11TH INTERNATIONAL
CRETACEOUS
SYMPOSIUM
Warsaw, Poland, 2022

CRETACEOUS OF THE NORTH SUDETIC SYNCLINORIUM (SOUTHWESTERN POLAND): STRATIGRAPHY, ORIGIN AND ECONOMIC IMPORTANCE

Stanisław Leszczyński[1]| Alina Chrząstek[2]| Adam T. Halamski[3]| Wojciech Nemec[4]| Jurand Wojewoda[5]

1| Jagiellonian University, Poland; e-mail: stan.leszczynski@uj.edu.pl

2| University of Wrocław, Poland; e-mail: alina.chrzastek@uwr.edu.pl

3| Instituite of Paleobiology, Polish Academy of Sciences, Warszawa, Poland; e-mail: ath@twarda.pan.pl

4| University of Bergen, {miasto}, Norway; e-mail: wojtek.nemec@uib.no

5| University of Wrocław, Poland; e-mail: jurand.wojewoda@uwr.edu.pl

ABSTRACT

The integrated stratigraphy, ichnology, depositional processes, sedimentary environments, and economic importance of the North Sudetic Cretaceous (Cenomanian to Santonian) are presented. The sediments of the North Sudetic Cretaceous were deposited in a narrow, northwest-trending basin at the northern periphery of the Bohemian Massif, between the West Sudetic Island to the southwest and the East Sudetic Island to the northeast. The basin was one of the Central European seaways linking the Boreal and Tethyan marine provinces. The sedimentary succession comprises shallow-marine, lagoonal, fluvio-deltaic, and paludal/lacustrine sediments deposited in response to the bathymetric configuration of the basin and contemporaneous sea-level changes controlled by eustasy and Alpine tectonism.

INTRODUCTION

The Cretaceous of the North Sudetic Synclinorium (NSS) constitutes an important part of the Cretaceous System in Central Europe, both from the point of view of pure geology, especially palaeontology, as well as for applied geology, especially its economic branch. The Cenomanian–Santonian part of the NSS is a mostly siliciclastic succession. The deposits have been explored in many respects and exploited for several hundred years. The first geological description of a small fragment of the area was given by Charpentier (1768), and the earliest, brief geological description of the basin by von Raumer (1819). Research conducted since the nineteenth century, first by German and then by Polish geologists, allowed for the recognition of the stratigraphic architecture of the sedimentary succession and the processes and palaeoenvironmental conditions of its accumulation. Research has provided valuable palaeontological and ichnological data, contributing significantly to the overall understanding of the Cretaceous System. Last, but not least, the NSS Cretaceous is of great regional economic importance because of the natural resources it hosts.

GEOLOGICAL SETTING

The NSS is a tectonic unit situated in the northern foreland of the Variscan Orogen of the Sudetes (Berg 1913; Born 1921), in the northern marginal zone of the Bohemian Massif (Fig. 1A). The unit extends SE-NW along the

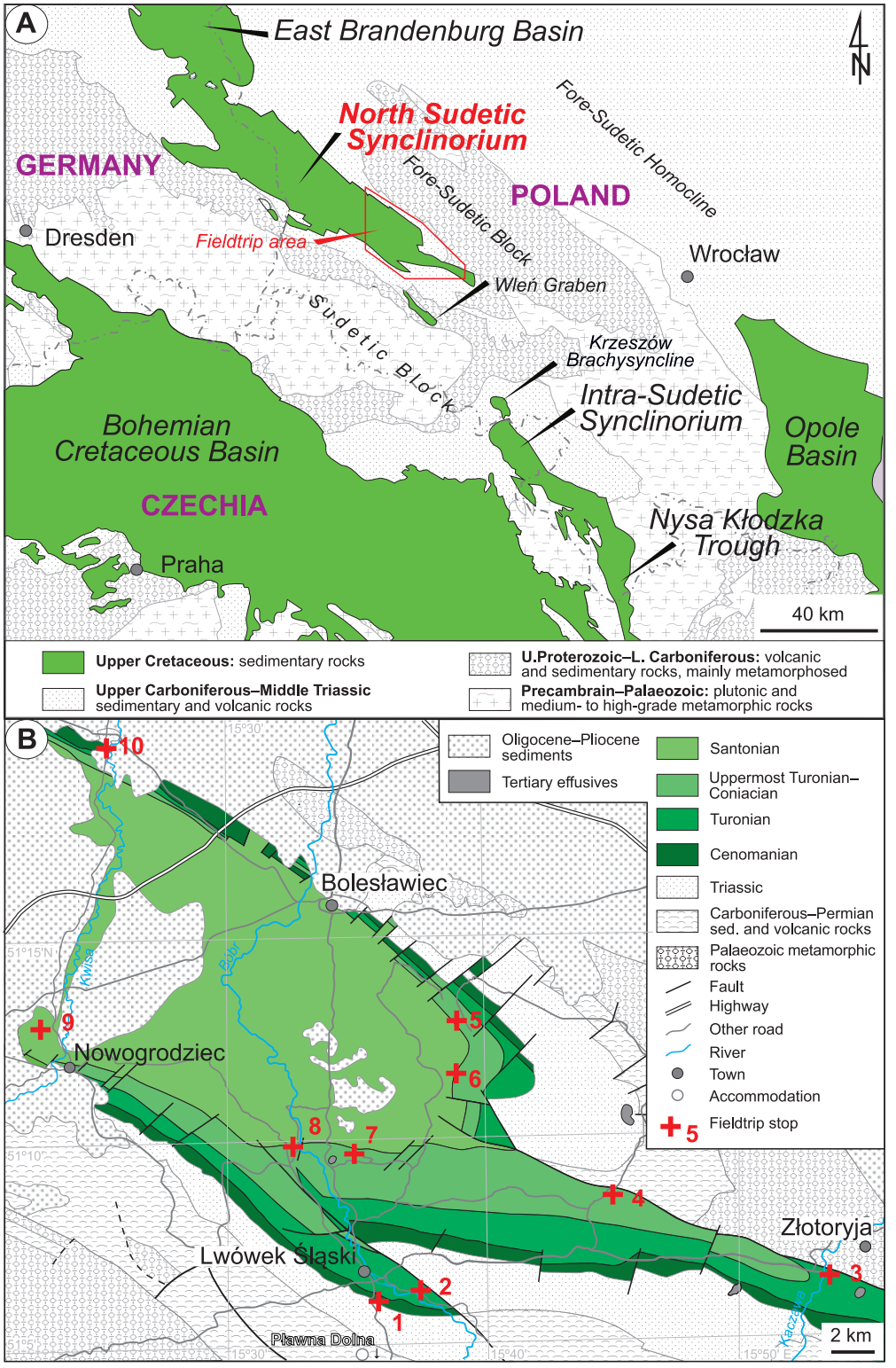

Fig. 1. Geological setting of the fieldtrip area. A – Location of the North Sudetic Synclinorium relative to the northern margin of the Bohemian Massif; geological map without Cenozoic, modified from Pożaryski et al. (1969). B – Geological map of the North-Sudetic Synclinorium and adjacent areas, without Quaternary deposits, compiled from Badura (2005), Cymerman et al. (2005a, b), Kozdrój et al. (2005), Przybylski et al. (2005), Sztromwasser (1995) and Halamski et al. (2020); partly reinterpreted by S. Leszczyński, with the location of fieldtrip stops marked.

Sudetic Boundary Fault and comprises a succession of Late Carboniferous, Permian, Early to Middle Triassic, and Late Cretaceous (Cenomanian–Santonian) strata, mostly siliciclastic sedimentary rocks and Late Palaeozoic volcanics, resting unconformably upon the Variscan basement (Scupin 1910; Oberc 1962; Śliwiński et al. 2003; Chrząstek and Wojewoda 2011). The NSS is bordered to the northeast by the elevated crystalline Fore-Sudetic Block, devoid of Mesozoic deposits, and by its northwestern envelope known as the Żary Pericline, with a Permian to Middle Triassic depositional cover. To the southwest, it is bordered by the elevated Görlitz and Kaczawa fold belts composed of pre-Permian metamorphic rocks (Żelaźniewicz et al. 2011). The complex internal structure of the NSS is due to faulting and inversion related to the multiphase convergence between Africa–Iberia and West-Central Europe (e.g., Kley and Voigt 2008) in the Cretaceous to Paleogene (Solecki 2011), the detailed timing of which is poorly constrained (Sobczyk et al. 2019 and references therein). Faults subdivide the NSS into subordinate units of various scale, most sharing the Cretaceous cover (Scupin 1913; 1931; Milewicz 1968). Only the southeastern part of the NSS Cretaceous crops out at the surface, with the rest hidden under various, mostly terrestrial, Cenozoic sediments and volcanics (Fig. 1B). The stratigraphy and lithofacies of these sediments, as well as the character and age of volcanics, indicate that in the Paleogene–Miocene this area was elevated and subject to peneplanation, basement weathering, and faulting (Oberc 1962; Jahn 1980; Migoń and Lidmar-Bergström 2001; Badura et al. 2004 and references therein). Differential subsidence with widespread terrestrial sedimentation occurred in the Miocene (Oberc, 1962; Dyjor 1995). The present-day relief shows a significant influence of prominent Oligocene–Miocene volcanism (Birkenmajer et al. 1966, 2004; Badura et al. 2005; Ulrych et al. 2011) and various Quaternary processes, particularly Pleistocene glaciation.

The NSS is a well-preserved axial relic of a Late Cretaceous sedimentary basin, called the North Sudetic Basin (NSB), that developed within the area of a former Late Palaeozoic–Jurassic(?) basin. Like the other Late Cretaceous basins of the Bohemian Massif, the NSB was formed at the Central European interface of the Tethyan and Boreal provinces by the regional reactivation of older, mainly Variscan fault zones dissecting the Bohemian Massif and its surroundings (Fig. 2). The initiation of these basins coincided with the worldwide Cenomanian transgression. As a result, a major part of Central Europe, including large areas of the Bohemian Massif, the present-day Sudetes, and their foreland, were flooded (Voigt et al. 2008), forming an island-dotted seaway, the so-called European Archipelago, between the Tethys and the Boreal Ocean (Csiki-Sava et al. 2015). The NSB formed a southeastern extension of the East Brandenburg Basin (Musstow 1968; Voigt et al. 2008) and was at least temporarily connected by hypothetical straits with the adjacent Intra-Sudetic Basin and further with the large Bohemian Basin (Fig. 2; Partsch 1896; Scupin 1910; Leszczyński 2018).

STRATIGRAPHY

The North Sudetic Cretaceous forms an over 1000 m thick sedimentary succession (Milewicz 2006) comprised of sandstones, mudstones, claystones, and marlstones, with subordinate limestone intercalations in the lower part and thin coal intercalations in the upper part. The limestones occur exclusively in the northwestern part of the NSS, and are known only from drill cores. The sediments are known to host a rich assemblage of body and trace fossils, both fauna and flora (Goeppert 1841, 1844; Drescher 1863; Williger 1882; Scupin 1913; Leszczyński 2010, 2018; Chrząstek and Wypych 2018; Halamski et al. 2020, and references therein), which – together with physical sedimentary features – indicate mostly nearshore, paralic, and offshore marine deposition (Beyrich 1849; Drescher 1863; Williger 1882; Partsch 1896; Scupin 1910; Milewicz 1965, 1996; Leszczyński 2010, 2018; Chrząstek and Wypych 2018; Leszczyński and Nemec 2020; Halamski 2020; Kowalski 2021). Outcrops and drill cores demonostrate considerable lateral and vertical variation of these lithofacies assemblages, with siliciclastic sandstone lithosomes dominant to the southeast and pinching out in mudstones and marlstones towards the northwest (Fig. 3).

The lithostratigraphic interpretation of the North Sudetic Cretaceous has evolved with

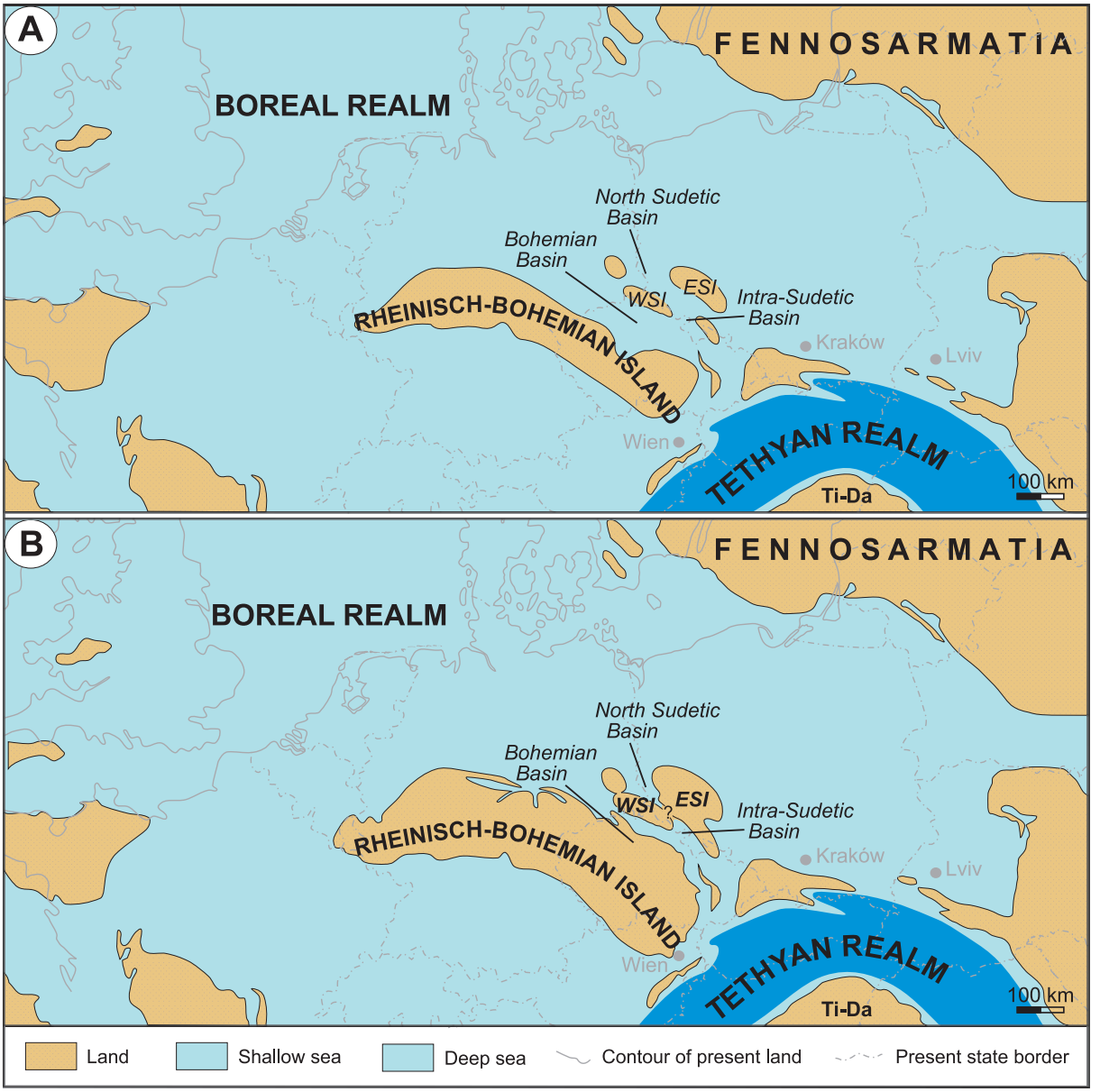

Fig. 2. Palaeogeography of southern Poland and adjacent areas during the Turonian (A) and the middle Coniacian regression (B); based on Ron Blakey from Csiki-Sava et al. (2015) and Kowalski (2021), modified for Poland and neighbouring areas by S. Leszczyński. Abbreviations: ESI – East Sudetic Island(s); WSI – West Sudetic Island(s); Ti-Da – Tisia-Dacia Block.

time (see review by Milewicz 1996). The existing lithostratigraphy (Fig. 3) was proposed by Milewicz (1985), who – based on earlier German and later Polish data – subdivided the succession into three formations. The marine lower half of the succession – dominated by sandstones to the southeast and by mudstones, marlstones, and limestones to the northwest – was designated the Rakowice Wielkie Formation, with its main sandstone lithosomes distinguished as separate members (the Wilków, Chmielno, Dobra, and Żerkowice Members; Fig. 3). The upper half of the succession was divided by Milewicz (1985) into two coeval formations, referred to as the Węgliniec Formation and the Czerna Formation (Fig. 3). The former is marine, ca. 250 m thick, and is composed chiefly of mudstones, whereas the latter to the southeast is paralic, attains a thickness of ca. 500–800 m, and comprises

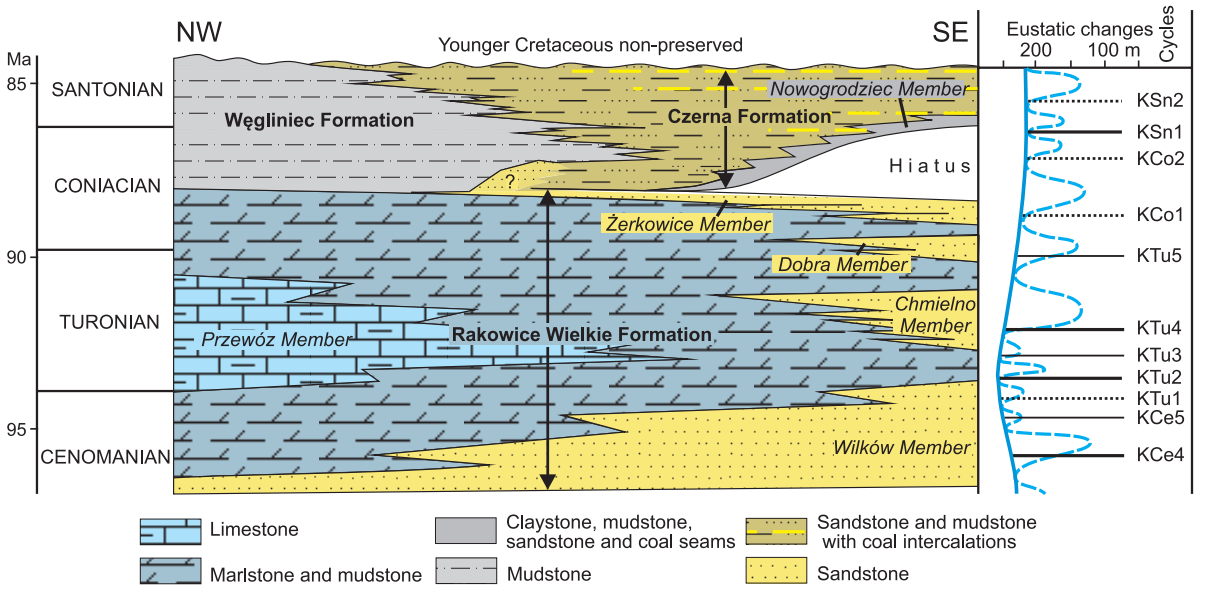

Fig. 3. The Upper Cretaceous stratigraphy of the North Sudetic Synclinorium, shown in axial cross-section. Lithostratigraphy is after Milewicz (1996), chronostratigraphy after Walaszczyk (2008) and Halamski et al. (2020), and numerical ages after Cohen et al. (2013); the corresponding eustatic curve is redrawn from Haq. (2014).

sandstones intercalated with mudstones, claystones, and thin coal seams, and is autochthonous to hypautochthonous (Milewicz 1985, 1996). The mud-dominated limnic lowermost part of the Czerna Formation, rich in coal and 2–50 m thick, was distinguished by Milewicz (1985) as the poorly defined Nowogrodziec Member (Fig. 3).

The first biostratigraphic dating of the sedimentary succession, based by Beyrich (1855) on bivalves and ammonites, indicated a Cenomanian–Senonian age. Milewicz (1958) limited the age of the upper part of the succession to the Santonian, and Krutzsch (1966) specified it further to the early Santonian. Milewicz (1956, 1969) also postulated a late Coniacian (late Emscherian) hiatus between the Rakowice Wielkie Formation and the Czerna Formation in the southeastern part of the North Sudetic Synclinorium, with a decrease in the duration of this stratigraphic gap towards the northwest (Fig. 3).

A more recent biostratigraphic study by Walaszczyk (2008) revised the succession chronostratigraphy. The boundary between the Rakowice Wielkie Formation and the overlying Węgliniec and Czerna Formations was assigned to the middle/late Coniacian transition, with the Coniacian/Santonian boundary in the middle of these latter formations, and the hiatus discussed above corresponding to the late middle Coniacian. Recent palaeobotanical studies by Halamski et al. (2020) speak for a local hiatus such as that indicated by Milewicz (1996). This revised chronostratigraphy is followed in the present guidebook (Fig. 3).

SEDIMENTOLOGICAL CHARACTERISTICS AND ORIGIN

The Rakowice Wielkie Formation

The sedimentary succession of the North Sudetic Cretaceous starts with a 5–40 cm thick pebbly conglomerate or pebbly sandstone resting almost conformably upon Late Carboniferous–Middle Triassic sedimentary and volcanic rocks, which are also found locally as clasts in the basal part of the unit (Fig. 4; see fieldtrip stops 1 and 10). The gravelly deposits pass upwards into very coarse- and medium-grained sandstones, and further into fine-grained sandstones. These are quartzose arenites to poor wackes with a small admixture of lydites and siliceous shists, mainly massive (structureless) or large-scale cross-stratified, and are largely unfossiliferous.

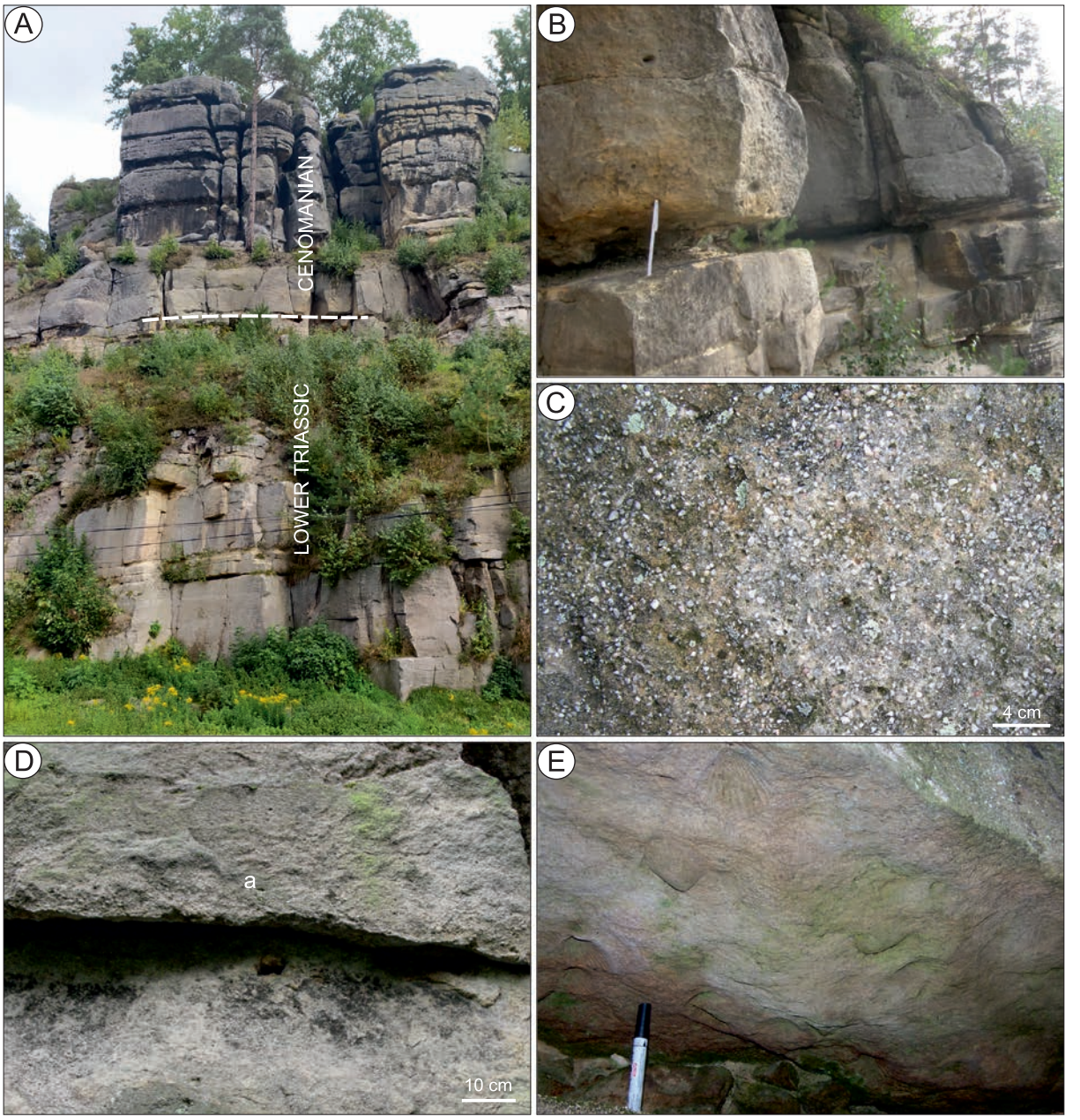

Fig. 4. The Cenomanian Wilków Member and its relationship to the underlying deposits. A – General view of the unit and its relationship to the underlying Early Triassic sandstones of the Radłówka Formation. B – The boundary (ravinement surface) between the Triassic and Cenomanian sediments. Note differences in sediment grain size. C – Texture of structureless Wilków Sandstone. D – Normal grading in structureless sandstone, highlighted by the granule sandstone tempestite located in the basal part of bed (a). E – Molds of bivalve shells at the sole of structureless tempestite sandstone bed. Pictures A to C are from fieldtrip stop 1 (in Lwówek Śląski), D and E are from the Wilków Sandstone in an abandoned quarry between the villages of Niwnice and Kotliska (7.5 km northwest of Lwówek Śląski). All photographs by S. Leszczyński.

The fossils consist of mostly bivalves (*Pecten asper* Lamarck, *P. hispidus* Goldfuss, *Exogyra columba* Lamarck, *Ostrea carinata* Lamarck, *Inoceramus bohemicus* Leonhard, *I. pictus* Sowerby, *Mytiloides hercynicus* (Petrascheck), single cephalopods, brachiopods, and echinoderms; numerous fish bones have been found in the sandstones (Drescher 1863; Scupin 1913; see Milewicz 1996). In the northwestern part of the NSS, the sandstones are calcareous and

glauconitic (Milewicz 1996). The deposits were called the *Unterquader* by German geologists (Scupin 1906, 1913). Milewicz (1985, 1996) distinguished them as the Wilków Sandstone and included them into the Rakowice Wielkie Formation. Their thickness reaches 135 m in the southeastern part of the NSS and decreases to several metres in the northwestern part of the unit (Milewicz 1996). The top part of the unit is locally marked by an iron hydroxide-impregnated layer, up to 30 cm thick.

The Wilków Sandstone is overlain by a succession of fine-grained sediments constituting the sedimentary background of the Rakowice Wielkie Formation. These start with dark-grey sandy and silty marls, marly siltstones, mudstones, and subordinately clayey ironstones, locally rich in various fossils and highly bioturbated (Milewicz 1960, 1996; *Pläner* in the German literature). The sediments become sandier upwards and are virtually sand-dominated to the southeast, where German geologists distinguished the *Pläner Sandstein* (e.g., Scupin 1913; see fieldtrip stop 2). In the northwestern part of the NSS, intercalations of grey to dark-grey, thin- to thick-bedded mudstone and wackestone- to packstone-, dolomitic, glauconite-bearing marly limestones appear in the higher part of succession. The latter subsequently develops into a homogenous limestone unit, up to 110 m thick, transitioning upward into a succession of interbedded, dark-grey to black, clayey, silty and sandy marls and calcareous mudstones (Milewicz 1996). The limestones are known from drillings in the northwestern part of the NSS and disappear to the southeast (Milewicz 1996). Rare fossils, mostly bivalves and brachiopods recorded in limestones from the lower part of the sedimentary succession, include *Inoceramus crippsi* Mantell, *I. pictus* Sowerby, and *Mytiloides hercynicus* (Petrascheck) (Milewicz 1966). Different inoceramids, including *Mytiloides labiatus* (Schlotheim), and *Mytiloides mytiloides* (Mantell), and foraminifers occur in the higher, lower Turonian part of the fine-grained succession (Milewicz 1996). Several inoceramid taxa, including *Inoceramus costellatus* Woods, *I. inaequivalensis modestus* Heinz, and *Cremnoceramus inconstans* (Woods) have been found higher, in the upper Turonian–lower Coniacian part of this succession, and *Volviceramus koeneni* (Müller) and *I. kleini* Müller are reported from its top in the northwestern part of the NSS (Milewicz 1996).

The fine-grained succession of the Rakowice Wielkie Formation thins to the southeast, where it is split by wedges of the Chmielno and Dobra Sandstone Members and topped by an extensive wedge of the Żerkowice Sandstone (Fig. 3).

The Chmielno Sandstone (*Mittelquader* according to Scupin 1913; *Rabendockensandstein* and *Ludwigsdorfer Sandstein* in Scupin 1935; see fieldtrip stop 3) is a unit composed of light-grey and beige, mostly coarse-grained, locally pebbly sandstone that is massive, faintly cross-stratified, and rarely plane-parallel stratified (Figs 5–9); compositionally, it is quartzose with a small admixture of feldspar and a sparse kaolinitic and ferrous cement. Numerous soft-sediment convectional disturbances with characteristic shapes (e.g., folds, helicoidal torsions) occur locally (Figs 6C, 7B, F). In some places, gravelly material is immersed in the underlying sand (drop-shaped load casts; Figs 6, 9B) The unit is up to 90 m thick, splitting to the northwest into two subordinate wedges (tongues). The lower one consists of coarse-grained sandstones in the lower part, whereas the upper shows an opposite vertical grain-size trend (Milewicz 1996). The lower and upper boundary of the unit are sharp. The top surface is covered by a layer of clayey ironstone. The sandstones contain fairly rich fossil fauna, including inoceramids (*M. labiatus*, *M. hercynicus*, *I. lamarcki* Parkinson, *I. costellatus*), other bivalves (*Pinna decussata* Goldfuss, *Lima canalifera* Goldfuss, *Pecten acuminatus* Geinitz, *Pectunculus geinitzi* d'Orbigny, *Cardita geinitzi* d'Orbigny), and some brachiopods, as well as trace fossils (mainly *Ophiomorpha nodosa*).

The Dobra Sandstone is a thinner unit, known from a narrow zone along the northern margin of the NSS southeast to northwest of Bolesławiec. The unit is composed of coarse- to fine-grained quartzose, and is mostly represented by cross-stratified sandstones. Their thickness does not exceed a few dozen metres (Milewicz 1985, 1996).

The Żerkowice Sandstone Member (*Oberquader* in German literature; see fieldtrip stops 4–8) is the uppermost lithostratigraphic division of the Rakowice Wielkie Formation in the southeastern part of the NSS, where this sandy

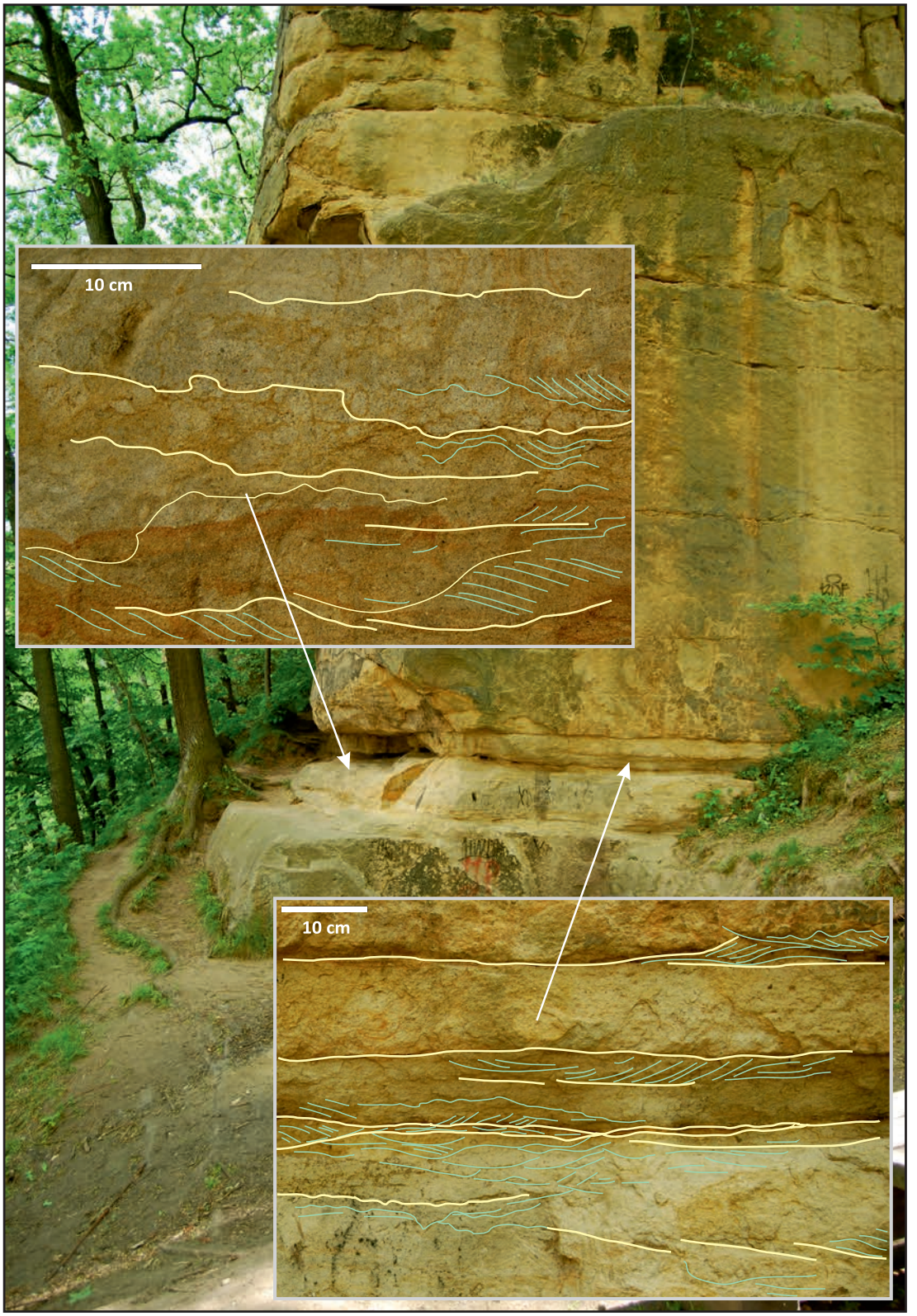

Fig. 5. Sandstones of the Chmielno Member at fieldtrip stop 3, site A (see Figs 1B and 33). Sandstones and gravelly sandstones of the lower part of the profile, mostly cross bedded in large- and small-scale cosets, with conglomeratic layers and highly bioturbed sediments. All photographs by J. Wojewoda.

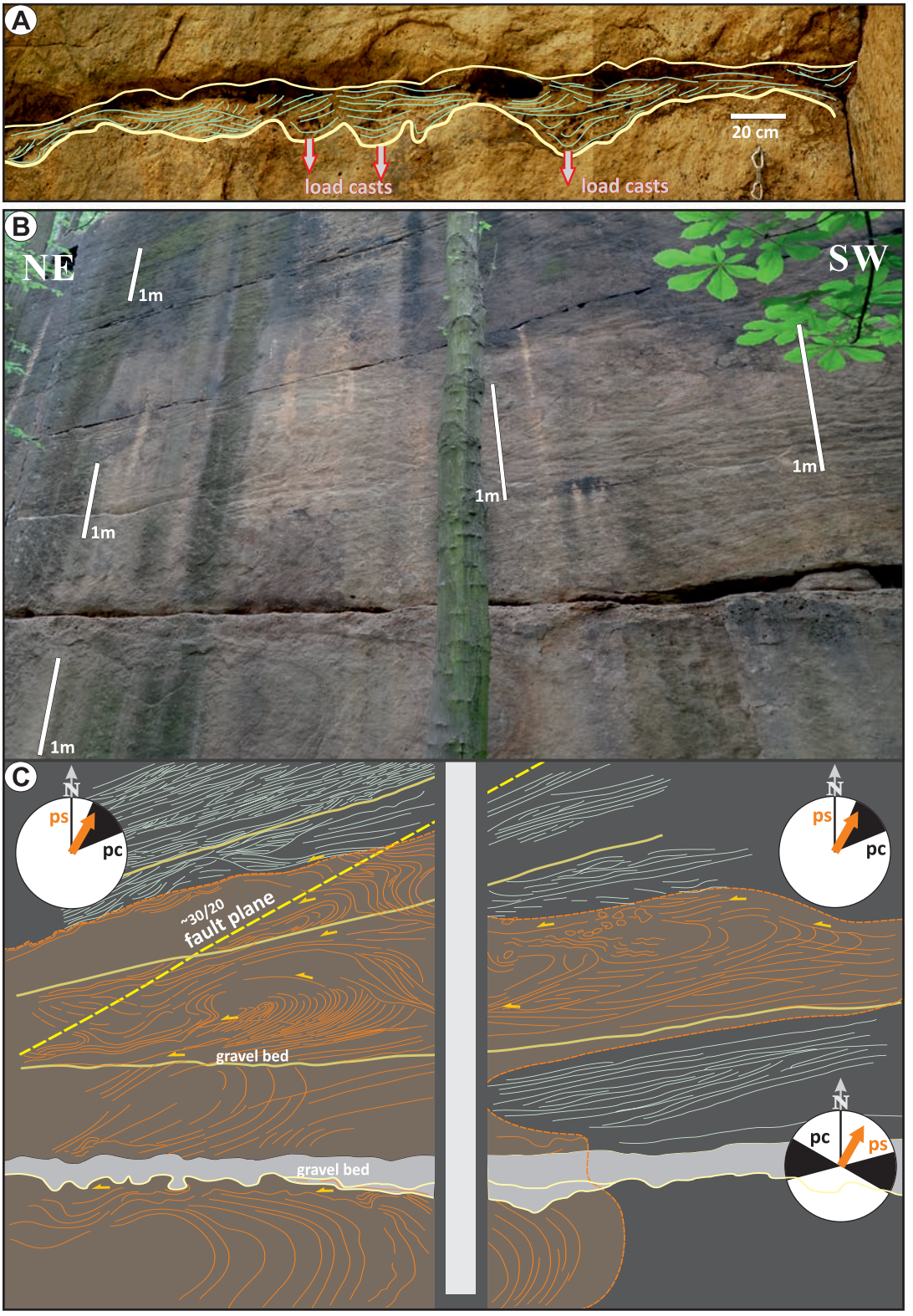

Fig. 6. Large-scale deformations of primary sedimentary structures in sandstones of the Chmielno Member at fieldtrip stop 3. A, B – from site I, C from site J (see Fig. 33); drop-like load structures in the conglomerates of the upper part of the "Krucze Skały" profile (contorsions and sinked gravel ripples?); the cross beddings indicate the dominant palaeocurrent was towards the north. All photographs by J. Wojewoda.

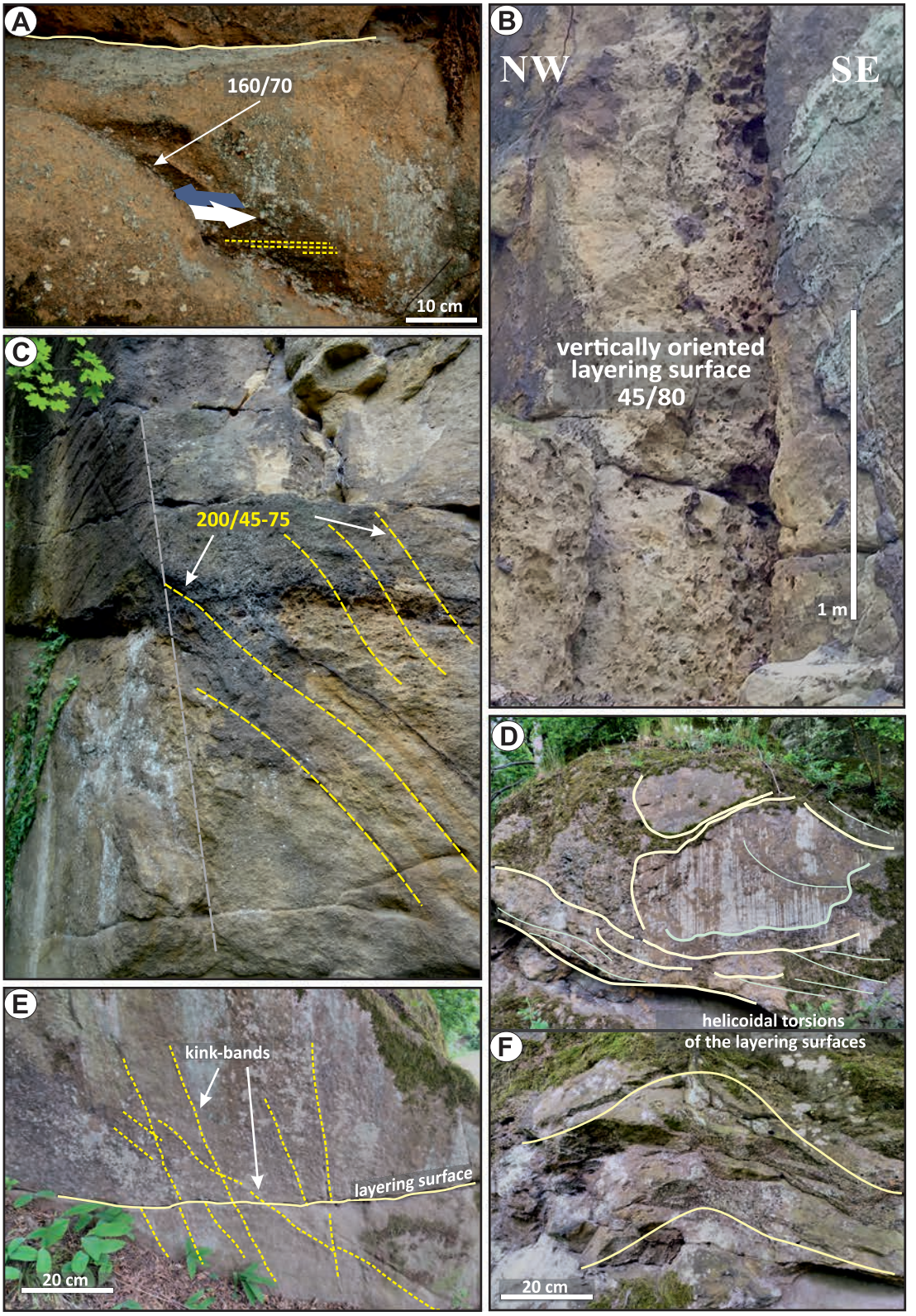

Fig. 7. Sandstones of the Chmielno Member. Examples of deformation structures within nonconsolidated sediments (kink bands, helicoidal torsions) and tectonic deformations (striation on tectonic mirrors, Riedel T-shears); fieldtrip stop 3. A – from site B. B – from site E. C – from site C. D – from site F. E – from site D (see Fig. 33). All photographs by J. Wojewoda.

Fig. 8. Sandstones of the Chmielno Member at fieldtrip stop 3, site K (see Fig. 33), approximately 400 m south of the previous sites, without any signs of deformation. Photograph by J. Wojewoda.

lithosome is exposed and has been subject to open-pit mining for several centuries as a highly valued dimension stone. The lower boundary of the unit is generally distinct, with fine-grained quartzose sandstones conformably overlying a lithosome of dark-grey mudstones, with a silty transition (Fig. 10). The boundary is less distinct and rather controversial in the northern part of the NSS, where the mudstone lithosome pinches out and the sandstones of the Żerkowice Member directly overlie the Dobra Sandstone (cf. Figs 3 and 10; Bossowski 1991). The top of the Żerkowice Member is the upper boundary of the Rakowice Wielkie Formation in the southeastern part of the synclinorium. This boundary is sharp and mainly erosional, with a stratigraphic hiatus (Fig. 3); the sandstones are overlain by a coal-bearing heterolithic unit dominated by mudstones and claystones (the Nowogrodziec Member of the Czerna Formation, *sensu* Milewicz 1985), increasingly ferruginized towards the southeast and containing local patches of ferricrust or ferruginized fossil turf (e.g., at fieldtrip stop 5).

Exploration boreholes show the sandstone lithosome of the Żerkowice Member thickens towards the northwest over 25 km along the synclinorium axis, from 50 m between fieldtrip stops 4 and 5, to 60 m roughly between fieldtrip stops 8 and 9, and up to 100 m ca. 10 km to northwest (Fig. 1B; see Leszczyński and Nemec 2020). Only a few kilometres farther to the northwest, the sandstone lithosome thickens abruptly to >200 m (corrected to >160 m on the account of local tectonic tilt) and virtually pinches out in a nearby borehole. This prominent thickening and abrupt pinch-out of the sandstone lithosome at its northwestern termination is meaningful, as discussed further in the text.

The Żerkowice Member consists of fine- to medium-grained and subordinately coarse-grained quartzose arenitic sandstones that are greyish white in colour, cream-yellow to light orange on weathered outcrop surfaces, and range in hardness from well cemented (mined as building blocks) to nearly soft (mined as glass sand). Mudstone interbeds are minor,

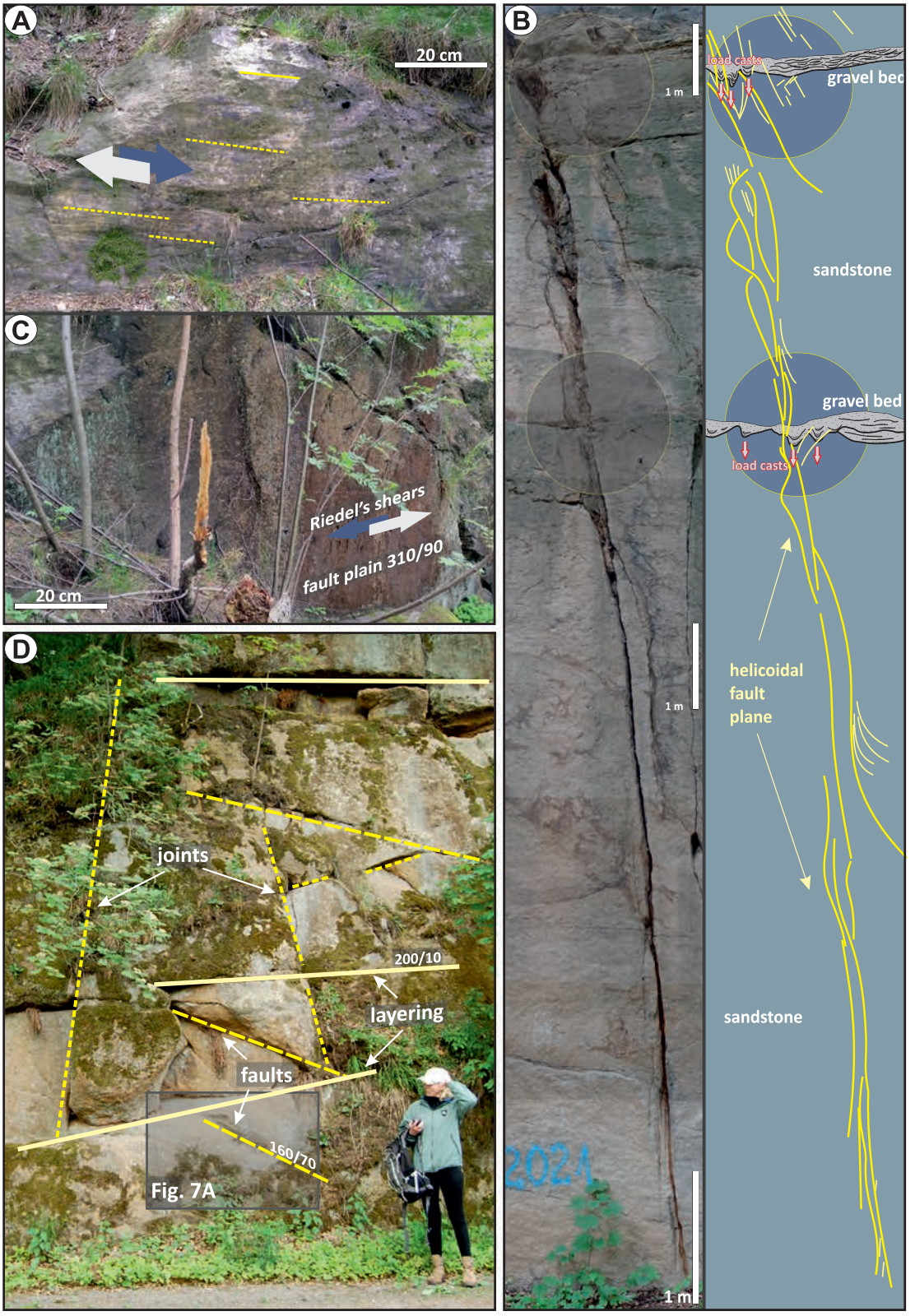

Fig. 9. Sandstones of the Chmielno Member displaying spatial change in interrelationships of stratification, tectonic deformations, and features formed in nonconsolidated sediments as they approach the Jerzmanice Fault. Fieldtrip stop 3. A, C – site G; B – site H; C – site G; D – site A". All photographs by J. Wojewoda.

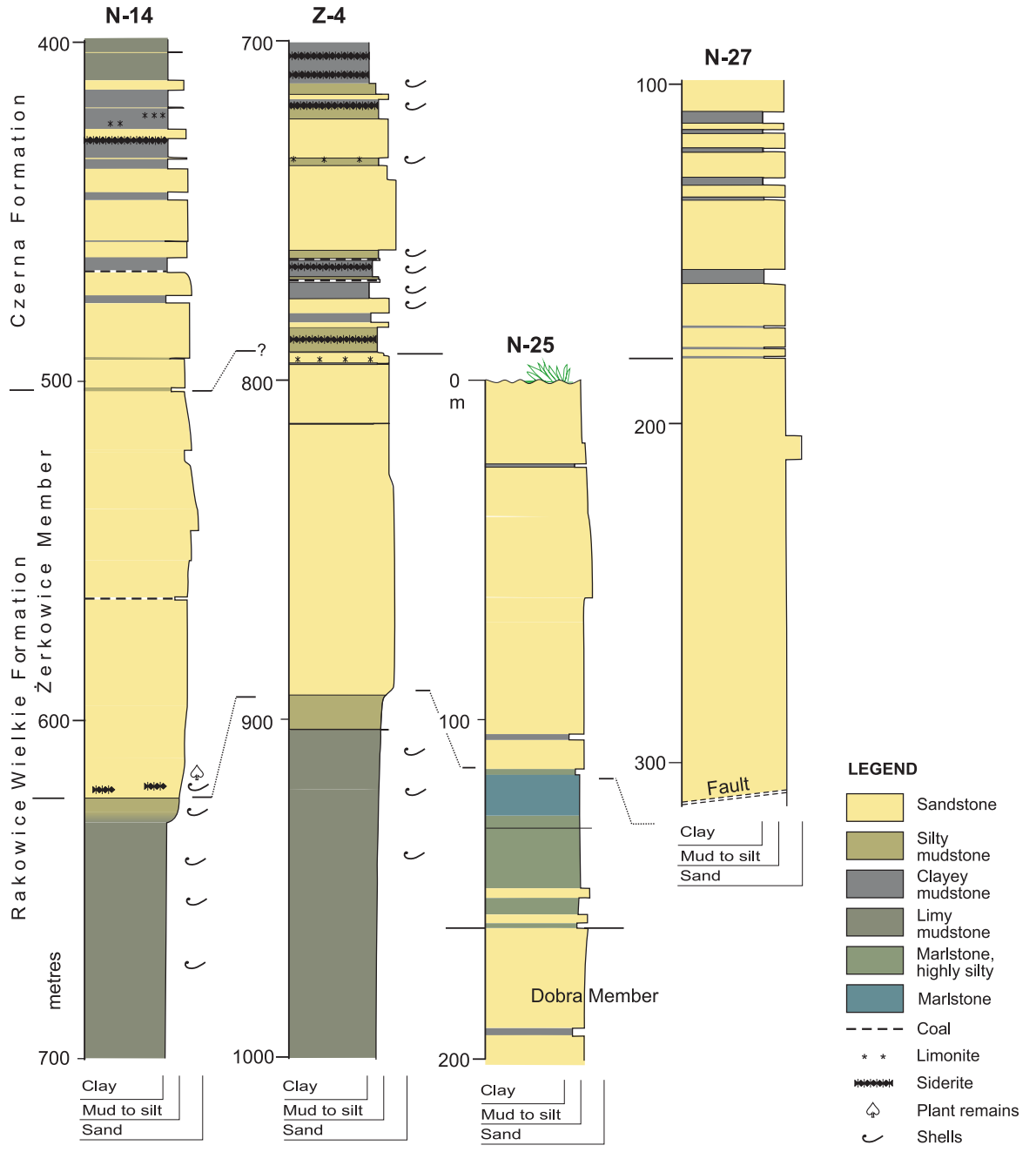

Fig. 10. Borehole logs showing the stratigraphic transition of the Rakowice Wielkie Formation to the Czerna Formation compiled by Leszczyński and Nemec (2020).

thin and laterally discontinuous. The sand is mainly very well sorted, which commonly renders its internal stratification and bed boundaries poorly visible.

The volumetrically dominant lithofacies are sandstones with large-scale planar or trough cross-stratification (lithofacies Sc in Leszczyński and Nemec 2020; Fig. 11A–C). Cross-strata sets range from a decimetre to 3.2 m in thickness, show variable and often bidirectional transport directions, and form laterally extensive cosets up to 15 m thick (Figs 13, 14; legend explained in Fig. 12). Some cross-strata sets show hydroplastic deformation and partial homogenization by liquefaction. Subordinate lithofacies distinguished

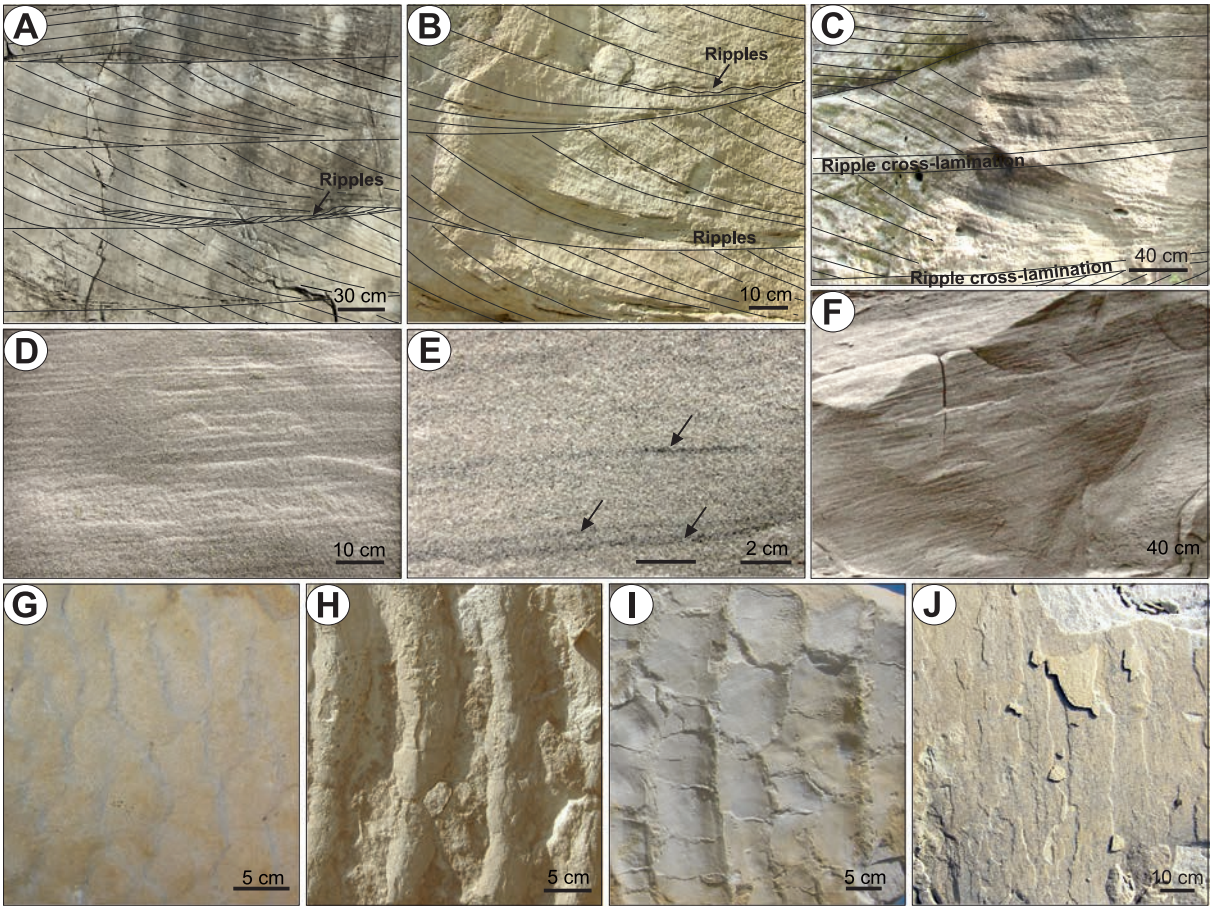

Fig. 11. Lithofacies and ichnofauna of the Żerkowice Member by Leszczyński and Nemec (2020). A – Sandstone with trough cross-stratification (lithofacies Sc) in vertical outcrop; fieldtrip stop 5A; note minor intrasets of reverse-flow ripple cross-lamination; main transport direction to the right, obliquely away from the viewer. B – Sandstone with planar tangential cross-stratification (lithofacies Sc) in vertical outcrop; fieldtrip stop 5A; note minor intrasets of reverse-flow ripple cross-lamination; main transport direction to the right, increasingly away from the viewer upwards. C – Sandstone with planar angular cross-stratification (lithofacies Sc) and interbeds of current ripple cross-lamination (lithofacies Sr) in vertical outcrop; fieldtrip stop 6B; transport direction to the right, obliquely towards the viewer. D – Sandstone with horizontal plane-parallel stratification (lithofacies Sp); vertical outcrop; active glass sand open pit ca. 2 km west of fieldtrip stop 10. E – Plane-parallel swash stratification in lithofacies Sp with dark laminae enriched in heavy minerals (arrows); vertical outcrop, locality as in D. F – Sandstone with gently inclined plane-parallel stratification (lithofacies Sp) in vertical outcrop, locality as in D. G – 3D current ripples exhumed on a bedding plane in sandstone lithofacies Sr; fieldtrip stop 7A. H – Symmetrical 2D wave ripples with rounded crests, exhumed on a bedding plane in sandstone lithofacies Sw; fieldtrip stop 5A. I – Sharp-crested symmetrical 2D wave ripples exhumed on a bedding plane in sandstone lithofacies Sw; fieldtrip stop 5A. J – Parting lineation on bedding surface in a swash-stratified sandstone of lithofacies Sp; fieldtrip stop 5A. All photographs by S. Leszczyński.

by Leszczyński and Nemec (2020) include sandstones with current ripple cross-lamination (lithofacies Sr, Fig. 11A–C, G), wave ripple cross-lamination (lithofacies Sw, Fig. 11H, I) and plane-parallel stratification (lithofacies Sp, Fig. 11D–F). Lithofacies Sr occurs as local intercalations, 5–50 cm thick, within the large-scale cross-strata cosets (Fig. 11C). Lithofacies Sp and Sw commonly alternate with each other, forming units 0.1–4 m thick that split or cap the cross-strata cosets of lithofacies Sc (Fig. 14, top). Lithofacies Sp dominates along the margins of the synclinorium, where it shows a gentle primary basinward inclination of 3–5° and forms basinward wedges up to 10 m thick. Where the inclination is steeper (10–15°, Fig. 11F), the plane-parallel stratification shows primary current lineation (Fig. 11J) and hosts laminae rich in heavy minerals (Fig. 11E). Clayey to silty grey mudstones (lithofacies M) are a minor component. This lithofacies occurs as thin (0.5–2 cm) and laterally

discontinuous drapes between some of the cross-strata sets of sandstone lithofacies Sc. Thicker mudstone units, up to 15 cm, are thinly interlayered with sand and/or silt, forming heterolithic beds (lithofacies H) beneath some of the sandstone cross-strata cosets.

Bioturbation occurs only locally in the sandstones (Milewicz 1965, 1996; Chrząstek and Wypych 2018; Leszczyński 2018). Burrows (Figs 15A–E, 16A–C) are concentrated as patches on the surfaces separating cross-strata cosets, especially where draped with mud, and in the topmost parts (10–15 cm) of cosets, which are often intensely bioturbated with single burrows reaching down nearly 1.5 m. Trace fossils include *Ophiomorpha* isp. (Fig. 15A–C), *Ophiomorpha nodosa* (Figs 15B, C; 16C), *Thalassinoides suevicus* (Fig. 15D), *T. paradoxicus* (Fig. 16B), *Rosarichnoides sudeticus* (Fig. 16A), *Nereites* isp., *Terptichnus* isp. and some small unidentified burrows (Fig. 15E). The trace-fossil assemblages seem to range between a stressed expression of the *Skolithos* Ichnofacies and a proximal expression of the *Cruziana* Ichnofacies (Chrząstek and Wypych 2018; Leszczyński 2018). Body fossils are rare, represented by bivalves (Fig. 16D–G; mainly inoceramids, e.g., Fig. 16D), including *Volviceramus involutus*, *I. percostatus* Müller), gastropods (Fig. 15F), ammonites, and echinoderms (Fig 16H; Milewicz 1965; Walaszczyk 2008). Some patchy shell pavements and discrete horizons rich with imprints and casts of shell debris (Figs 11F, 15F, 16E–G) were found at fieldtrip stops 5 and 6 (Leszczyński 2010, 2018; Chrząstek and Wypych 2018). Scattered wood fragments of various sizes and aggregated imprints of large fishbones are sporadically present at fieldtrip stops 5, 6A and 8. Some large driftwood fragments are preserved solely as clustered *Teredolites*, casts of wood-boring bivalves (Leszczyński 2018).

According to Leszczyński and Nemec (2020), the spatially and genetically related lithofacies of the Żerkowice Member represent several sedimentary systems (environments), reviewed below. Sediment assemblages dominated by the cross-stratified sandstones of lithofacies Sc form mounded elongate sandbodies (longitudinal sand bars) roughly parallel to the synclinorium axis and virtually dominant in the axial zone to the southeast (Figs 13–17). Quarry outcrops show that these sandbodies are 5–15 m

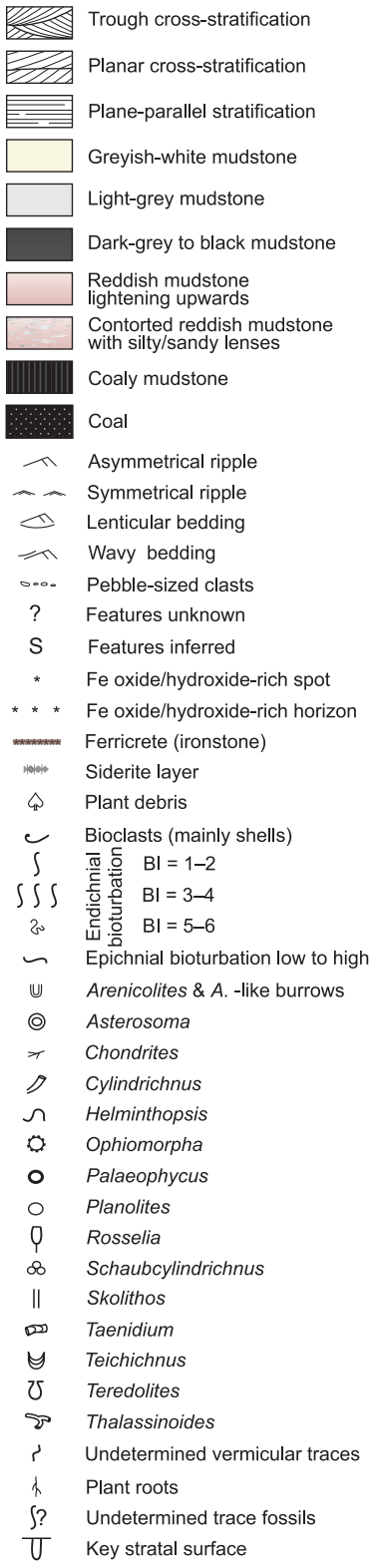

Fig. 12. Review of sedimentological and ichnological features recognized in Coniacian outcrops, given as a legend to the outcrop logs shown farther in this guide (after Leszczyński and Nemec 2020).

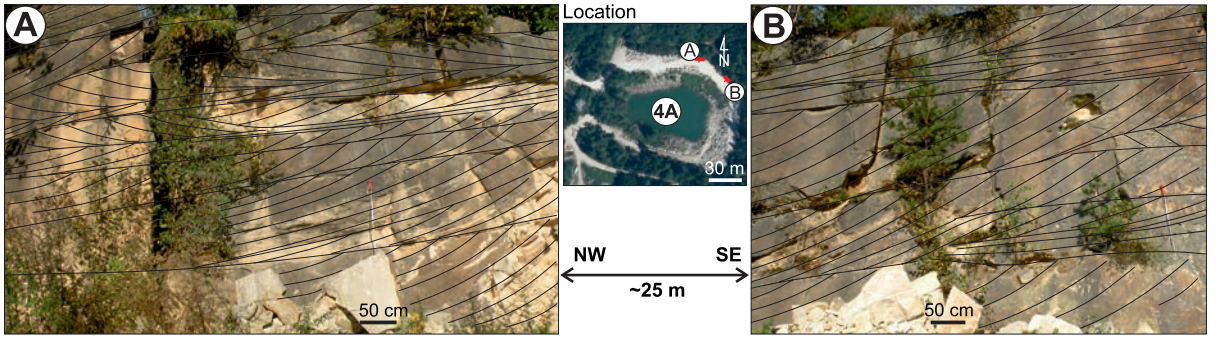

Fig. 13. Succession of vertically stacked, bidirectional dune cross-strata sets (lithofacies Sc) interpreted as a northwest-trending longitudinal tidal bar (sand ridge). Outcrop photographs A and B (by S. Leszczyński) show cliff portions of the abandoned quarry (fieldtrip stop 4A), as indicated in the inset image from Google Earth. From Leszczyński and Nemec (2020).

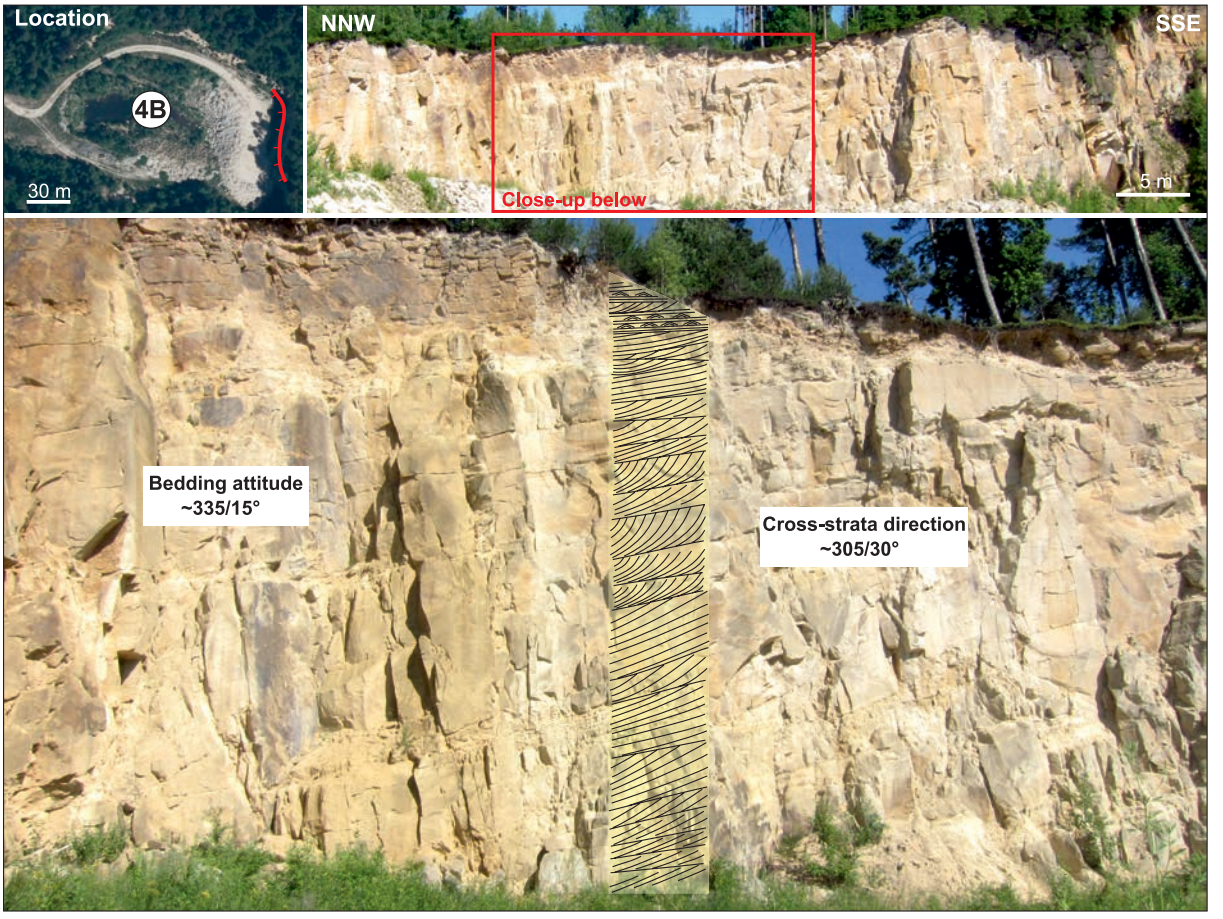

Fig. 14. Succession of vertically stacked dune cross-strata sets (lithofacies Sc) interpreted as a northwest-trending longitudinal tidal bar (sand ridge). The bedding inclination at this locality includes at least 5° of secondary tectonic tilt. Abandoned quarry in Czaple (fieldtrip stop 4B, Fig. 1B); the quarry and cliff location are shown in the inset image from Google Earth. From Leszczyński and Nemec (2020). Phohotographs by S. Leszczyński.

thick and apparently several kilometres long, stacked laterally and vertically into complexes up to 50 m thick. Their internal architecture displays vertically stacked 2D and 3D dune cross-strata sets, with bedding surfaces slightly rising or subhorizontal and gently falling to the northwest (Figs 13, 14). Transport directions to the northwest locally dominate (Fig. 14), but

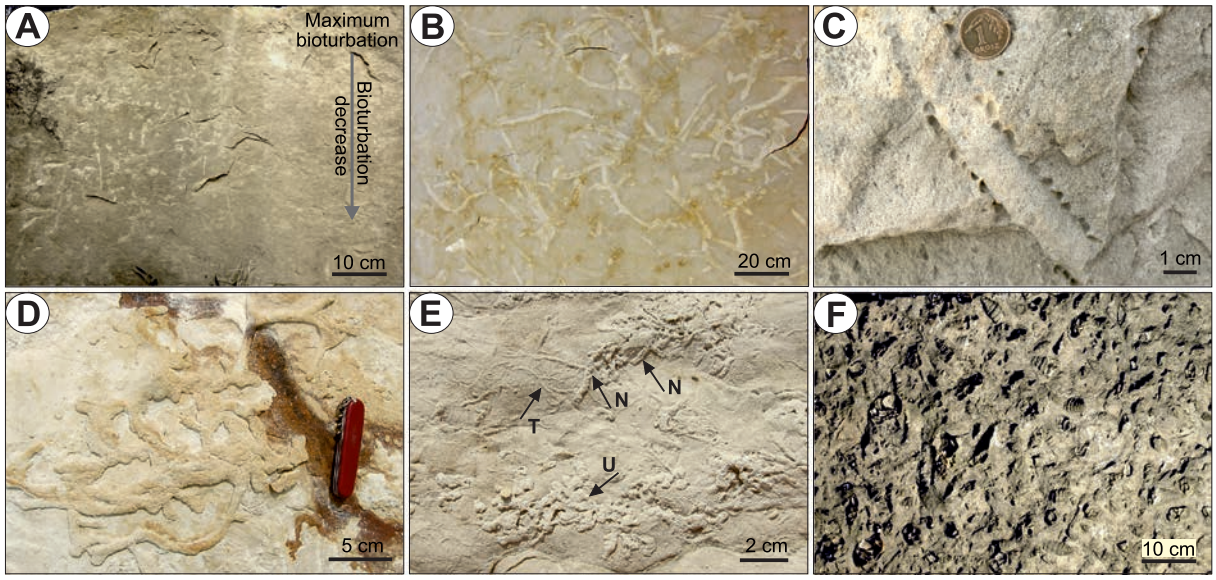

Fig. 15. Trace fossils and body fossils of the Żerkowice Member by Leszczyński and Nemec (2020). A – *Ophiomorpha* with density decreasing downwards in sandstone lithofacies Sc at fieldtrip stop 5A. B – *Ophiomorpha nodosa* network on sandstone bedding surface at fieldtrip stop 5A. C – Subvertical *Ophiomorpha nodosa* in sandstone at fieldtrip stop 6. D – *Thalassinoides suevicus*, slightly flattened by compaction, on sandstone bedding plane at Locality 8 in Leszczyński and Nemec (2020), neighbouring to fieldtrip stop 7. E – ?*Nereites* isp. (N); *Terptichnus* isp. (T) and undetermined burrows (U) on sandstone bedding surface at fieldtrip stop 6A. F – Shell lag (*Nerinea*) on a bedding plane in sandstone lithofacies Sp at fieldtrip stop 6. All photographs by S. Leszczyński.

the dune cross-sets are generally bidirectional (Fig. 13A) and show a wide range of transport directions (see rose diagram in Fig. 17). Some cross-sets are underlain by local drapes of lithofacies M. Interbeds of lithofacies Sw and Sr are minor, with the latter showing mainly reverse flow directions relative to those of the adjacent dune cross-strata (Fig. 11A–C). The basal parts of sand bodies consist of smaller dune cross-sets (Figs 14, 17) and are occasionally underlain by a heterolithic unit of lithofacies H, whereas their top parts are commonly packages of interbedded lithofacies Sp and Sw (Figs 10 and 13). Some of the sandbodies show shallow, isolated palaeochannels at the top (Fig. 18) filled with lithofacies Sc and trending slightly obliquely to the estimated long axis of the sandbody.

The elongate cross-stratified sand bodies are interpreted as longitudinal tidal sand bars (Leszczyński and Nemec 2020), also known as tidal sand ridges (Allen 1982; McBride 2003; Fig. 19A, B). They extend roughly parallel to the direction of tidal currents and grow seawards with a lateral migration component. The component tidal dunes migrate through the bars (lithofacies Sc in Fig. 11A–C), range from 2- to 3-dimensional, commonly grow in thickness by overstepping one another (Fig. 13B), and often show hydroplastic deformation of various origins. Tidal sand ridges are commonly associated with estuaries, tidal inlet deltas, and narrow straits (see Leszczyński and Nemec 2020 and references therein).

The bars interpreted in the Żerkowice Member are often underlain by inter-bar muddy heterolithic lithofacies H (cf. Hein 1986) and show an upward increase in flow energy (dune and grain sizes), indicating aggradational shallowing culminating in reworking by sea waves (Figs 14, 17) after reaching fairweather wave base. The alternation of lithofacies Sw and Sp in bar cappings indicates considerably fluctuating wave orbital velocity (Komar and Miller 1965), possibly including episodic erosion by storm waves (Clifton and Dingler 1984). Isolated palaeochannel features (Fig. 22) are interpreted as tidal conduits cut over the sand-ridge top, probably to accommodate local storm-boosted tidal current flows (cf. Dalrymple 1984).

Based on measurements in the rock tor "Skała z Medalionem" (fieldtrip stop 6B; Fig. 17) and the neighbouring, now abandoned, Żerkowice Quarry, Leszczyński and Nemec (2020) estimated the mean thickness of cross-sets

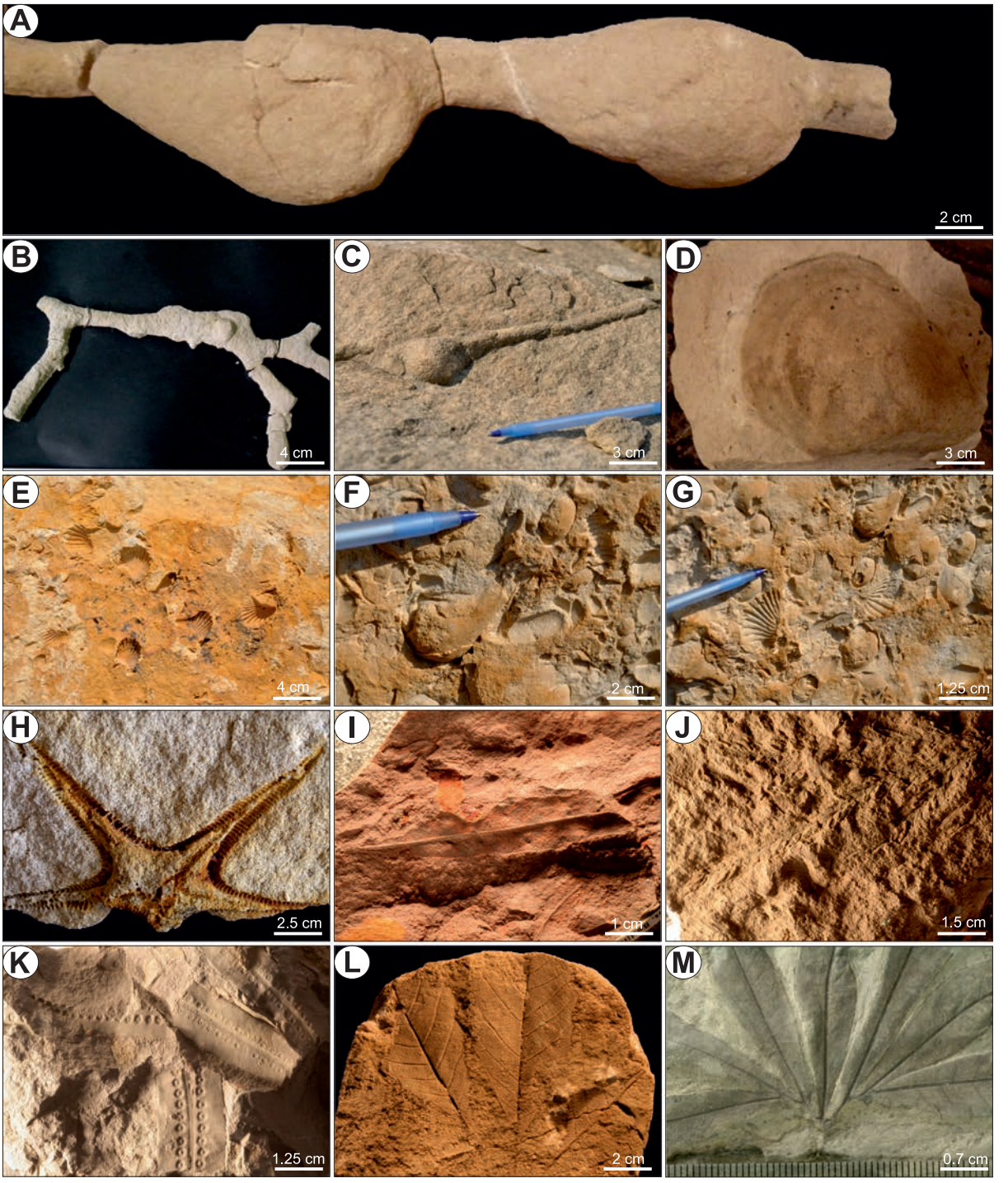

Fig. 16. Plant, macrofaunal body, and trace fossils from the Upper Cretaceous of the North Sudetic Synclinorium. A–H – Macrofaunal body fossils and trace fossils from the Żerkowice Member. A – Full relief of *Rosarichnoides sudeticus* Chrząstek, Muszer, Solecki, Sroka, 2018 from quarry at fieldtrip stop 4B (Chrząstek et al., 2018). Specimen MGUWr-6650s. B – Full relief of *Thalassinoides paradoxicus* Kennedy, 1967, from the quarry at Żerkowice (ca. 250 m to the north of fieldtrip stop 7; Chrząstek et al., 2018). C – Full relief of *Ophiomorpha nodosa* Lundgren, 1891, in loose block of sandstone at the quarry in Żerkowice (cf. B; Chrząstek and Jewticz, 2019). D – A cast of *Inoceramus* sp. in sandstone of the quarry at fieldtrip stop 4A (Chrząstek et al., 2018). E – Imprints of bivalves *Trigonia glaciana* Stürm, 1901 at bedding surface of sandstone in loose block (quarry at fieldtrip stop 6; Chrząstek and Jewticz, 2019). F – Internal mold of bivalve *Anatina* (*Cercomya*) *lanceolata* Geinitz, 1871–1875 in loose block of sandstone (quarry at fieldtrip stop 6). G – Bivalve shell lag (imprints and internal molds) on a →

in individual tidal bars as ranging from 50 to 66 cm, with a consistent median value of 40 cm. The mean cross-set thicknesses are consistently higher than the median values, which indicates a positively skewed thickness frequency distribution and implies a moderate excess of larger dunes. This is probably an effect of local dune overstepping and thickness amplification (Fig. 13B). The standard deviations of dune cross-set thickness show bar-to-bar differences in the range of 38–69 cm, which is probably an artefact of the derivation of data from different parts of laterally stacked asymmetrical bars.

Based on the approximate equations given by McBride (2003), the maximum bar thicknesses measured in the Żerkowice Member (10–15 m) suggest bar lengths of 12–18 km and widths of 1–1.5 km, with formative water depth of bars at 15–20 m (Fig. 19A). The palaeocurrent data (rose diagram in Fig. 17) are broadly compatible with the flow pattern expected for in-

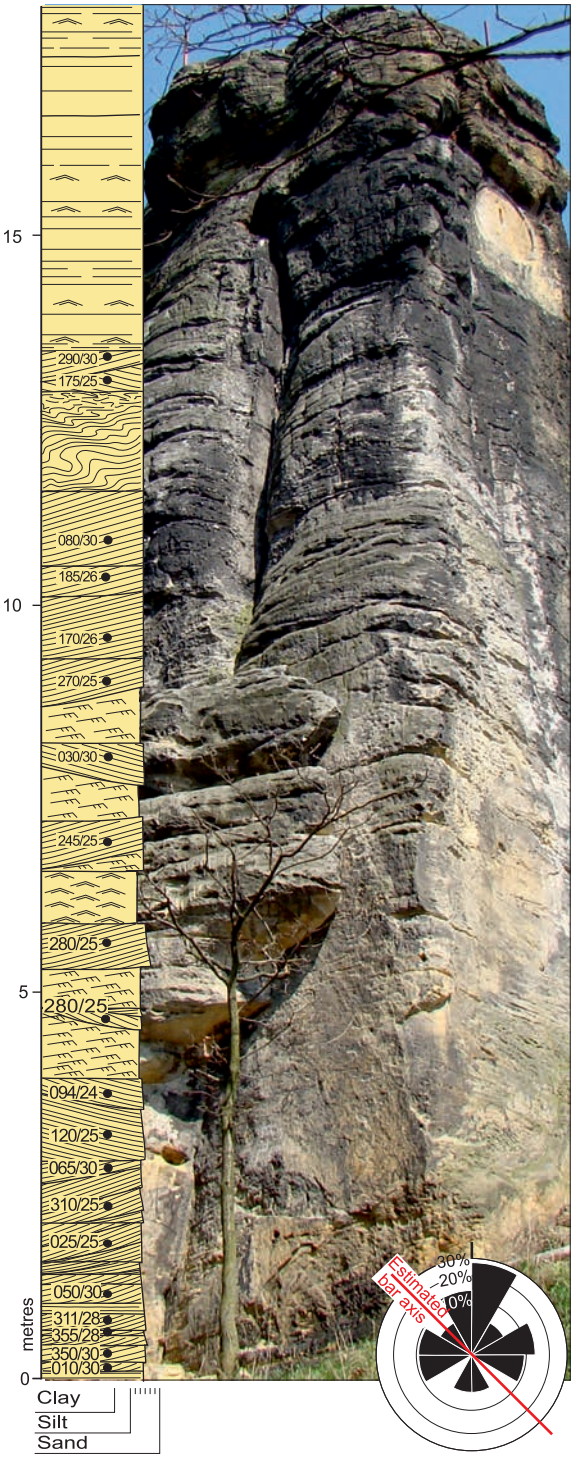

Fig. 17. Succession of vertically stacked dune cross-strata sets of lithofacies Sc with interbeds of current- and wave-ripple cross-laminated lithofacies Sr and SW, increasingly wave worked at the top (lithofacies Sw and Sp). "Skała z Medalionem" tor, fieldtrip stop 7B. The succession is thought to represent a shoaling-upwards bar. The inset rose diagram summarizes cross-strata palaeocurrent directions. From Leszczyński and Nemec (2020).

sandstone bedding plane at fieldtrip stop 6. H – Imprint of the starfish *Lophidiaster scupini* (Andert, 1934), formerly *Astropecten scupini* Andert, 1934, in sandstone (quarry at fieldtrip stop 4B; Chrząstek et al., 2018). I–M – Plant fossils and their assignment to the assemblages distinguished by Halamski et al. (2020). I – Imprint of an isolated leaflet of *Dewalquea haldemiana* Debey ex de Saporta and Marion, 1873. Specimen MB.Pb.2008/320. Rakowice Małe, detailed locality unknown; Nowogrodziec Member, lower part (Assemblage 4), upper Coniacian?–lower Santonian? J – Imprint of a twig of *Geinitzia reichenbachii* (Geinitz, 1842) Hollick and Jeffrey, 1909 (Gymnospermae, Coniferae, family unknown). Specimen MB.Pb.2008/0252. Ołdrzychów, Nowogrodziec Member, upper part (Assemblage 5), upper Coniacian?–lower Santonian? K – Accumulation of imprints of fertile pinnules of *Konijnenburgia* cf. *galleyi* (Miner, 1935) Kvaček and Dašková, 2010 (Filicophyta, Leptosporangiatae, Matoniaceae). Specimen MB.Pb.2008/373.2a. Żerkowice, detailed location unknown; Nowogrodziec Member, lower part (Assemblage 4), upper Coniacian?–lower Santonian? L – Imprint of a trifoliolate leaf of *Dryophyllum westerhausianum* (Richter, 1904) Halamski and Kvaček in Halamski et al., 2020 (Angiospermae, Dictotyledoneae, Fagales). Specimen MB.Pb.2008/346. Ulina, detailed location unknown; Czerna Formation (Assemblage 6), lower–middle Santonian. M – Imprint of a subcomplete compound leaf of *Dewalquea* aff. *gelindenensis* de Saporta and Marion, 1873 (Angiospermae, Dicotyledoneae, Eudicotyledoneae). Bolesławiec (former quarry southeast of the town centre, between Miłosza, Starzyńskiego, and Kosiby Streets). Specimen MGUWr 2880p. Czerna Formation (Assemblage 8), lower–middle Santonian. MB – Museum für Naturkunde, Berlin. MGUWr – Muzeum Geologiczne Uniwersytetu Wrocławskiego, Wrocław. Photographs A – H by A. Chrząstek, I – M by A. Halamski.

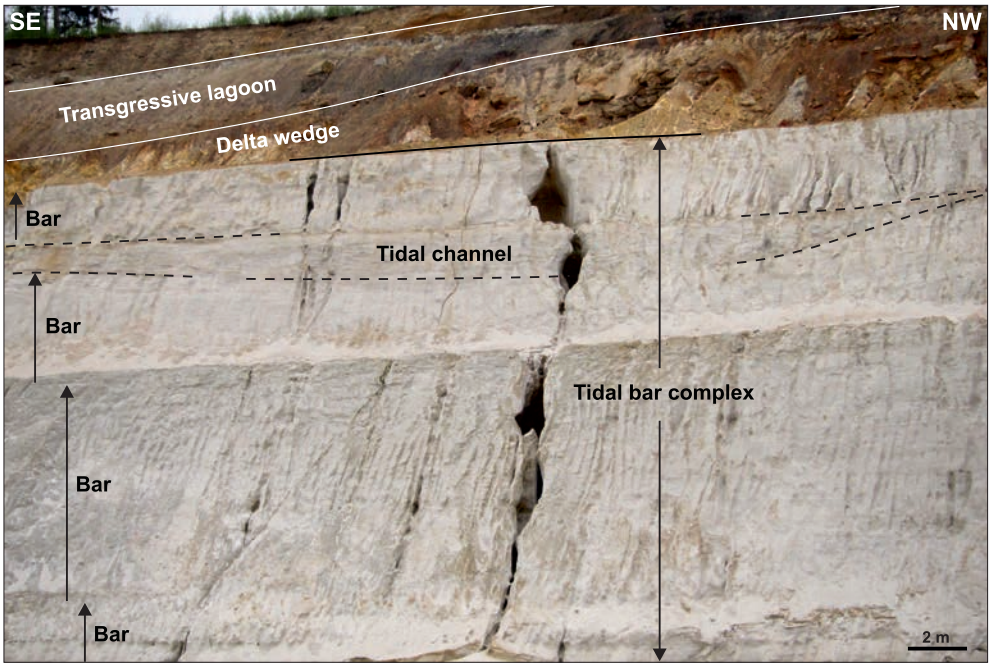

Fig. 18. Portion of outcrop section in active glass sand open pit ca. 2 km west of fieldtrip stop 10 (Fig. 1B). Here, the topmost part of Żerkowice Member comprises a northwest-prograding tidal bar complex with an embedded tidal palaeochannel, overlain by a southwest-advancing basin-margin delta wedge. The overlying basal part of the Czerna Formation consists of transgressive lagoon deposits. From Leszczyński and Nemec (2020).

stantaneous tidal current reversals over a sand ridge (Fig. 19D; cf. Snedden and Dalrymple, 1999; Reynaud et al., 1999), while the lateral and vertical stacking of sand ridges into complexes implies groups of coalescing adjacent coeval bars (Fig. 19C).

The local wedge-shaped sediment assemblages composed of lithofacies Sp, with subordinate intercalations of lithofacies Sr and Sw and sporadic isolated dune cross-sets of lithofacies Sc – which extend from the synclinorium outcrop margins towards its axis, transverse to the inferred tidal sand ridges and effectively interfingering with or onlapping the latter (Figs 20–22) – are interpreted by Leszczyński and Nemec (2020) as basin margin shoal-water deltas (*sensu* Leeder et al. 1988; Postma 1990) or mouth bar-type deltas (*sensu* Dunne and Hempton 1984; Wood and Ethridge 1988). These deltas are dominated by river frictional effluent (lithofacies Sp, Wright, 1966) and fluctuating wave action (lithofacies Sp and Sw; Komar and Miller 1965), with basin-axis tidal current influence (lithofacies Sc; Dalrymple 1984, 2010). The deltaic sandbodies in the Żerkowice Member extend basinwards from both the southwestern (Figs 20, 21) and the northeastern (Figs 22, 23) of the original synclinal basin; near the synclinorium margins, their maximum preserved thicknesses are up to 20 m. Drifted plant fragments are common. Trace fossils are mainly indicative of a shore-proximal expression of the *Cruziana* Ichnofacies (Leszczyński 2018). Advancing deltas apparently impinged sidewise onto the basin-axis tidal bars (Figs 20 to 23). The shore-proximal subaerial parts of the deltas are scarcely preserved, removed by the erosion of the synclinorium flanks (cf. Fig. 22). The outcrop that comes closest to showing a fluvial feeder system is the delta wedge near fieldtrip stop 10 (Fig. 23), where delta-top distributary palaeochannels are recognizable (see the top photograph, Fig. 23), represented by coarser-grained, cross-stratified sandstones (log interval 23–26 m in Fig. 23) and interpreted as fluvial channel-mouth deposits.

The sand wedges with thicknesses of up to 5 m, consisting of gently basinwards inclined (3–5°) deposits of alternating lithofacies Sp and Sw (log interval 6–10 m in Fig. 23; intervals separating tidal bars in log interval 0–20 m in Fig. 23), are interpreted by Leszczyński and

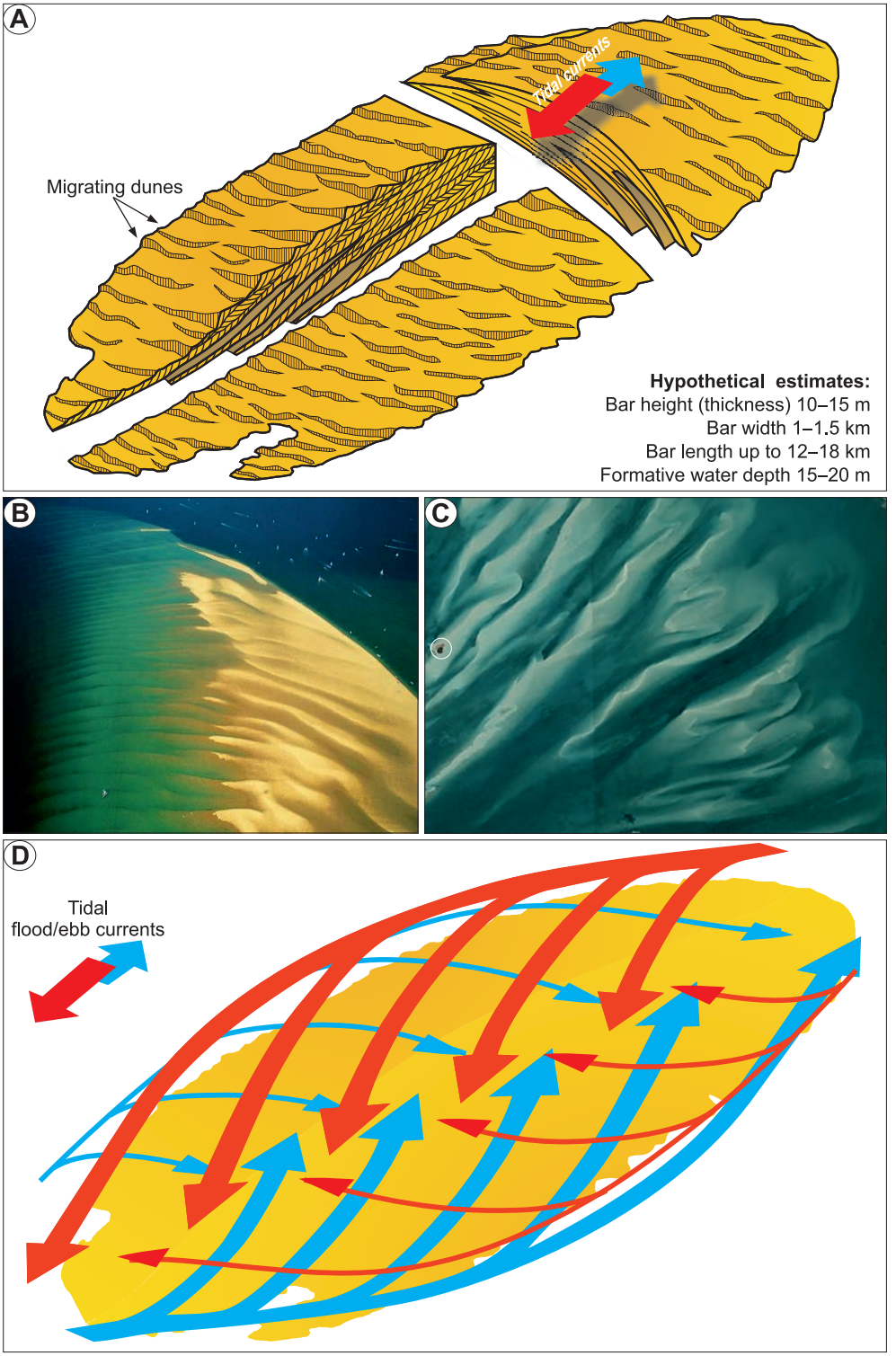

Fig. 19. Longitudinal tidal bar (sand ridge) features and their development. A – Idealized model of a prograding bar with hypothetical estimates of its dimensions and formative water depth pertaining to the Żerkowice Member. B – Modern tidal sand ridge in the southern North Sea; the white spots on the water surface (top right) are wakes of small motorboats. C – An array of coalescing tidal sand ridges, fanning out from a strait in the Bahamas; large cruise ship (encircled) for scale. D – Interpreted pattern of instantaneously reversing tidal currents over a tidal sand ridge inferred from palaeocurrent measurements (e.g., Fig. 17). From Leszczyński and Nemec (2020). Aerial images from Google Earth.

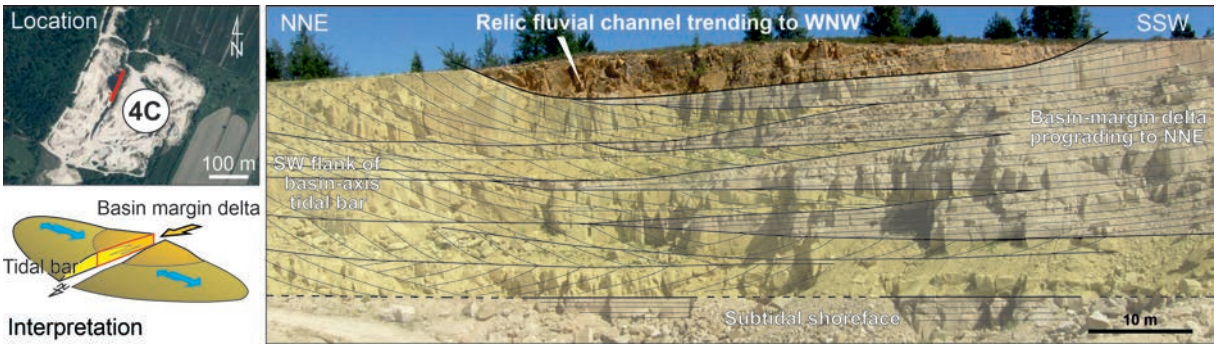

Fig. 20. Outcrop section in the active quarry in Czaple (fieldtrip stop 4C; see Fig. 1B and inset Google Earth image), showing a basin-margin delta interfingering with the southwest flank of a basin-axis tidal sand bar (see inset interpretative diagram). The relic fluvial palaeochannel at the top represents the forced regression that terminated the deposition of the Żerkowice Member. From Leszczyński and Nemec (2020). Photograph by S. Leszczyński.

Fig. 21. Outcrop detail from active quarry in Czaple (fieldtrip stop 4C, Fig. 1B; and inset Google Earth image) from Leszczyński and Nemec (2020), showing a basin-margin shoal-water delta wedge onlapping the southwest flank of basin-axis longitudinal tidal bar. Photograph by S. Leszczyński.

Nemec (2020) as wave-dominated upper shoreface deposits (Komar and Miller, 1965; Clifton and Dingler, 1984) that prograded from both sides of the basin jointly with the basin-margin local river deltas. The sediments commonly display subtle angular unconformities in the form of planar erosional surfaces. The plane-parallel stratification in some units of lithofacies Sp is as steep as 10–15° (Fig. 11F), showing heavy-mineral placers (Fig. 11E) and primary current lineation (Fig. 11J). The sand is nearly pure quartz, very well sorted and poorly cemented. Trace fossils are uncommon, and those present represent an environmentally stressed version of the *Skolithos* Ichnofacies (Leszczyński 2018). Internal planar unconformities are attributed to episodic erosion by storm waves. The advancing shoreface deposits locally interfinger with basin-axis tidal bars (Fig. 23). The more steeply inclined packages of lithofacies Sp, with heavy-mineral placers and parting lineation, are interpreted as fore-

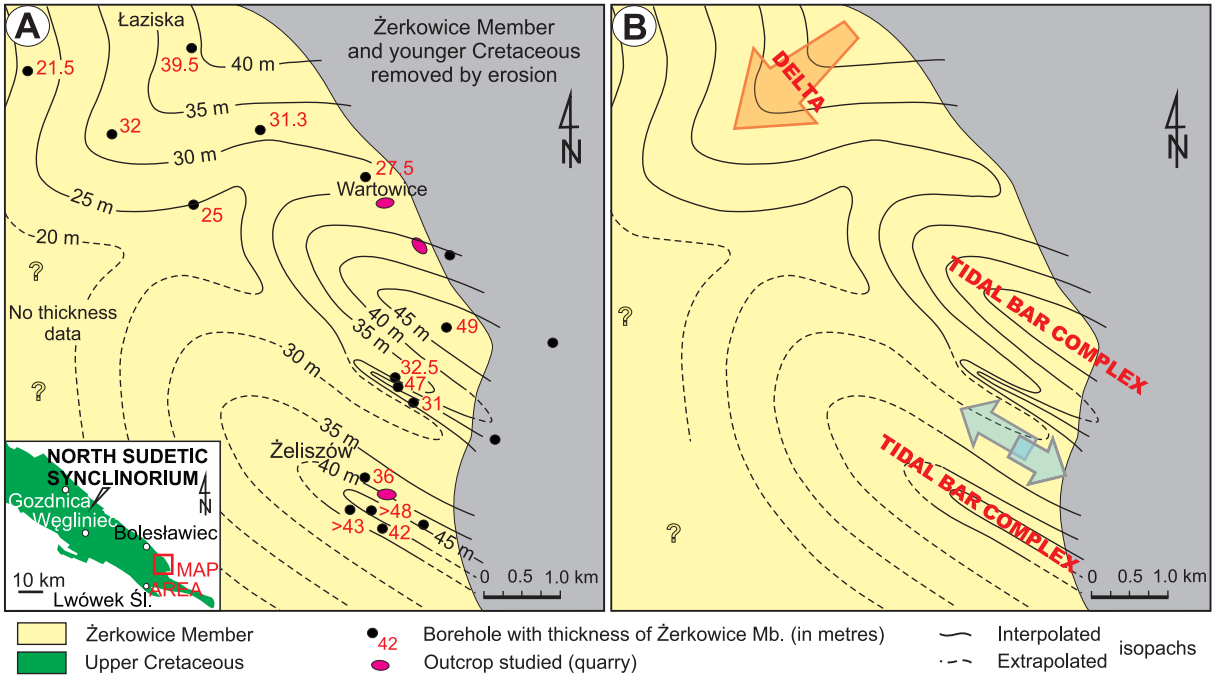

Fig. 22. A – Local sandstone isopach map of the Żerkowice Member (area indicated in the inset map) with the location of boreholes and quarries in Wartowice (fieldtrip stop 5) and Żeliszów (fieldtrip stop 6); see localities in Fig. 1B. Borehole data from Drozdowski et al. (1978). B – Interpretation of the isopach map as a basin-margin delta that interfered with northwest-prograding tidal bar complexes. Note the large extent of basin-fill erosion due to the end-Cretaceous tectonic inversion of the basin. From Leszczyński and Nemec (2020).

shore swash deposits (Allen 1982), implying local encroachment of the basin shoreline (e.g., Fig. 23, log interval 9.5–10 m).

The Czerna Formation

The Czerna Formation begins with a prominent mudstone distinguished by Leszczyński and Nemec (2020; Figs 10, 23–25). It forms units up to a few metres thick, ranging in colour from maroon and orange, with ferricrete (ironstone) concretions or bands up to 5 cm thick, to greenish and dark grey with local siderite interlayers up to 6 cm thick. Some mudstone units are densely interspersed with sand and/or silt streaks and thin interlayers, forming the heterolithic lithofacies H that is often strongly bioturbated and occurs as units up to a few metres thick (Figs 23B, 26K–O). The mudstones are also intercalated with claystone lithofacies CL (Figs 23B, 26J) that forms 0.1–1.2 m thick units, ranging in colour from maroon and orange with clayey ironstone interlayers to greenish and dark grey or subordinately black (coaly). Another new facies are the coal beds of lithofacies C, up to 25 cm thick and ranging from autochthonous, underlain by seat-earth, to hypautochthonous (Figs 23D, 25, 26D). Fine-grained, ripple cross-laminated sandstone beds of lithofacies Sr and Sw, 10–25 cm thick, occur as sheet-like intercalations in lithofacies H or are overlain by the planar parallel-stratified sandstones of lithofacies Sp as upwards coarsening couplets 0.5–2 m thick (Figs 23A, 25, 26E, F). Many sandstone beds are variably homogenized by bioturbation. The cross-stratified sandstones of lithofacies Sc are commonly medium- to coarse-grained, with an admixture of granules and small pebbles. This lithofacies occurs solely as the infill of local palaeochannels, each a few metres deep and less than 100 m wide, trending to the northwest and dominated by trough (3D dune) cross-stratification (Figs 25, top, 26G).

Trace fossils abound, including rhizoliths, rhizocretions (Fig. 26A), and densely plant root-penetrated palaeosols (Fig. 26B, C), classified as vertisol to histosol (cf. Retallack 2001). Only some of the palaeosol horizons are actual seat-earths to coal beds (Fig. 25). Common

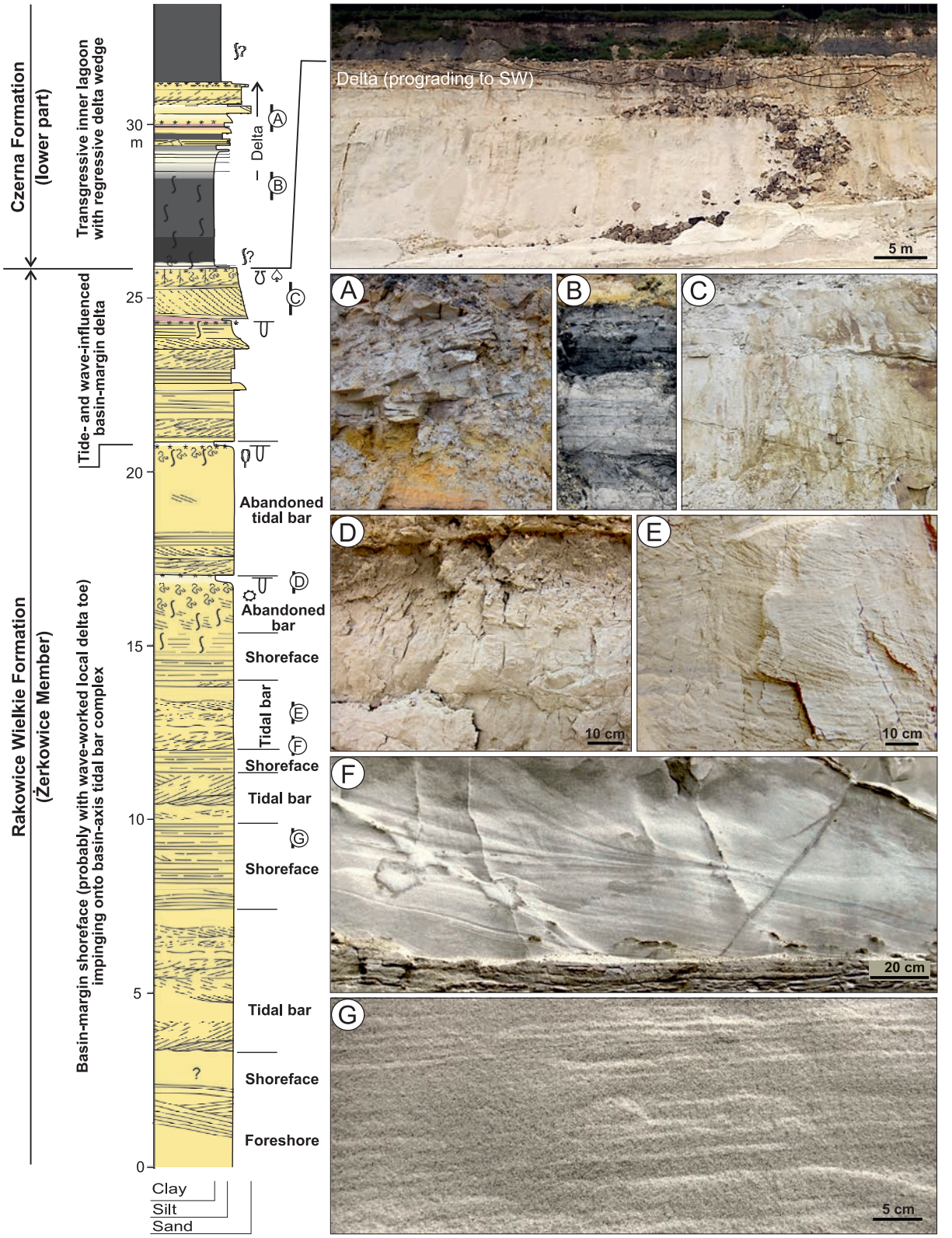

Fig. 23. Sedimentological log and corresponding outcrop photograph (top) of the upper part of Żerkowice Member and the lowermost Czerna Formation in the glass sand pit at Osiecznica (~2 km west of fieldtrip stop 10, Fig. 1B). From Leszczyński and Nemec (2020). Note the basin-margin delta wedge impinged sidewise onto the basin-axis tidal system at the top of the →

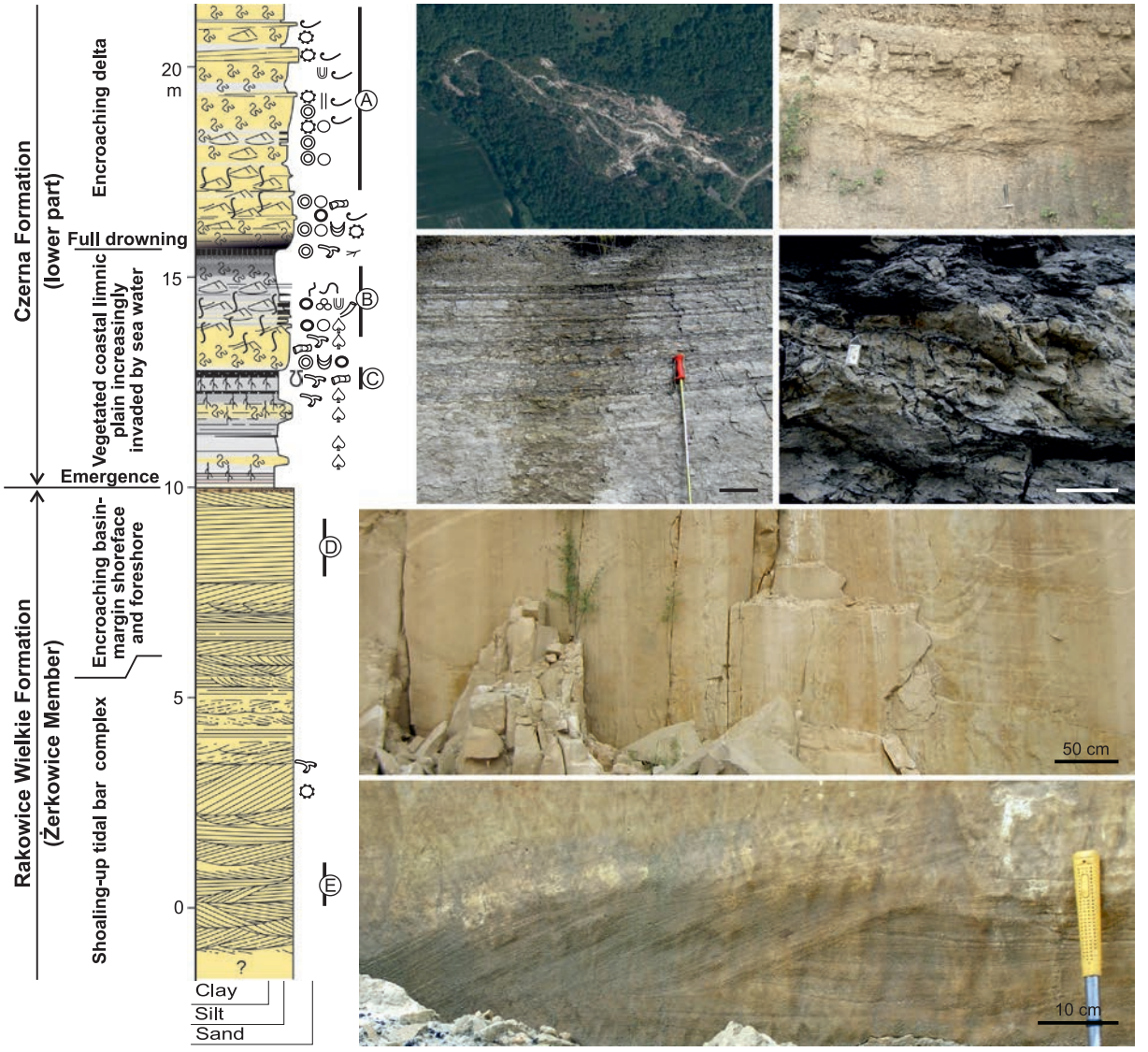

Fig. 24. Sedimentological log of the uppermost Żerkowice Member and lower Czerna Formation at the Rakowiczki quarry (fieldtrip stop 8, Fig. 1B), from Leszczyński and Nemec (2020). The tidal sand bar complex here was covered by a regressive sandy wedge of basin-margin shoreface to foreshore deposits prior to emergence. The overlying paralic deposits indicate gradual marine inundation and eventual full flooding, followed by encroachment of a basin-margin wedge of prodelta deposits. For log legend, see Fig. 12. Outcrop details (indicated at the log margin and in the inset Google Earth image). A – Coarsening-upwards packages of bioturbated progradational prodelta deposits of lithofacies Sr. B – Thin-bedded, bioturbated lagoonal deposits of lithofacies H. C – Paludal deposits of lithofacies M with horizons of plant-root traces and brackish marine burrows in the coal bed. D – Wave-worked upper shoreface sandstone of planar parallel-stratified lithofacies Sp. E – Dune cross-stratified sandstone of lithofacies Sc. All photographs by S. Leszczyński.

Żerkowice Member and the overlying transgressive lagoon deposits of the basal Czerna Formation, split by the minor delta re-advance. For log legend, see Fig. 12. Outcrop details (indicated at the log margin): A – Sandy mouth bar of the coarsening-upwards minor deltaic wedge. B – Muddy lagoonal deposits directly below deltaic wedge. C – Sandy mouth bar of the main delta wedge. D – Bioturbated top of quasi-abandoned tidal bar. E – Bidirectional dune cross-stratification in tidal bar. F – Gently northwest-descending tangential cross-strata sets in lower part of prograding tidal bar. G – Plane-parallel stratification in wave-worked upper part of tidal bar. All photographs by S. Leszczyński.

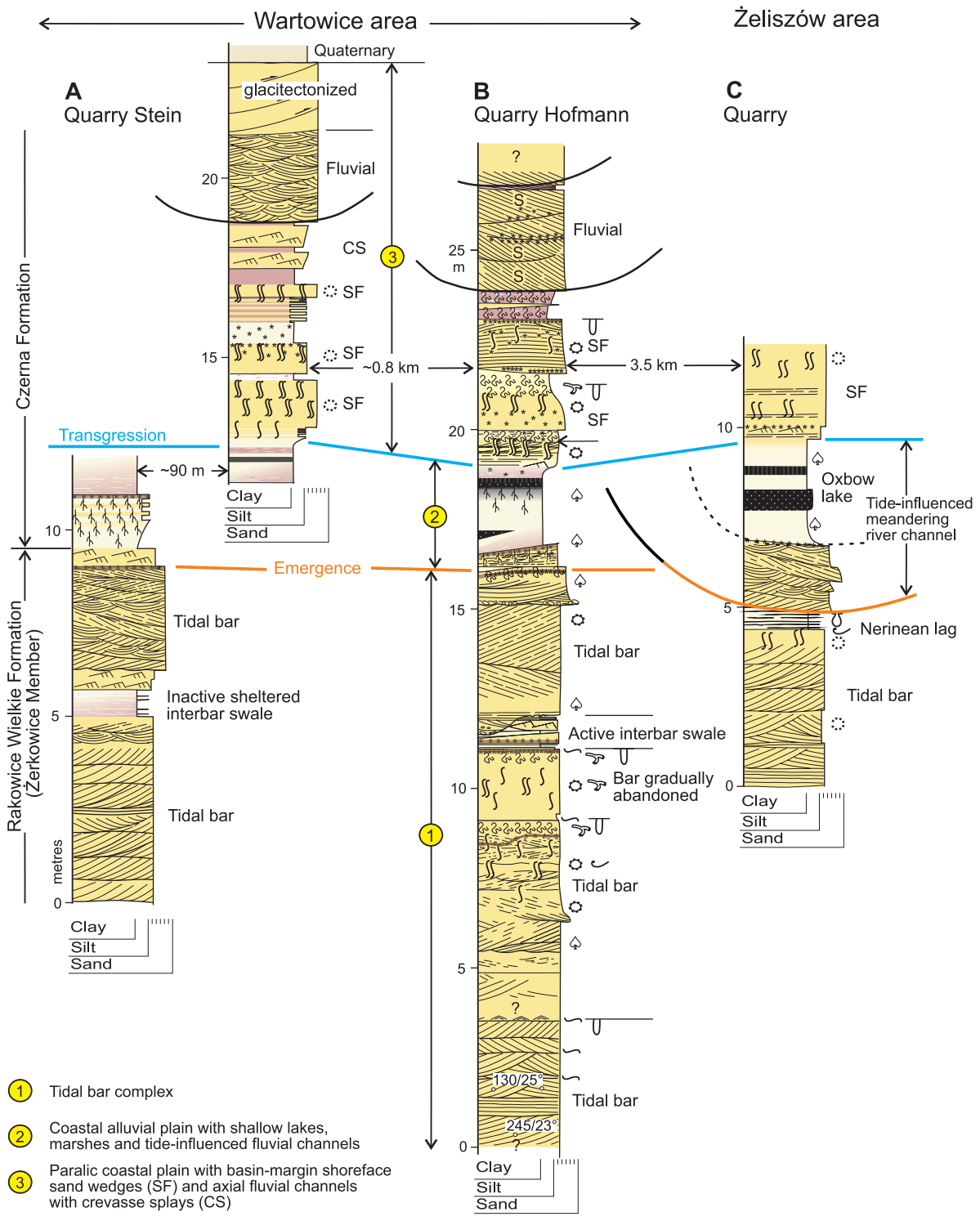

Fig. 25. Sedimentological logs from quarries at fieldtrip stops 5C (A), 5A (B) and 6 (C) (see Fig. 1B), showing the upward passage of the Żerkowice Member of the Rakowice Wielkie Formation to the Czerna Formation. From Leszczyński and Nemec (2020). Note that the deposition of Żerkowice Member was terminated by emergence, with the tide-influenced fluvial palaeochannel probably a time-equivalent of the fluvial palaeochannel at fieldtrip stop 4 (Fig. 20). The deposition of the Czerna Formation in this area commenced in a peat-forming coastal-plain environment, which was eventually flooded by marine transgression. The subsequent highstand normal regression involved rapid advances of the basin-margin shoreface, culminating in the expansion of a basin-margin fluvio-deltaic system.

animal traces include *Ophiomorpha* (Fig. 26I), *Palaeophycus* (Fig. 26L), *Arenicolites* (Fig. 26M), *Thalassinoides* and *Asterosoma* (Fig. 26N). Leszczyński (2010, 2018) reported in detail the rich ichnofauna assemblages in the quarry associated with fieldtrip stop 8 (Fig. 1B), while pointing to the sparse bioturbation at some other localities, such as the rare, taxonomically undetermined ichnofossils at the glass sand pit in Osiecznica (ca. 2 km west of fieldtrip stop 10; Figs 1B and 23). Leszczyński (2010) also reported on scattered mollusc shells, some buried in life position, and on shell lags preserved solely as imprints. Sporadic horizons with brackish-water bivalve and gastropod shells were described earlier by Drescher (1863) and Milewicz (1965, 1996).

The sedimentary succession of the Czerna Formation, which roughly corresponds to that distinguished as the *Überquader* by Beyrich (1855), rests upon the Rakowice Wielkie Formation in the southeastern part of the NSS, with a stratigraphic hiatus (Fig. 3) composed of an erosional unconformity that decreases in duration to the northwest along the basin axis and passes seawards into a correlative conformity (Milewicz 1956, 1969; Walaszczyk 2008). This erosional boundary demarcates a dramatic change in the sedimentary facies and depositional environment of the Coniacian North Sudetic Basin (Figs 3 and 23–25).

The lower boundary of the Czerna Formation, a subaerial unconformity surface, is locally incised by northwest-trending isolated fluvial palaeochannels filled with lithofacies Sc (Fig. 20), some tidally-influenced before abandonment (Fig. 25C). These palaeochannels are interpreted as representing an incised fluvial drainage system directed along the basin axis towards the northwest and frontally influenced by marine tides. The incision of fluvial channels directly in littoral deposits (Figs 20 and 21C) strongly supports the idea of a forced marine regression (Leszczyński and Nemec 2020).

The overlying sedimentary succession of the Czerna Formation commences with a widespread unit of fined-grained deposits, 2–5 m thick, dominated by lithofacies M, CL, and H with subordinate intercalations of sandstone lithofacies Sr and autochthonous or hypautochthonous coal beds of lithofacies C (Figs 23–25; fieldtrip stops 5, 6, 8). Brackish shelly fauna and ichnofauna accompany palaeosols and accumulations of plant debris in this unit, locally even directly at its base and within the same depositional bed. This unit of coal-bearing muddy deposits is presumably the poorly defined Nowogrodziec Member of Milewicz (1985) (Fig. 3).

The short-distance lateral variation in the thickness of this unit and the relative proportion of its component lithofacies is noteworthy (cf. Figs 23–25; Leszczyński and Nemec 2020). In the glass sand pit 2 km west of fieldtrip stop 10, this muddy unit is at least 9 m thick and split in the middle by a coarsening-upwards sandstone wedge, 2–4 m thick, composed of lithofacies Sr, Sp, and Sc (Fig. 23, top). The nearby boreholes N-14 and N-26 (Fig. 10; see Leszczyński and Nemec 2020) show that the unit pinches out abruptly towards the northwest by interfingering with a coeval, few dozen metre thick prominent sandbody that rests directly on the sandstones of the Żerkowice Member. This thick sandstone body, earlier considered to be part of the Żerkowice Member, is interpreted by Leszczyński and Nemec (2020) as an integral part of the lowermost Czerna Formation (see below).

According to Leszczyński and Nemec (2020), the coal-bearing muddy basal unit of the Czerna Formation (i.e., the Nowogrodziec Member of Milewicz, 1985), with its brackish/marine fauna, represents a paralic environment comprising extensive shallow lakes with peat-forming mires and small stream deltas. The thick, muddy deposits at the glass sand pit in Osiecznica (near fieldtrip stop 10; Fig. 23, top) are considered to represent a transgressive lagoon intruded sidewise by a southwest-prograding basin-margin sandy delta wedge. The lagoon was apparently sheltered from the open sea by the thick and narrow sandbody mentioned above and recognized in boreholes N-14 and N-26 (Fig. 10), interpreted by Leszczyński and Nemec (2020) as a cross-basinal transgressive coastal sand barrier. The formation and in-place growth of this barrier would have blocked the earlier fluvial drainage of the emerged southeastern part of the basin and turned this area into a peat-forming paralic lacustrine plain with local stream deltas. The eventual in-place drowning of the barrier (cf. Sanders and Kumar 1965; Rampino and Sanders 1981) would then bring about another change to the basin environment.

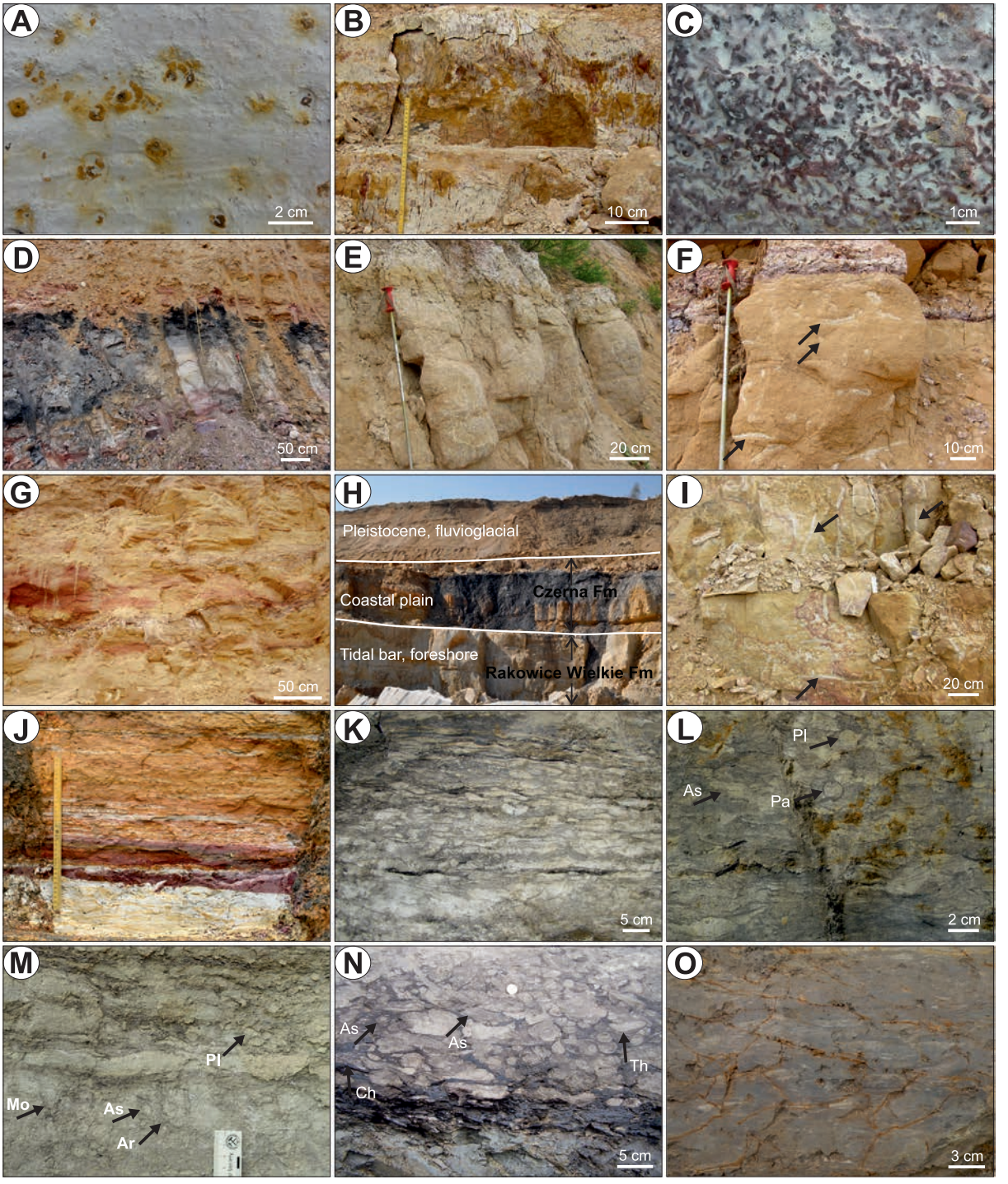

Fig. 26. Lithofacies and ichnofauna of the lower Czerna Formation according to Leszczyński and Nemec (2020). A – Rhizocretions, and in B, C – denser plant-root penetration structures at the formation base at fieldtrip stop 5A (cf. Fig. 25A). D – Dark-grey claystone of lithofacies CL overlain by autochthonous coal of lithofacies C in the basal part of the formation at fieldtrip stop 5A (Fig. 25B). E, F – The overlying shoreface lithofacies Sp at fieldtrip stop 5A (Fig. 25B), showing a variable degree of bioturbation with Ophiomorpha (two fragments are indicated by arrows). G – Cross-stratified fluvial sandstone of lithofacies Sc in the top part of outcrop at the same locality (Fig. 25B). H – Tidally influenced fluvial palaeochannel incised in the underlying formation at fieldtrip stop 6 (Fig. 25C). I – Ophiomorpha burrows (three cases indicated by arrows) in shoreface lithofacies Sp in the uppermost part of outcrop at fieldtrip stop 6 (Fig. 25C). J – Light-grey to reddish claystone with ferricrete (lithofacies CL) passing upwards into iron oxyhydroxide-stained yellowish mudstone (lithofacies M) in the basal part of the formation at fieldtrip stop 8. →

The overlying deposits – ca. 10 m thick (Figs 23–25), in the lower part of the Czerna Formation, consisting of muddy heterolithic lithofacies H intercalated with sheets of sandstone lithofacies Sr, Sp and minor Sw forming coarsening-upwards or sporadically fining-upwards packages, 0.5–1.5 m thick (Figs 23, 25) and variably bioturbated – are thought to represent a marine offshore-transition environment that underwent rapid shallowing by the spasmodic encroachment of basin-margin shoreface and prodelta sand wedges (Leszczyński and Nemec, 2020). The uppermost exposed cross-stratified deposits (lithofacies Sc; Fig. 25, top) are interpreted to be laterally and vertically stacked palaeochannels, 3–4 m deep and 100–120 m wide. These channels record the shallowing of the marine environment and expansion of the basin-margin alluvial plain with small shoal-water deltas, fluvial channels, and associated crevasse-splays (Fig. 25, top).

The remaining, major part of the Czerna Formation, up to 500 m thick, is almost exclusively comprised of siliciclastic deposits, predominantly sandy (from nearly loose sands to sandstones), muddy, and clayey (partly plastic), subordinately gravely, with thin intercalations of coal, ironstone, and siderite (Scupin 1913; Milewicz 1996). The relative proportion of the individual lithologies, their features, and their vertical arrangement vary both laterally and vertically in the sedimentary succession. Its lower part consists mainly of grey to dark grey fine-grained deposits, locally with red-brown or cherry colouration and with frequent thin xylite-rich coal interlayers (Górniak 1991), coalified wood fragments, and numerous mollusc fossils. In the upper part, the fine-grained deposits show lighter colouration, mostly light grey to whitish towards the top, and lack fossil fauna (Górniak 1991). The fine-grained sediments contain predominantly detrital-like kaolinite and up to 20% mica group minerals (illite, muscovite; Górniak 1991, 1996).

The sandy and gravelly sediments in the Czerna Formation (Fig. 27, fieldtrip stop 9; Górniak 1991) are whitish, drab to cream-yellow, locally orange, brown or cherry red in colour. Sandstones are mainly fine- to medium-grained, quartzose, with kaolinite matrix and cement. Weathered feldspars, micas, halloysite-goethite-hematite-siliceous impregnation (ironstone, ferruginous silcrete), and coalified plant remains (leaf fragments, wood; Górniak 1996) are present as accessorary constituents. The sandstones occur as thin to several metre thick beds, massive (structureless) or with planar or cross-stratification, plant-root horizons, and casts or molds of fossil fauna (Górniak 1991; Milewicz 1996). Pebble admixtures and thin pebbly conglomerate layers/lenses occur in the basal parts of sandy trough cross-strata sets, particularly in the uppermost preserved part of the Czerna Formation (fieldtrip stop 9; Fig. 27; Górniak 1991).

In the Santonian, coarse-grained sediments (mainly sandstone or sands) prevail in the eastern part of the NSS (see Górniak 1996, fig. 1). Towards the west and northwest, they form two leading divisions – one in the lower part of the Santonian succession and the other at the top (Milewicz 2006). These divisions are separated by a wedge of almost exclusively fine-grained, dark coloured, muddy and clayey sediments, poorly calcareous to non-calcareous, defining the Węgliniec Formation. The thickness of this fine-grained wedge grows to the northwest, associated with the wedging out of the lower coarser-grained division. The thickness of the upper coarser-grained division grows towards the basin centre and further decreases towards the northwest, ultimately pinching-out (Milewicz, 2006). Fossil fauna, almost exclusively brackish molluscs (bivalves and gastropods, e.g., *Cucullaea zimmermanni* Andert, *Cyrena lischkei* Andert, *Cytherea kruschi* Andert, *Ceromya cretacea* Müller, *Natica geinitzi* Holzapf, *Mytilus rackwitzensis* Scupin, *Cerithium dressleri* Scupin, *Turitella acanthophora* Müller; see Williger 1882; Milewicz 1996 and references therein), occur in the lower coarser-grained division and in the lower part of the overlying fine-grained wedge.

K–M – Lagoonal heterolithic deposits of lithofacies H, highly to totally bioturbated, enclosing ichnogenera *Arenicolites* (Ar), *Asterosoma* (As), *Monocraterion*? (Mo), and Palaeophycus (Pa) at fieldtrip stop 8. N – Prodelta heterolithic sediments of lithofacies H, highly bioturbated, including ichnogenera *Asterosoma* (As), *Chondrites* (Ch) and Thalassinoides (Th) at fieldtrip stop 8. O – Offshore-transition lithofacies H with interlayers of fine-sand lithofacies Sw heavily obliterated by bioturbation at fieldtrip stop 8. Fieldtrip stop numbers as in Fig. 1B. Photographs A–G and I–O by S. Leszczyński, and H by A. Chrząstek.

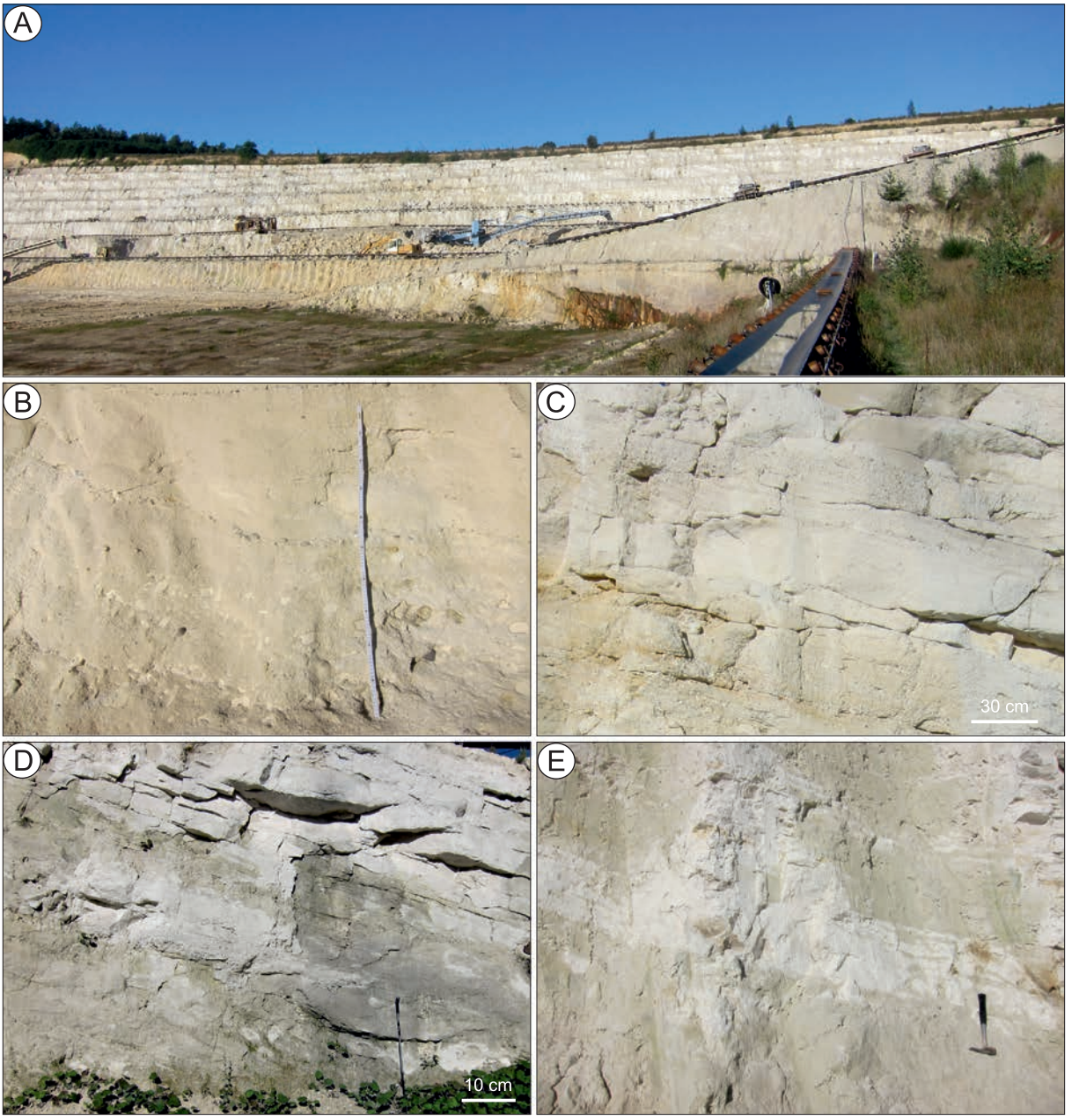

Fig. 27. The Czerna Formation in the kaolin open pit of the Kopalnie Surowców Mineralnych Surmin-Kaolin S.A. in Nowogrodziec (fieldtrip stop 9, Fig. 1B). A – general view of the western pit wall. Note the homoclinal dipping of the sedimentary succession to the right (northeast) B – Agglomeration of claystone intraclasts, small quartz pebble stringers and crudely stratified coarse-grained sandstone of a channel fill. C – Conglomerate of quartz pebbles and claystone intraclasts (cream-yellow) overlain by high-angle and low-angle cross-stratified fine sandy conglomerate. D – Package of lenses, irregular bodies and tabular beds of small-pebble conglomerate, sandstone and siltstone; the walking stick (scale) is 1 m. E – Plane-parallel stratified siltstone with fine-grained sandstone stringers and thin layers; the hammer (scale) is 35 cm. All photographs by S. Leszczyński.

The lithofacies are indicative of a marine to terrestrial, generally deltaic and prodeltaic origin of these deposits. The coarse-grained divisions are delta-front deposits, while the others represent delta-plain palaeochannels and inter-channel zones with swamps and ponds (Williger 1882; Scupin 1913; Milewicz 1996, 2006; Górniak 1991, 1996).

Rich kaolinite occurrences in both fine-grained and sandy sediments render them an

important raw material for the ceramics industry; indeed, the kaolin has been exploited for several centuries.

PALAEOBOTANY

The Upper Cretaceous of the NSS has yielded a moderately diverse fossil flora (Fig. 16I–M) that has only recently received a modern comprehensive analysis. The megaflora, microflora, and palaeoecology were treated by Halamski et al. (2020). Fern tree stem casts were described by Greguš et al. (2013) and the mesoflora by Heřmanová et al. (2019, 2020). An exceptional specimen of an angiosperm leaf overgrown by marine bryozoans was described by Halamski and Taylor (2022). The historical aspects of collections were discussed by Mohr (2009), whereas short overviews of all Polish Cretaceous palaeofloras, including extensive reference lists, may be found in Halamski (2020) and Barbacka et al. (in press).

The Late Cretaceous palaeoflora from the NSS, like others from Central and Northern Europe, is preserved in marine and marginal marine strata, which means the plant remains were washed out from land and are dispersed within the sections. No "plant beds" have been found. From a methodological point of view, this means the systematic revision of megafloras is conducted mostly on the basis of ancient collections, assembled over many years when numerous small local quarries were active. In contrast, the biostratigraphy, taphonomy, mesoflora, and microflora are studied based on new observations and newly collected material.

The palaeoflora of the North Sudetic Basin is composed of 29 megafloral taxa, 9 mesofloral taxa, and >126 microfloral taxa (Halamski et al. 2020; Heřmanová et al. 2020). It is worth mentioning that the microflora from strata overlying the Nowogrodziec Member (*sensu* Milewicz 1985; Fig. 3) was studied for decades by the Polish palaeobotanist Jadwiga Raniecka-Bobrowska, but her voluminous memoir (with several hundred taxa) unfortunately remains at a preliminary stage and unpublished. Moreover, the exact location and stratigraphy of boreholes from which the palynomorphs were extracted remains unclear.

The mega- and mesoflora are dominated by angiosperms, while the most common microfloral elements are ferns. The plant palaeocommunities may thus be interpreted as generally intermediate between those pre-dating the Cretaceous Terrestrial Revolution and modern, angiosperm-dominated vegetation (Halamski et al. 2020).

The megaflora was grouped by Halamski et al. (2020) into eight assemblages, consisting of localities grouped by their similar stratigraphy and floral content. Assemblages 1–3 belong to the Rakowice Wielkie Formation, Assemblages 4 and 5 to the Nowogrodziec Member of the Czerna Formation, and Assemblages 6–8 to the part of the Czerna Formation overlying the Nowogrodziec Member. Assemblage 3 contains fern tree stems preserved as casts (Greguš et al. 2013). Assemblage 6 (sandstones of the higher Czerna Formation) contains mainly the fagalean angiosperm *Dryophyllum westerhausianum*. Assemblage 8 (ceramic clays in the Bolesławiec area and other localities) is relatively diversified, including, in particular, the trifoliolate platanoid *Platanites willigeri*. Further descriptions of Assembleges 4 and 5 are provided below.

Plant palaeocommunities interpreted on the basis of the fossil mega-, meso- and microflora to have grown on the East Sudetic Islands include: (i) back-swamp forests dominated by the conifer *Geinitzia*, with ferns; (ii) several varieties of angiosperm-dominated riparian and alluvial-plain forests with *Dryophyllum* and platanoids; (iii) fern savanna with patches of *Pinus* woodlands; (iv) dunes; (v) halophytic vegetation (mangroves) with *Frenelopsis*: a single grain of *Spinizonocolpites* sp. suggests *Nypa* is a part of this community, but requires confirmation; and (vi) pioneer vegetation with lycophytes and ferns (Halamski et al. 2020).

Finally, it should be mentioned that the palaeobiogeographic patterns identified on the basis of fossil flora are in striking contrast to those based on palaeofauna (Csiki-Sava et al. 2015). While faunal reconstructions indicate the Cretaceous European Archipelago was a highly endemic zone, with strong differentiation among individual islands, the plant cover of the same area and interval is mainly comprised of widely distributed species, some of which were similar or possibly identical to those found in North America.

DEVELOPMENT OF SEDIMENTATION

Palaeontological data collected over nearly two centuries indicate that Cretaceous sedimentation in the North Sudetic Basin commenced in the Cenomanian and proceeded until at least the middle Santonian (Walaszczyk 2008). Scupin (1910) suggested that the basin, which he referred to as the *Löwenberger Becken*, was situated between two elevated island areas: one to the northeast, which he called the *Ostsudetische Landmasse* (East Sudetic Landmass), and the other to the southwest named the *Riesengebirgsinsel* (West Sudetic Island; Fig. 2A). The notion that the Late Cretaceous basin lied between two Sudetic landmasses was supported by Andert (1934), although he postulated that the East Sudetic Landmass was much smaller, limited only to an area in the southeastern part of that suggested by Scupin. Recently, two islands have been shown to exist both southwest and northeast of the North Sudetic Basin, and in its southeastern prolongation (Wilmsen et al. 2014; Kowalski 2021). It is generally accepted that the size and relief of the islands changed during their existence (Scupin 1936), due to the influence of eustasy and Alpine tectonism. Therefore, the exact location of the basin coastlines remains a subject of controversy (Biernacka and Józefiak 2009; Biernacka 2012). It is worth noting that Scupin (1913) correctly recognized the northwesterly transition of sandy deposits into mudstones and marlstones (cf. Fig. 3) as the longitudinal direction of bathymetric deepening of the basin.

According to Leszczyński (2018), the two islands mentioned above existed as separate landmasses until the middle Coniacian (Fig. 28A, B). The mid-Coniacian forced regression resulted in a retreat of the sea to the northwest, which merged the two islands and drove the formation of an erosional hiatus in the southeastern part of the basin (Milewicz 1956; Figs 3 and 28B, C). Consequently, the late Coniacian transgression occurred in an embayment open to the northwest, ca. 35 km long and 15 km wide (Leszczyński 2018; Fig. 28D–F), with sedimentation persisting until the final retreat of the sea around the middle Santonian or later.

Palaeogeographic reconstructions suggest that the North Sudetic Basin, in its southern prolongation, had at least two narrow linking straits: one near the town of Złotoryja (which closed in the mid-Coniacian) and another preserved as a relic in the Wleń Graben (Fig. 1B; Kowalski 2021). The latter author has suggested that marine sedimentation in the Wleń strait persisted long after the mid-Coniacian closure of the Złotoryja strait. However, this opinion is questionable, because the youngest Cretaceous deposits in the Wleń Graben are poorly dated and, given their carbonate content, seem to correspond to those documented as predating the mid-Coniacian regression in other areas of the NSS; hence, they may be older than the Żerkowice Member in the excursion area (Fig. 3).

According to Leszczyński and Nemec (2020), the Cretaceous North Sudetic Basin formed as an early, synclinal side effect of the Alpine orogeny, in combination with eustatic forces; crucial stages of basin evolution occurred in the Coniacian. In the early Coniacian, the basin was a long and narrow shallow-marine embayment with the hypothetical (non-preserved) Złotoryja bayhead strait funnelling tidal currents. Input from Wleń strait is unrecognizable in the basin – additionally, the the timespan of this strait's activity is uncertain. Coalescing tidal sand ridges extending from the Złotoryja strait formed a littoral platform that prograded from the bayhead zone along the basin axis, laterally impinged on by the basin-margin shoreface and local river deltas. A mid-Coniacian forced marine regression and closure of the bayhead strait, attributed to Alpine tectonism combined with eustasy, brought about a dramatic change in the ba-

Fig. 28. Schematic interpretative reconstruction of the Coniacian palaeogeography and sedimentation pattern in the inner, southeastern part of the North Sudetic Basin; after Leszczyński and Nemec (2020). A – The littoral system of coalescing tidal sand ridges of the Żerkowice Member (Fig. 3) progrades to the northwest, impinged on laterally by the basin-margin nearshore and deltaic sandy systems. B – This tide-driven littoral sand platform reaches its maximum basinward extent, terminated by the closure of the basin bayhead tidal strait and a forced marine regression. C – The emerged former littoral sand platform is denudated and incised by river channels, with the coastal area of paralic sedimentation shrinking basinwards; this stage of development marks the top of the Żerkowice Member. D – The onset of subsequent eustatic sea-level rise creates a transgressive, aggrading coastal sand barrier at the outer edge of the former littoral sand platform, with a barrier-sheltered →

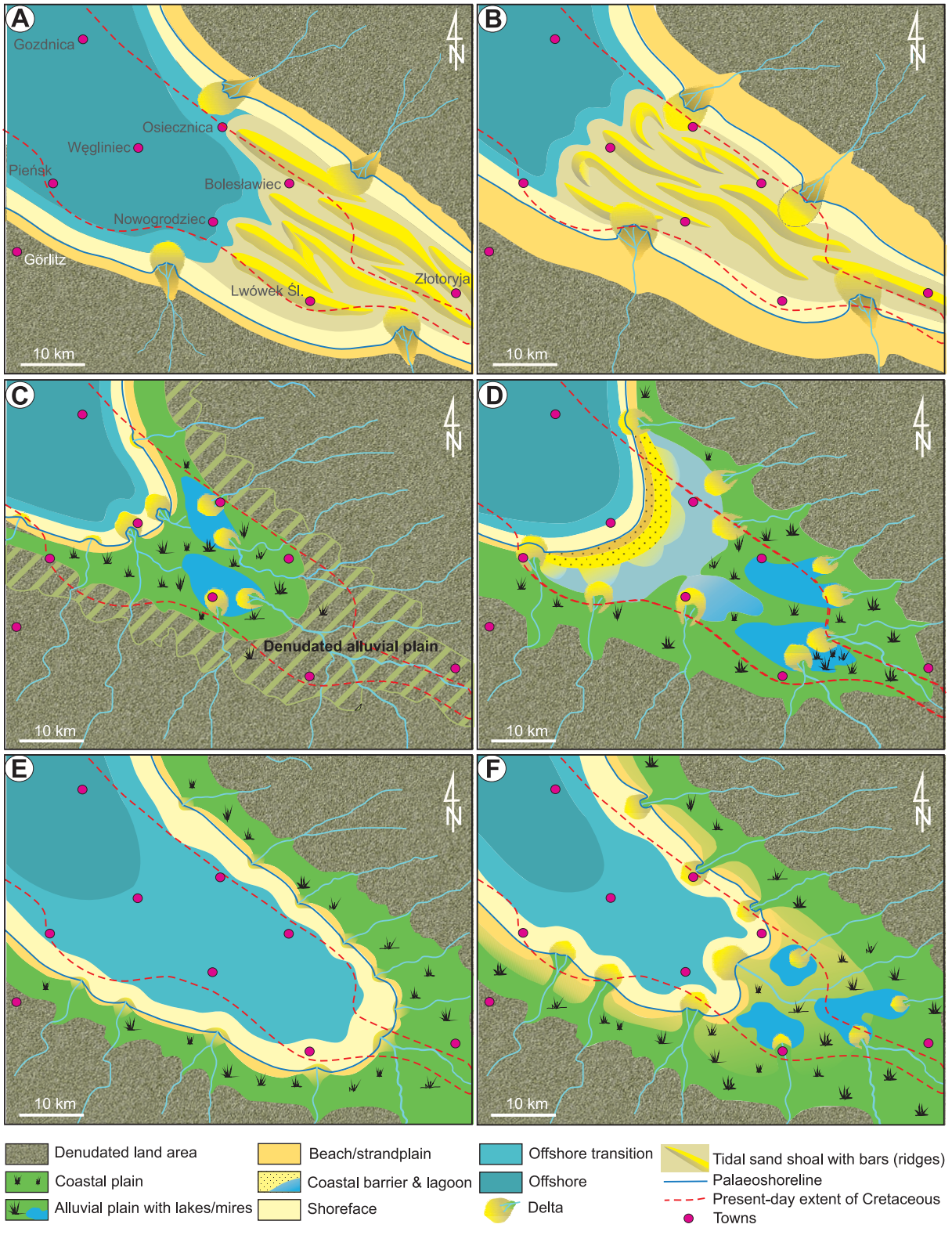

lagoonal to paralic bayhead alluvial plain. E – The aggrading coastal sand barrier is eventually drowned by the sea, whereby the bayhead paralic plain briefly becomes an offshore-transition marine zone. F – The rebounding sediment yield from the elevated margins of the basin causes rapid shallowing by the lateral encroachment of nearshore and fluvio-deltaic systems; the diagram portrays the beginning of the late Coniacian normal-regressive advance of the Czerna Formation (cf. Fig. 3).

sin, through which the basin-wide littoral sand platform emerged and briefly turned into a denudated coastal plain. The late Coniacian eustatic transgression formed an in-place, growing coastal sand barrier at the outer edge of the former littoral platform, sheltering a paralic limno-lagoonal plain with peat-forming mires (the Nowogrodziec Member of Milewicz (1997). The coastal barrier was eventually drowned and maximum marine flooding occurred, followed by a normal regression recorded as a rapidly upward-shallowing succession of offshore-transition to fluvio-deltaic deposits. The sedimentation pattern in an palaeogeographically evolving, tectonically controlled marine embayment contributes to existing models for estuarine sedimentary environments.

Sequence stratigraphy

According to Walaszczyk (2008), the Cretaceous of the NSS represents a single sedimentary cycle including two or three poorly regressive cycles. The Coniacian–Santonian part of the sedimentary succession was interpreted by Milewicz (1997) as representing the latest regressive phase of a transgressive-regressive (T-R) cycle and the earliest transgressive phase of the next T-R cycle. His recognition of a hiatus between the Rakowice Wielkie Formation and the Czerna Formation in the southeastern part of the basin, which he attributed to a northwesterly retreat of the sea from a large inner part of the basin and terrestrial erosion in this emerged area, was particularly important. Walaszczyk (2008) dated this event to the late mid-Coniacian, and Leszczyński (2018) translated it as a forced regression in the parlance of sequence stratigraphy. Leszczyński (2010) interpreted the Żerkowice Member of the Rakowice Wielkie Formation as a regressive systems tract formed at the culmination of the regressive phase and separated by a hiatus from the overlying transgressive systems tract of a 3rd-order eustatic cycle. Later, Leszczyński (2018) attributed the deposition of the Żerkowice Member to the KCo1 eustatic sea-level fall (Haq 2014).

More recently, Leszczyński and Nemec (2020) interpreted the Żerkowice Member as representing a normal-regressive highstand systems tract (Fig. 28A, B) that ended in a forced regression (Fig. 28C) caused by a combination of regional tectonics and eustatic sea-level fall (cf. curve in Fig. 3). The resulting erosional hiatus in the southeastern part of the basin predictably passes into a correlative, normal-regressive deltaic lowstand systems tract in the unexposed northwestern part of the basin (Fig. 29). The forced-regressive unconformity is overlain by a transgressive systems tract represented by the Nowogrodziec Member of Milewicz (1985), including the hypothetical, grown in-place transgressive coastal sand barrier (Figs 28D, 29). Maximum marine flooding occurred during the in-place drowning of the barrier (Figs 25, 28E). The overlying exposed deposits of the lower Czerna Formation (Fig. 25, upper part) are considered by Leszczyński and Nemec (2020) as representing a normal-regressive highstand systems tract (Figs 28F, 29). The thick and narrow sandbody found in boreholes N-14 and N-27 (Fig. 10) is interpreted as an in-place drowned transgressive coastal sand barrier (Fig. 29), stratigraphically belonging to the lowest part of the Czerna Formation as a lateral equivalent of the Nowogrodziec Member of Milewicz (1985).

Leszczyński and Nemec (2020) further observed that the Late Cretaceous pattern of marine transgression and regression in the North Sudetic Basin correlates well with eustatic sea-level changes (Fig. 3), and in particular coincides with the mid-Coniacian pulse of regional Alpine tectonism that critically amplified the eustatic impact on the basin. As such, this Late Cretaceous sequence-stratigraphic record from the northern, outer part of the Central European Boreal–Tethys seaway differs from that in the large, intermediately-located Bohemian Basin (Fig. 1A; Voigt et al. 2008; Mitchell et al. 2010; Nádaskay and Uličný 2014), where the eustatic signal may have been obscured by complicated palaeogeography and local Alpine tectonism.

Apart from regional stratigraphic debates, the Cretaceous seaway eventually retreated from the North Sudetic Basin and the other basins surrounding the Bohemian Massif around the latest Cretaceous to early Palaeogene(?) (Kley and Voigt 2008; Voigt et al. 2021), as evidenced by the shallowing-upward top part of the sedimentary succession and the cessation of marine sedimentation. The retreat resulted from the ultimate Alpine uplift of the region, documented through the deformation of Cretaceous strata and as distinct basement

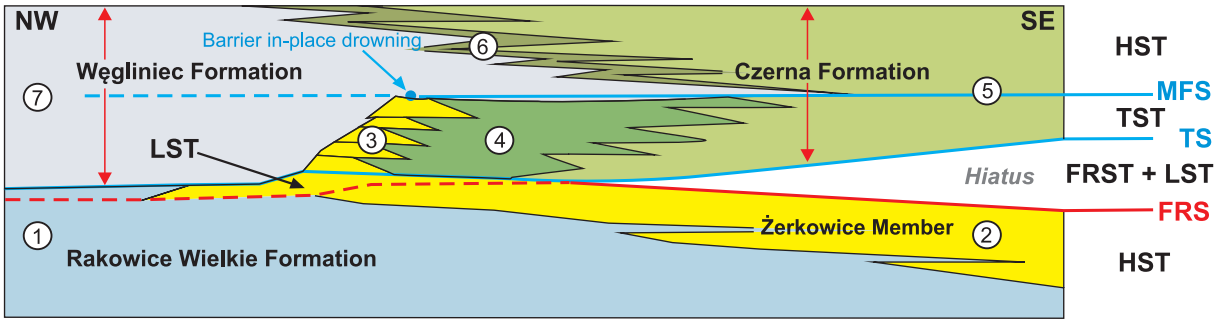

Main sedimentary environments of the Coniacian–Santonian succession:

1. Carbonate-rich, distal muddy offshore zone
2. Subtidal sand platform with laterally impinging deltas and shoreface to beach zone
3. Hypothetical transgressive sand barrier complex (unexposed, inferred from boreholes)
4. Lagoonal zone with sand supply by barrier washover and fluvio-deltaic processes
5. Paralic alluvial plain with rivers, lakes, lacustrine deltas and peat-forming mires
6. Shoreface with shoal-water deltas and prodelta zone
7. Carbonate-poor, distal muddy offshore zone

Sequence-stratigraphy code:

FRS – Forced-regression surface
MFS – Maximum-flooding surface
TS – Transgression surface
FRST – Forced-regressive systems tract
HST – Highstand systems tract
LST – Lowstand systems tract
TST – Transgressive systems tract

Fig. 29. Sequence-stratigraphic interpretation of the Coniacian–early Santonian sedimentary succession in the southeastern part of the North Sudetic Basin, displayed as a basin longitudinal cross-section (schematic, not to scale); slightly modified from Leszczyński and Nemec (2020). The hypothetical notion of an in-place aggrading transgressive coastal sand barrier (unexposed) is based on the great thickness of sandstones in borehole N-27 and their apparent absence in borehole J-1 located ~9 km farther northwest relative to the basin axis.

cooling recorded by thermochronological data (Skoček and Valečka 1983; Jarmołowicz-Szulc 1984; Ziegler 1986; Milewicz 1996; Wojewoda 1996; Uličný 2001; Aramowicz et al. 2006; Ventura et al. 2009; Danisik et al. 2010; Botor et al. 2019). According to Kley and Voigt (2008), this uplift was caused by compression and transpression induced by the Europe–Iberia–Africa plate convergence.

NATURAL RESOURCES

The Cretaceous of the NSS is known for its various natural resources, including, in particular, building stones, ceramic clays, and glass sands. The first consist of sandstones that have been quarried for several hundred years as dimension and carving stones. The oldest mentions of their extraction come from the 12th century (Walendowski 2001). They are highly valued due to their excellent workability and high resistance to weathering. In stone masonry, they were previously used as ashlar, but later and recently have mostly served as veneer. Several quarries between the towns of Lwówek and Bolesławiec are currently active, and some others are ready to begin mining operations.

The early recognition of the value of these sandstones as building and decoration material is documented in the old local architecture, which is richly preserved in Lwówek Śląski and Bolesławiec. The early Coniacian fine-grained sandstones from the top part of the Żerkowice Member south and southeast of Bolesławiec (fieldtrip stops 4–8) are particularly valuable. Farther to the northwest, their quality decreases due to declines in rock strength. The exploited sandstones are divided into several categories differing in colour and texture, and are named after their extraction localities. These sandstones, and coeval sandstones from the Intra-Sudetic Synclinorium, are still considered to be some of the most important building sandstones in Germany (Ehling 2006). They were the dominant natural stone in Berlin's architecture for many decades (1880–1942), and were also used in other German and European cities during that period. After World War II, and especially after the fall of communist regime, they also became important dimension stones in Poland, where recently they have been used mainly as the veneer material of important, official, and exclusive buildings. A renaissance in their use in Germany occurred in 1990 (Ehling 2006). They are still highly prized for their high

degree of homogeneity and attractive physical properties.

Ceramic clay deposits occur in the lower part of the Santonian Czerna Formation, in a ca. 200 m thick succession that abounds in beds and lenses of clay-rich sandstones, kaolinitic white-firing clays, stoneware clays, and refractory clays (Milewicz 1964; Galos 2010). These clay lenses and beds have thickness of 0.2–3.0 m, and constitute ca. 25% of the whole succession. Originally, white-firing clays were extracted from clay beds and lenses. Later, they were extracted by washing from the bulk sediment, if it contained more than 20% good quality clay minerals (Nieć and Ratajczak 2004).The deposits contain diagenetic and secondary kaolin, redeposited to streams and lakes (oxbow lakes) on a delta plain due to the erosion of residual deposits.

White-firing and stoneware clay deposits are recognized mainly in the southern limb of the NSS, in the vicinity of Węgliniec and Nowogrodziec, as well as between Bolesławiec and Lwówek Śląski. Since the Middle Ages, they have been extracted here in open pits; in some intervals in the 20th century, they were also exploited in underground mines. The sediments display differentiated mineralogical composition, with the percentage of grains coarser than 0.063 mm exceeding, in some cases, 50%. The main components are well-ordered kaolinite, illite, and muscovite, although the quartz content varies from 15 to 80% (Stoch 1962; Galos 2010). Due to their large lithological and mineralogical variability, numerous varieties have been distinguished, according to bending strength after drying, >0.063 mm grain content, water absorption, and whiteness after firing (Nieć and Ratajczak, 2004). Kaolin extracted here (e.g., from the Maria III deposit exploited by the Surmin Kaolin plant in Nowogrodziec; fieldtrip stop 9) is used in the ceramic industry for the production of fine pottery products, as well as in the refractory, paper, glass, and cement industries.

White-firing clay resources are currently recognized in six deposits in the Bolesławiec area. The total estimate reservoir of this raw material amounts to ca. 59.6 million t, but a total of ca. 1.1 million t of pure clays in seams and lenses are recognized in three abandoned deposits. In the other three deposits (Janina I, Nowe Jaroszowice, and Ocice), a total of ca. 58.6 million t of sandy-clayey raw material, used for the production of white-firing clay by washing, have been recognized, enabling the production of ca. 16.2 million t of raw white-firing clayey material. Some white firing clay varieties occur in the two nearby, undeveloped stoneware clay deposits (Anna-Włodzice Małe and Ocice II), with total resources estimated as ca. 11.5 million t (see Galos 2010 and references therein). Moreover, the adjacent Czerwona Woda sandy-clayey deposit, recognized previously as a natural foundry sand, has recently started to be used for the production of raw white-firing clayey material, with ca. 5.0 million t available (Galos 2010 and references therein). Prospective areas between Bolesławiec and Nowogrodziec that have tentatively considered for industrial exploration have total estimated resources of ca. 132 million t sandy-clayey sediment, which might allow the production of ca. 40 million t of raw white-firing clay (Galos 2010).

Due to the Cretaceous ceramic clay deposits and local usage, Bolesławiec has been known since the Middle Ages as a town of pottery industry. Unique, stamp-ornamented Bolesławiec ceramic products attract collectors from all over the world.

Another major regional resource are glass sand deposits, which occur in the Coniacian, and subordinately in the Santonian, succession of the Bolesławiec area. They are the second most-important sand glass deposits in Poland (Burkowicz et al. 2020). Top-quality glass sand is mined at the plant Kopalnia i Zakład Przeróbczy Piasków Szklarskich Osiecznica sp. z o.o. (which, since 1995, has belonged to the Quarzwerke GmbH group), and is sold both within the country and abroad. Glass sand of slightly lower quality, spoiled by colouring oxides, is also obtained as a by-product from the processing of kaolinitic sandstone in the plant Kopalnie Surowców Mineralnych Surmin Kaolin S.A. in Nowogrodziec (since 1998, in the Quarzwerke GmbH group). The mining sites between the Osiecznica and Nowogrodziec are particularly famous for the production of glass sands and fine ceramic clays.

Natural resources of subordinate significance in the NSS Cretaceous include foundry sands, which have been documented within the Czerna Formation in the village of Czerwona Woda, northwest of Bolesławiec.

FIELD STOPS

Stop 1

Rock tors "Szwajcaria Lwówecka" (German *Löwenberger Schweiz,* English *Switzerland of Lwówek*) in Lwówek Śląski (German *Löwenberg in Schlesien*) (Fig. 30);

51° 6' 6.4'' N, 15° 35' 37.4'' E; A rocky, wooded ridge on the southern outskirts of Lwówek Śląski between the Bóbr River and the main road to the town of Jelenia Góra, rising up to 40 m above the bottom of surrounding valleys, limited by a cliff from the west and featuring numerous tors, each several metres high (Fig. 4A).

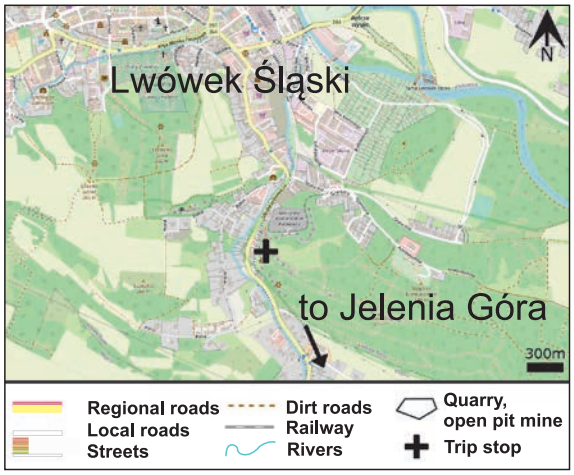

Fig. 30. Location of fieldtrip stop 1.

Structure and stratigraphy: Lwówek Syncline; Radłówka Formation (Lower Triassic Buntsandstein) and the Wilków Member (upper Cenomanian) of the Rakowice Wielkie Formation

Subject: Stratigraphy (Triassic–Cretaceous contact) and sedimentology (lithofacies record of the Cenomanian transgression)

Remarks: Thick- and medium-bedded, pinkish and light grey, quartzose and arkosic sandstones, medium- to coarse-grained with admixture of granules and small pebbles, plane-parallel stratified and cross-stratified, overlain almost conformably by light grey and drab sandstones with quartz pebbles, 0.3 to 0.8 cm in size, scattered in the sandy groundmass (Fig. 4C). The first lithology represents the Early Triassic Radłówka Sandstone Formation, whereas the second belongs to the late Cenomanian Wilków Member of the Rakowice Wielkie Formation. The boundary between the two lithostratigraphic units is a sharp surface overlain by pebbly sandstone (ravinement surface; Fig. 4B). The individual beds of the Wilków Sandstone are 0.5 to 1.5 m thick, structureless, occasionally normally graded, crudely plane-parallel and cross-stratified.

Genesis: Deposition by longshore currents and mass settling from storm-derived suspension clouds in the upper shoreface zone of a high energy coast. Episodic local sediment homogenization by benthic fauna.

Stop 2

Former quarry on the eastern side of the road from Lwówek Śląski to the village of Sobota (German *Zobten am Bober*), 1.8 km from the intersection of Złotoryjska and Widokowa Streets, towards the village of Sobota (Fig. 31); 51° 6' 20'' N, 15° 37' 19.4'' E; Land depression in the woods, bounded by a rock cliff to the north, below a small cave called Zimna Dziura (in English, cold hole).

Structure and stratigraphy: Lwówek Syncline; Chmielno Member (?) and overlying part of the Rakowice Wielkie Formation (Turonian)

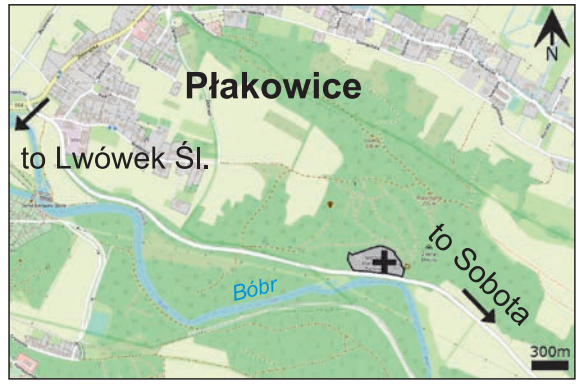

Fig. 31. Location of stop 2. For explanation of symbols see Fig. 30.

Subject: Stratigraphy and sedimentology; features of the top part of the Chmielno Sandstone and the overlying fine-grained sediments of the Rakowice Wielkie Formation, with focus on the appearance of the boundary between two lithostratigraphic units.

Remarks: Ca. 12 m thick portion of the uppermost Chmielno Sandstone, composed of structureless or faintly cross-stratified, medium- to coarse-grained, noncalcareous sandstone with small pebbles, friable in the higher part, delimited at the top by a 20 cm thick transition zone to the overlying grey, brittle, silty to sandy marlstones, crudely thin-bedded, strongly to totally bioturbated with frequent, poorly preserved, deformed macrofossils. Sandstone cross-stratification occurs in 30–50 cm thick sets, with strata dipping to the northeast.

Genesis: Sandstone of shoreface origin (basin margin nearshore sedimentation by longshore currents and reworking by waves) overlain by lower shoreface to upper offshore marly sediments.

Stop 3

Rock tors "Krucze Skały" (English *Raven's Rocks*; German *Rabenfelsen*) in Jerzmanice Zdrój (German *Hermsdorf*; Fig. 32); 51° 6' 46.1'' N, 15° 53' 30.5'' E; Sandstone bluff up to 25 m high, marking the eastern bank of the Kaczawa River valley, near the train station in the village of Jerzmanice Zdrój.

Structure and stratigraphy: Leszczyna half-graben; Chmielno Member (middle Turonian, Inoceramus lamarcki horizon) of the Rakowice Wielkie Formation; so-called "Middle Jointed Sandstone" (German Mittel Quadersandstein).

Subject: Sedimentological features; ichnofossils and sedimentary environment; depositional and post-depositional processes; large scale seismotectonic deformations; soft-sediment shears and kink-bands.

Remarks: The sand and gravel rocks in the vicinity of Jerzmanice Zdrój were first stratigraphically classified by Scupin (1910, 1913) as Lower Turonian. In later studies and on subsequent geological maps (Jerzmański 1955; Śliwiński et al. 2003; Chrząstek and Wojewoda 2011), it was included into the Middle Turonian, what is probably justified as its petrography and sedimentological features are same to those of the paleontologically well-documented Radków Bluff Sandstones in the Intra-Sudetic Basin, which belong to the Inoceramus lamarcki horizon (Wojewoda 1997, 2020).

Fig. 32. Location of 3. For explanation of symbols see Fig. 30.

The sedimentary succession is bipartite. Its lower part (Fig. 5) consists of strongly homogenized conglomeratic sandstone units, which locally show relics of low-angle and large-scale cross-bedding (sediments of lateral accretion of nearshore bars (?)). Layers reach up to 4 m thickness and mostly consist of sand size material, with admixture of scattered pebbles up to 6 cm in size. Usually near the bottom of layers, the grains are visibly coarser and sediment shows relics of swaley and hummocky cross stratification. Primary sedimentary structures are largely oblitered, mostly due to locally high trace fossil concentrations, dominantly of the Ophiomorpha type. The layer at the base of the quarry shows large-scale trough cross-stratification resulting from the migration of large current-formed bedforms (paleocurrent direction is bimodal 175–225°) on the shoreface bar slopes.

The sandstone layers are separated by layers of pebbly conglomerate with thicknesses of up to 0.5 m. The bottom surfaces of these layers are usually irregular. Within them, relics of the stratification characteristic of wave-generated bedforms are present (Fig. 6A). In the lowest part of the Chmielno Member succession, which only outcrops in the tectonically disturbed zone at the Jerzmanice Fault in the

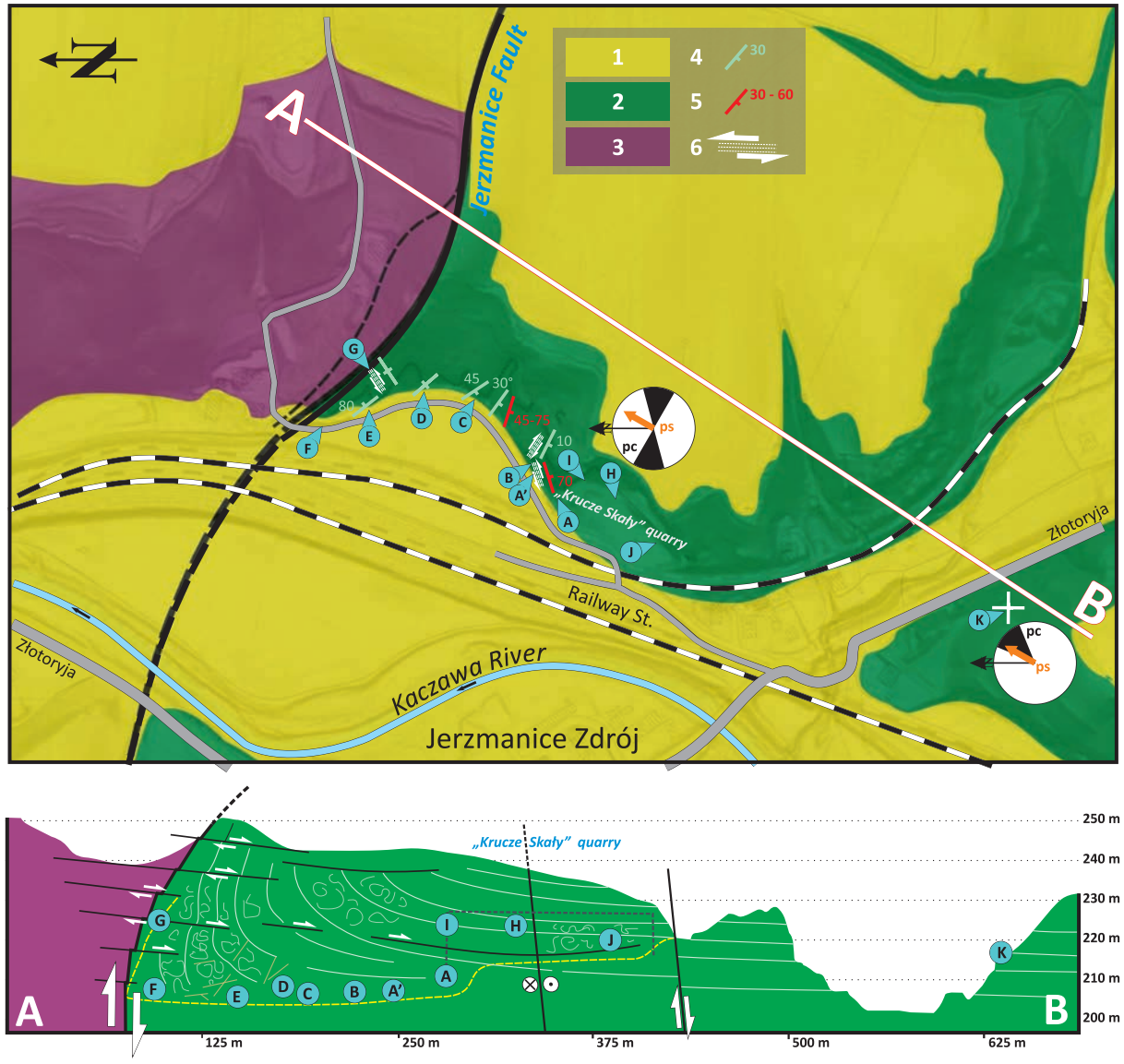

Fig. 33. Schematic map and cross-section illustrating the geological structure of the "Krucze Skały" geosite in Jerzmanice Zdrój. Explanation: 1 – unseparated Neogene deposits, 2 – Cretaceous, 3 – metamorphic rocks of the Kaczawa Complex, 3 – layering, 4 – local fault surfaces, 5 – vertical or steeply inclined surfaces of horizontal shearing; rose diagrams: pc – palaeocurrent, ps – paleoslope; black lines: solid – certain faults, dashed – suspected faults; X – X': geological cross-section: lines – continuous white (layering surfaces), dashed yellow (trip route), explaned sites from A to K.

north, these conglomeratic beds can reach thicknesses of up to 1.5 m (cf. Fig. 7E, F). No escape trace fossils were found on these areas of rapid sediment accretion. The upper part of the succession consists of cosets of large-scale tabular and trough cross-stratification. Transport directions to the northeast predominate here (Figs 6C, 8).

In summary, the clastic material of the Chmielno Member sandstones and conglomerates was deposited close to storm wave base, not far from shore, in an area with relatively slow sediment accumulation rates. At the same time, this area was dominated by offshore (longshore?) currents towards the north and northeast, which excludes the present-day Jerzmanice Fault as a zone delimiting the contemporaneous shoreline of the basin.

A significant proportion of sediments inside the layers in the lower part of the succession,

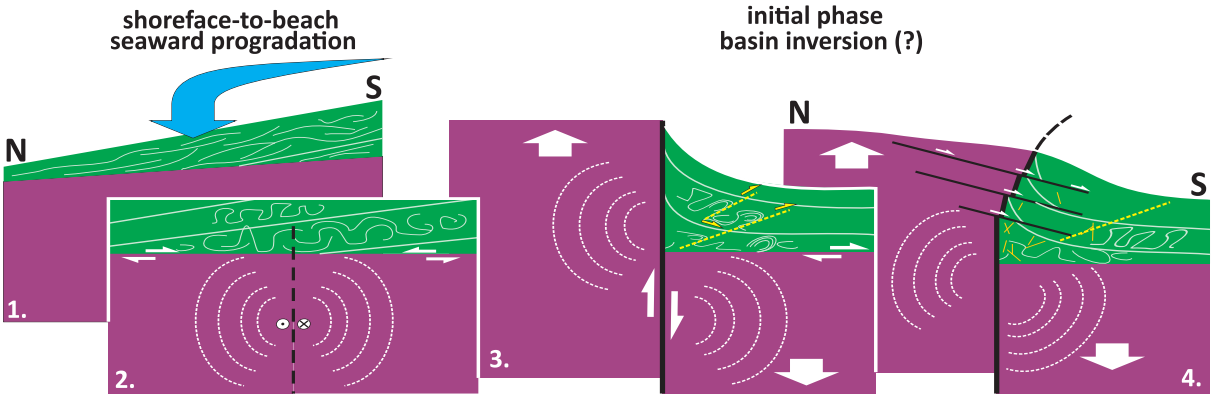

Fig. 34. Diagram explaining the probable sequence of sedimentation (1–2) and geodynamic (3–4) phenomena at Krucze Skały.

as well as within the cosets of the upper part of the unit, exhibit numerous soft-sediment convectional disturbances with characteristic shapes (e.g., folds, helicoidal torsions) (Figs 6C; 7B, F). In some places, the gravel material are immersed in the underlying sand (drop-shaped load casts) (Figs 6A; 9B). All of these deformations, especially in the upper part of the Chmielno Member, gradually disappear towards the southwest (cf. Fig. 6), where they have not been documented in natural exposures to date. Most of the deformations show a clear northward vergence, which is in accordance with the direction of local sedimentary redeposition, as well as the direction of the local palaeoslope during sedimentation. This, in turn, places the Late Cretaceous North-Sudetic Basin shoreline to the south or southwest of the sites discussed here. Some of the nearly vertical faults observed also have soft sediment features (helicodal torsions and shears, complementary kink bands) (Figs 7C, E, F; 9B). Probably some of these faulted zones were later reactivated as typical tectonic deformations of Cretaceous rocks during the regional inversion of the sedimentary basin.

As we approach the Jerzmanice Fault zone, the sediments of the Chmielno Member dip progressively steeper towards the south-southwest (cf. Figs 33, 7B, 9D). Close to the fault zone, the conglomerate and conglomeratic sandstone layers are vertically oriented and even inverted. In the latter, there are autobreccias – that is, deformations typical of local *in situ* redeposition or tectonic destruction of still unlithified sediment. Some fractures, especially low-angle, coupled shear surfaces of the R type (Riedel's shears), and kink-bands surfaces have features typical of incompletely lithified sediment (Figs 7C, E; cf. Solecki, 2011). In addition, numerous subhorizontal, inclined, and vertical surfaces have typical indicators of fault surfaces including lineation and slickenside features, and/or are covered with recrystallization slickenfibres, which indicate a generally oblique and overthrusting movement direction of approximately 190–170° (Figs 9A, D). Interestingly, the majority of horizontally oriented layers have boundaries and/or subhorizontal tectonic surfaces within them – classic signs of overthrust slides – which allows for a slightly different interpretation of the "inversional" nature of the Jerzmanice Fault than would appear from the cartographic image (see Fig. 34).

Genesis: Sand-gravely deposits of the shelf and shoreface, forming cyclic layers with slightly coarsening upwards grains, partially obliterated primary sedimentary structures, and storm-induced gravel accumulations. Numerous soft sediment deformation structures (convectional, helicoidal torsions, load casts) indicate high synsedimentary seismotectonic activity of the Jerzmanice Fault.

Stop 4

Kopka Hill (German *Hockenberg*) between the villages of Czaple (German *Hockenau*) and Nowa Wieś Grodziska (German *Neudorf am Groditzberg*) (Fig. 35); **Stop 4A**: 51° 8' 40.5'' N, 15° 44' 53'' E; **Stop 4B**: 51° 8' 32.4'' N, 15° 45'

Fig. 35. Location of stop 4. For explanation of symbols see Fig. 30.

9.9'' E; **Stop 4C**: 51° 45' 9.9'' N, 15° 45' 9.8'' E; Stop 4A: Abandoned quarry at the western foot of Kopka Hill, by the road from the village of Czaple to the village of Nowa Wieś Grodziska. Stop 4B: Abandoned quarry on the southwestern slope of the hill. Stop 4C: Active quarry at the top part of the hill. All quarries are operated by the Polish company "Kamieniarz", Tadeusz Modliński, Kielce.

Structure and stratigraphy: Leszczyna half-graben; Żerkowice Member (lower Coniacian). The sub-stops (individual quarries) are labelled in stratigraphic order, with stop 4A showing the lowest part of the Żerkowice Member and stop 4C its top part. Relics of the basal Czerna Formation (lower Santonian) seem to occur at stop 4C.

Subject: Sedimentological features; depositional processes; ichnofossils and depositional environment; normal-regression deposits; economic importance.

Remarks: A sedimentary succession composed of mostly medium-grained, quartzose, noncalcareous, moderately to weakly cemented sandstones with dune-scale, bidirectional planar and trough cross-stratification (lithofacies Sc of Leszczyński and Nemec 2020) is exposed at stops 4A–C (Figs 13, 14, 20, 21). Some admixture of coarse sand and granules occurs at stop 4C. Cross-strata sets are up to 1.5 m thick with foreset dip mostly towards the northwest (ca. 330°), and less often towards the southeast. Intercalations of plane-parallel stratified and ripple cross-laminated sandstone are subordinate (e.g., in the quarry at stop 4B; Fig. 14) The local bedding inclination includes at least 5° of secondary tectonic tilt. The top part of the sedimentary succession exposed in the eastern quarry wall at stop 4C shows a sandstone lens, ca. 50 m wide and 4 m thick, incised in the substrate (Fig. 20). In contrast, the topmost western wall of the quarry at stop 4C used to show a ca. 4 m thick succession comprised of pinkish-red clayey mudstone overlain by two cross-stratified sandstone bodies separated by a white mudstone layer (Leszczyński observation from 2010). The prominent variegated mudstones with sandstone interbeds suggest a basal relic of the Czerna Formation, as exposed at stop 5.

No trace fossils and only a few body fossils (*Inoceramus* sp., Fig. 16D; *Inoceramus kleini* Müller, 1888; Chrząstek et al. 2018) have been found in the quarry at stop 4A. Rare trace fossils occur at stop 4B, including vertical Ophiomorpha nodosa shafts, *Rosarichnoides sudeticus* (Chrząstek et al. 2018), *Thalassinoides suevicus*, *T. paradoxicus*, *Phycodes* cf. *palmatus*, and *Gyrochorte* isp.; additionally, body fossils of the starfish *Lophidiaster scupini* Andert, 1934 (formerly *Astropecten scupini* Andert 1934; Fig. 16H) have been recovered (Chrząstek and Wypych 2018). Intense bioturbation occurs at stop 4C, with bedding surfaces densely covered with burrows such as *Gyrochorte* isp., *Ophiomorpha nodosa*, *Phycodes* cf. *curvipalmatum*, *Phycodes* isp., *Planolites* cf. *beverleyensis*, and ?*Thalassinoides–Phycodes* compound burrows (Chrząstek and Wyoych 2018; Chrząstek et al. 2018).

The presence of the starfish Lophidiaster scupini Andert, 1934 (formerly Astropecten scupini; Fig. 16H) suggests a shallow-marine setting (shoreface). These fossils used to occur in abundance down to a water depth of usually 30–50 m (Beddingfield and McClintock 1993; Villier et al. 2004). They are well-adapted to soft-bottom substrates, as detrivores and predators of gastropods, bivalves, and crustaceans (Caregnato et al. 2009; Blake and Guensburg 2016). Inoceramids are very common and cosmopolitan in Upper Cretaceous marine shelf environments and had broad ecological tolerances (Harries and Ozanne 1998).

The sandstones at the Kopka hill have been exploited since the Middle Ages as valuable dimension stones.

Genesis: The sediment packages mainly composed of dune-scale cross-stratified sandstones are interpreted as longitudinal tidal bars, up to 10–15 m thick, with complexes of vertically and laterally stacked bars reaching several dozen metres. The planar cross-strata sets were deposited as 2D dunes, and the trough cross-strata sets as 3D dunes. Both indicate transport mainly to the northwest, and evidence for opposite transport directions supports the existence of tidal flows. The top part of the sedimentary succession exposed at stop 4C shows a basin-margin delta prograding to the north-northeast and interfingering with the southwest flank of a tidal sand bar. The incised sandstone lens at the succession top is a fluvial palaeochannel formed during the forced regression that terminated the deposition of the Żerkowice Member. The relic, topmost part of the succession in the western quarry wall at stop 4C comprises lacustrine clayey mudstone and fluvial channel sandstones.

Stop 5

Quarries south of the village of Wartowice (German *Warthau*) (Fig. 36); **Stop 5A**: 51° 12' 45.3'' N, 15° 39' 12'' E; **Stop 5B**: 51° 12' 53.6'' N, 15° 39' 2.8'' E; **Stop 5C**: 51° 18' 37.5'' N, 15° 45' 42'' E; all stops are active quarries; Stop 5A: Quarry currently operated by Hofmann Natursteinwerke Polen Sp. z o.o., Kraków; Stop 5B: Quarry currently operated by Geiger Stein- und Schotterwerke GmBH, Kinding, Germany; Stop 5C: Quarry currently operated by ATS-Stein Sp. z o.o. Kopalnie piaskowca, Bolesławiec.

Structure and stratigraphy: Bolesławiec (Grodziec) Syncline; Upper part of the Żerkowice Member (lower Coniacian) of the Rakowice Wielkie Formation and lower part of the Czerna Formation with Nowogrodziec Member (lower Santonian)

Subject: Sedimentological features; lateral change of the succession; depositional processes; body fossils and ichnofossils; palaeosols and depositional environment; normal regression and transgressive deposits; economic importance.

Remarks: The lower part of the sedimentary succession exposed in all three quarries

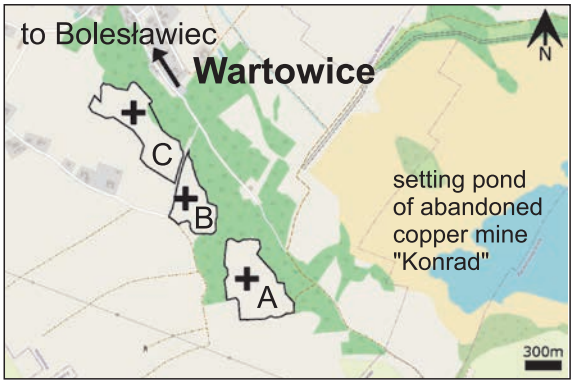

Fig. 36. Location of stop 5. For explanation of symbols see Fig. 30.

shows the uppermost part of the Żerkowice Sandstone Member, exploited here as valuable dimension stone. The upper part of the succession represents the lower part of the overlying Czerna Formation (Fig. 25A, B, 37).

The Żerkowice Member exposed at the visited quarries is up to ca. 17 m thick at stop 5A, 7 m at stop 5B, and 9 m at stop 5C. The general appearance of the succession varies with the nature of the exposure. On the surfaces of older natural joints, portions of the succession with thicknesses of several metres look massive, divided into two sandstone beds as much as 4 m thick, separated from each other by a flat to highly irregular discontinuity surface (e.g., in the quarry at stop 5B; Fig. 37B). Elsewhere, a packet of heterolithic sediment occurs, up to 1 m thick (lithofacies H in Leszczyński and Nemec 2020; quarries at stops 5A and 5C; Fig. 37A, D). Weathered surfaces tend to show thinner bedding, tabular and lenticular in vertical section, with beds up to 1.5 m thick (Fig. 37A left side of photo). On closer inspection, one can see dune-scale cross-stratification (lithofacies Sc of Leszczyński and Nemec 2020; Fig. 11A, B), plane-parallel stratification (lithofacies Sp in Leszczyński and Nemec 2020), and rarely ripple cross-lamination, besides the massive structure. Cross-stratification occurs as 30–95 cm thick sets. The thinner sets are bounded either by discontinuity surfaces or by laterally discontinuous siltstone or mudstone drapes 0.5–2 cm thick (lithofacies M in Leszczyński and Nemec 2020). The sandstone is mostly fine- to medium-grained, arenitic, quartzose, noncalcareous with kaolinitic and generally ferrous-poor cement. An admixture

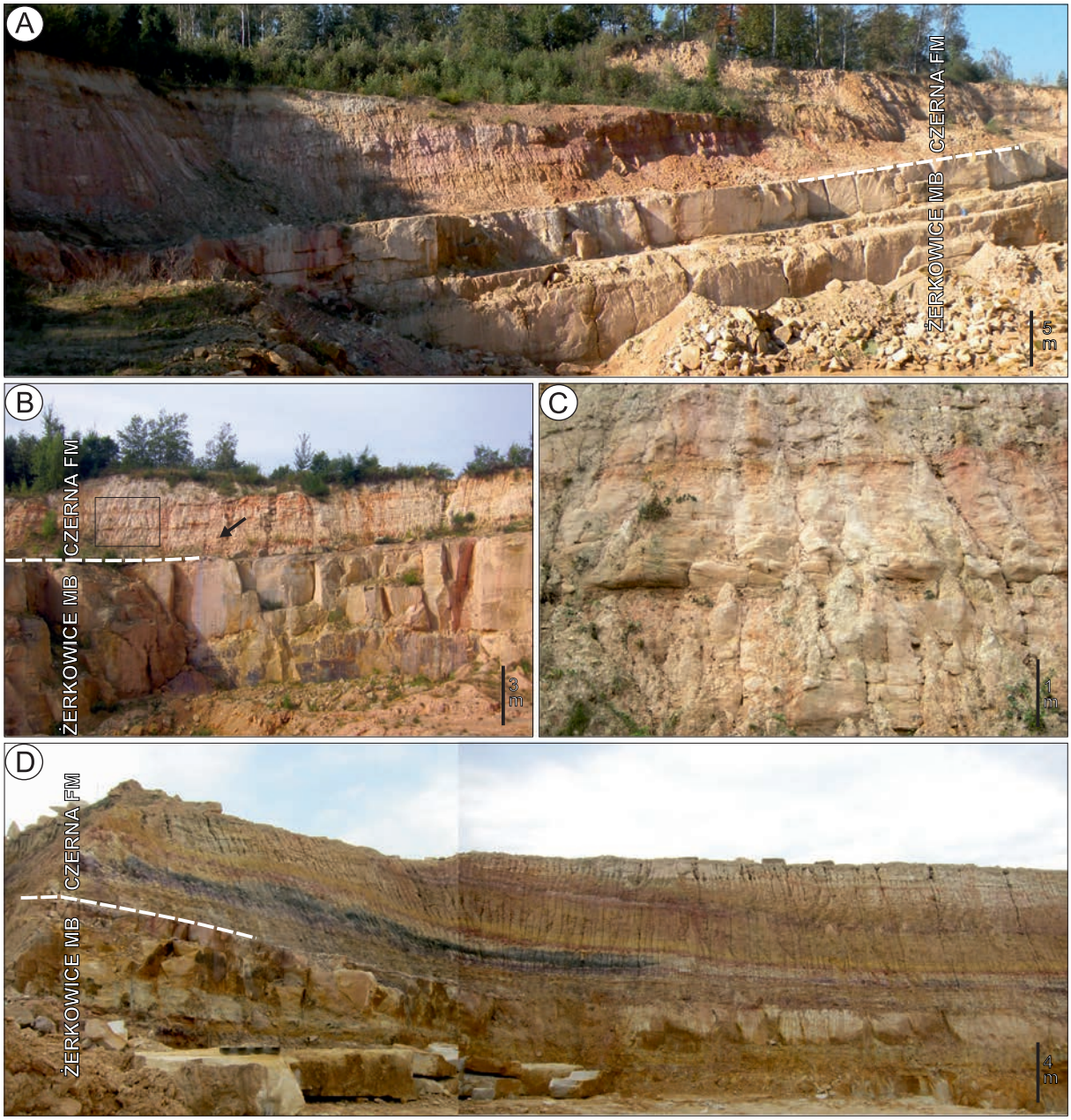

Fig. 37. General appearance of outcrops at stop 5. A – View of fieldstop 5A on October 10, 2010. B – View of fieldstop 5B view September 29, 2021. The arrow indicates location of numerous *Ophiomorpha nodosa*. The black rectangle indicates close-up in C. C – Portion of the Czerna Formation at fieldstop 5B on September 29, 2010. D – View of fieldstop 5C on September 29, 2021.

of coarser grains up to small quartz pebbles (1 cm in size) occurs in the highest bed.

Isolated and clustered fishbones (Leszczyński 2018, fig. 11F) as well as single imprints of driftwood fragments with clustered casts of wood boring bivalves (*Teredolites clavatus*) were found in the sandstones at stop 5A (Leszczyński 2018, fig. 12B). Claystone intraclasts occur in the fills of large gutters. The bedding surfaces of sandstone, particularly the scoop-shaped surfaces bounding trough cross-strata sets, are covered with wave or combined-flow ripple marks (Fig. 11H, I), bioturbation structures (Fig. 15A, B), and rarely molds and casts of body fossils, mostly bivalves (Leszczyński 2018, fig. 11A). The bioturbation structures include trace

fossils ranging between a stressed expression of the *Skolithos* Ichnofacies and a proximal expression of the *Cruziana* Ichnofacies (Leszczyński, 2018). Two thick sandstone beds in the top part of the Żerkowice Member at stop 5A show a totally bioturbated, locally ferruginized, sharp top (Fig. 25A, B; Leszczyński 2018, fig. 10A–C). Some bioturbation structures reminisce rhizoliths (Leszczyński 2018, fig. 10B). Moreover, numerous *Ophiomorpha nodosa* occur locally in the lower bed, up to 3 m below its top. At stop 5A, local ferruginization occurs in the two highest thick sandstone beds, at their top and up to ca. 1 m below it. The ferruginized layer is up to 10 cm thick.

In all three quarries, the Czerna Formation begins with a heterolithic unit dominated by mudstones and claystones, locally containing ferricrete or bands up to 5 cm thick and globular to vermicular hematitic concretions (the Nowogrodziec Member of Milewicz 1985). This unit is up to 7 m thick, and its basal part is marked by a packet of mostly greyish white or variegated silty mudstone overlain by very fine sandstone with siltstone interlayers and rhizoliths (Figs 25A, B; 26A–C; Leszczyński 2018; Leszczyński and Nemec 2020). In quarry 5A, the unit contains two coal lenses up to 25 cm thick. The lower one encloses coalified trunks of driftwood with diameters of up to 12 cm. The upper lens rests on a clay layer enclosing plant roots in its top part (Figs 25B; 26D). In quarry 5C, a coal and coaly mudstone lens, ca. 20 m long and up to 1 m thick, has recently been exposed. It occurs approximately 2 m above the base of the Czerna Formation (Fig. 37D). Some mudstone layers therein are densely interspersed with sand and/or silt streaks and thin interlayers, forming the heterolithic lithofacies H of Leszczyński and Nemec (2020), which occurs as beds up to 2 m thick and is often strongly bioturbated (in part abiotically contorted?) in the upper part of the unit (Fig. 25A, B). The heterolithic deposits pass upwards into fine-grained and further medium- to coarse-grained sandstones, mostly homogenized by bioturbation (Fig. 26E, F), locally showing ripple cross-lamination (lithofacies Sr and Sw of Leszczyński and Nemec 2020), up to 2 m thick, variably ferruginized, with local ferricrete at their top. Some sandstone beds have both sharp bases and tops and show plane-parallel stratification and cross-stratification.

The overlying part of the Czerna Formation, up to 8 m thick, is dominated by medium- to coarse-grained sandstones with an admixture of small pebbles, planar-parallel stratified and trough cross-stratified (lithofacies Sp and Sc of Leszczyński and Nemec 2020). They occur as beds up to several metres thick, separated by sheet-like heterolithic units of lithofacies H, 10–25 cm thick. The lowest thick sandstone bed locally captures *Ophiomorpha nodosa* (Fig. 26F).

Genesis: As with the sandstones of the Żerkowice Member at stop 4, the dune-scale cross-stratified sandstones at stop 5 are interpreted as representing longitudinal tidal bars elongated roughly parallel to the basin axis. Their planar cross-strata sets were deposited as 2D dunes, and the trough cross-sets as 3D dunes. Foreset dip directions indicate a dominant transport direction to the northwest, but the cross-sets are generally bidirectional and show a wide range of transport directions (cf. Fig. 19D). The heterolithic interbeds were deposited in inactive, sheltered interbar swales.

The lower part of the Czerna Formation is interpreted as deposits of a coastal alluvial plain with shallow lakes (ponds and oxbow lakes), peat-forming mires, and tide-influenced fluvial channels. The upper part includes deposits of a paralic coastal plain with basin-margin sand wedges and axial fluvial channels with crevasse splays (referred to as minor mouth bars where spread into lacustrine ponds).

Stop 6

Active quarry near the village of Żeliszów (German *Giersdorf;* Fig. 38); 51° 11' 3'' N, 15° 38' 54.92'' E; Active quarry owned by the company "Kamieniarz", Tadeusz Modliński, Kielce

Structure and stratigraphy: Bolesławiec (Grodziec) Syncline; Żerkowice Member (lower Coniacian) and Nowogrodziec Member (lower Santonian).

Subject: Sedimentological features; depositional processes; ichnofossils and depositional environment; normal- to forced-regressive and transgressive to normal-regressive systems tracts; economic importance.

Fig. 38. Location of stop 6. For explanation of symbols see Fig. 30.

Remarks: The lower part of the sedimentary succession exposed in the quarry is up to ca. 10 m thick and represents the uppermost part of the Żerkowice Member, exploited here as dimension stone. The upper part, up to 7 m thick, represents the lower part of the Czerna Formation (Fig. 25C). The deposits are overlain by a several metre thick succession of fluvioglacial gravels. The Żerkowice Member consists of several beds of fine- to medium-grained, quartzose, noncalcareous, arenitic, cream-yellow sandstone up to 4 m thick, separated from one another by flat to irregular (erosional) discontinuity surfaces (Fig. 26H) or packets of heterolithic sediment up to 0.7 m thick (lithofacies H in Leszczyński and Nemec 2020). The sandstones appear either structureless or show planar and trough bidirectional cross-stratification and plane-parallel stratification. Cross stratification occurs in 15–35 cm thick sets. The top surface of the uppermost bed exhibits a shell lag (Leszczyński and Nemec, fig. 5K) dominated by casts and molds of the gastropod *Nerinea bicincta* and rare trace fossils, mostly *Ophiomorpha nodosa* (Fig. 15C). The latter can also be rarely found in bed cross-sections.

The Czerna Formation begins with a 0.5 m thick heterolithic packet (lithofacies H), with bioturbated greyish-white to yellow claystone and fine-grained sandstone. An imprint of a driftwood fragment with clustered *Teredolites clavatus* (casts of wood-boring bivalves) has been found in the middle part of this packet. The packet is overlain by a ca. 1.8–3 m thick composite bed of fine- to very coarse-grained sandstone, trough cross-stratified, with thin siltstone and mudstone interlayers and rare *Ophiomorpha nodosa*. The cross-strata sets are inclined toward the southwest. The unit in its thinner segment is overlain by a lens of light-grey to orange claystone, sandy mudstone, and two coal beds (0.6 m and 0.25 m thick). The lens has an SE-NW (150–330°) extent of ca. 30 m and is up to ca. 3 m thick. It is overlain by a 0.35 m thick bed of planar-parallel-laminated siltstone passing upwards into ripple cross-laminated, very fine-grained sandstone. The succession is topped with a 2.3 m thick bed of sandstone with clustered occurrences of mostly vertically oriented *Ophiomorpha nodosa* (Fig. 26I), indicating the *Skolithos* Ichnofacies.

Genesis: Similar to the sandstones of the Żerkowice Member at stops 4 and 5, the sandstones at this stop are interpreted as representing a tidal sand bar, with planar cross-strata sets deposited as 2D dunes and the trough cross-sets as 3D dunes. Like in stops 4 and 5, foreset dips indicate a dominant transport direction to the northwest. The top surface of the Żerkowice Member, covered by a shell lag, may represent the shoreface of a retreating sea.

The Czerna Formation sediments are interpreted as deposits of a coastal alluvial plain with shallow lakes (ponds and oxbow lakes) and tide-influenced fluvial channels. The upper part includes deposits of a paralic coastal alluvial plain with basin-margin sand wedges (Fig. 26H).

Stop 7

Active quarry and a rock tor between the villages of Skała (German *Hohlstein*) **and Żerkowice** (German *Sirgwitz*; Fig. 39); **Stop 7A**: 51° 9' 34.9'' E, 15°3 4' 55.8'' E; **Stop 7B**: 51° 9' 30.6'' E, 15° 34' 33.4'' E; Stop 7A: Active quarry currently owned by Hofmann Natursteinwerke Polen Sp. z o.o., Kraków; Stop 7B: "Skała z Medalionem" tor, 26 m high, in the woods on the southern slope of Wieżyca Hill.

Structure and stratigraphy: Southern outskirts of the Bolesławiec Syncline; Żerkowice Sandstone Member (lower Coniacian).

Subject: Sedimentological features; ichnofossils; depositional processes and environment; economic importance.

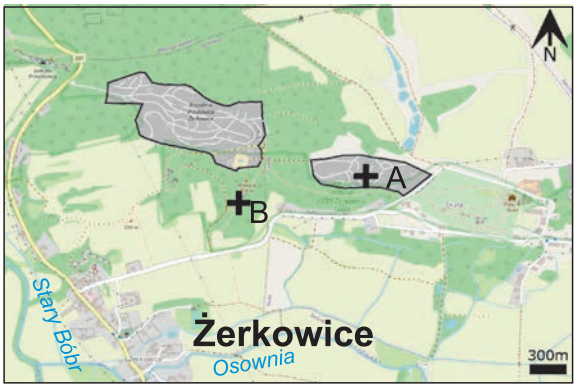

Fig. 39. Location of stop 7. For explanation of symbols see Fig. 30.

Remarks: Approximately the same part of the Żerkowice Member is exposed in both sub-stops, which are separated by about 400 m, although the quarry outcrop is stratigraphically less than half the length of the rock tor and corresponds to the upper part of the tor. Both the quarry and the tor expose mostly fine- to medium-grained, quartzose sandstones with planar and trough cross-stratification (lithofacies Sc of Leszczyński and Nemec 2020; Figs 11A–C, 17) as well as planar-parallel stratification (lithofacies Sp of Leszczyński and Nemec 2020; Fig. 17) with surfaces covered by parting lineation (Fig. 11J). Cross-strata sets range from a decimetre to 0.9 m in thickness and show variable and often bidirectional transport directions (Fig. 17). Thinner sets occur in the lower part of the succession, whereas the thickest are characteristic of the middle part (Fig. 17). Sandstones with current ripple cross-lamination (lithofacies Sr of Leszczyński and Nemec 2020; Fig. 17) and wave ripple cross-lamination (lithofacies Sw of Leszczyński and Nemec 2020; Fig. 17) constitute subordinate lithofacies. The top part of the sedimentary succession, best preserved in the tor, shows only faint, bioturbated planar-parallel stratification and ripple-cross lamination. Wave and current ripples (Fig. 11G–I) and bioturbation structures (mainly ichnogenus *Thalassinoides*, rarely *Ophiomorpha*, *Treptichnus*, *Planolites, Nereites*, and other; see Leszczyński 2018; Fig. 15E), are frequently encountered on cross-set bounding surfaces. However, bioturbation is restricted to these bedding surfaces and is rarely visible in vertical bed cross-sections. The trace fossil assemblage represents a proximal expression of the *Cruziana* Ichnofacies. Some cross-strata sets show hydroplastic deformation and partial homogenization by liquefaction (Fig. 17). The sandstone in the quarry is exploited as a building stone.

Genesis: The sedimentary succession at both sub-stops is thought to represent a shoaling-upwards tidal bar, increasingly wave-worked at the top (lithofacies Sw and Sp). The cross-strata sets represent 2D and 3D dunes migrating over an accreting tidal bar, obliquely to its axis (cf. Fig. 19). Plane-parallel stratified and ripple cross-laminated sandstones in the top part of the tor are thought to represent a wave-dominated bar top shoal, probably merged with the upper shoreface environment of the basin shoreline.

Stop 8

Rakowiczki, abandoned quarry in the village of Rakowice Małe (German *Wenig Rackwitz*) (Fig. 40); 51° 9' 55.6'' E, 15° 32' 33.8'' E; Abandoned quarry now mostly overgrown with young trees. The southern wall, up to 10 m high, shows sandstones. The northern wall, now up to 15 m high, shows sandstones in the lower part, up to 4 m high, and claystones, mudstones, siltstones and sandstones in the upper part (Fig. 24).

Structure and stratigraphy: Southwestern outskirts of the Bolesławiec Syncline; Żerkowice Member of the Rakowice Wielkie Formation (lower Coniacian) and Nowogrodziec Member of the Czerna Formation (lower Santonian; Fig. 24).

Subject: Fully marine to brackish shoreface; lagoonal and paludal sediments; palaeosol; marine regression/transgression record; fossils; bioturbation.

Remarks: Rakowice Małe is one of the main localities for the extraction of Cretaceous sandstones and for studies of North-Sudetic Cretaceous stratigraphy and related historical collections of Cretaceous megaflora. The extraction of sandstone from here lasted several hundred years. Rich floral collections have been collected from this quarry and other outcrops in the area, and palaeobotanical issues

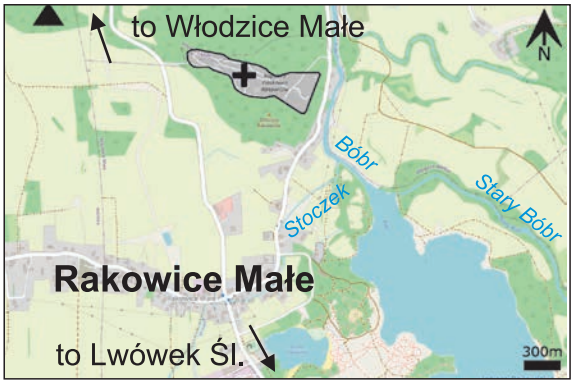

Fig. 40. Location of stop 8. For explanation of symbols see Fig. 30.

are discussed separately at the end of the stop description.

The sedimentary succession in the quarry, particularly the part representing the Czerna Formation, has been described in many papers since the 19th century. The Żerkowice Member below consists predominantly of fine- and medium-grained, cream-yellow to locally orange-brown, moderately hard, non-calcareous quartzose sandstones, plane-parallel and through cross-stratified (lithofacies Sp and Sc of Leszczyński and Nemec, 2020), partly massive-looking and indistinctly bedded (Fig. 24D, E). The massive-looking and planar parallel-stratified lithofacies form the topmost part of the unit. Cross-strata sets range from a decimetre to 1 m thickness and show variable, often bidirectional transport directions. Rare, taxonomically undefined bioturbation structures (ethologically mostly pascichnia) and the ichnogenera *Ophiomorpha* and *Thalassinoides* are encountered on the bedding surfaces (Leszczyński 2010, 2018; Fig. 15D). The upper boundary of the Żerkowice Member is sharp, flat, ferruginized, and covered with ironstone crust. Until 2012, the sandstones of this unit were extracted in this quarry as valuable buildingstone, whetstone, and carvingstone for several hundred years.

The overlying Czerna Formation begins with a layer of cream-yellow, cherry-red, and orange banded, streaked, and mottled muddy claystone, 0.65 m thick (Fig. 26J). The cherry-red variety displays vertically elongate, white-coloured root-like structures. X-ray diffraction analysis revealed that this is a kaolinite-dominated deposit (average kaolinite content 53.9% by weight). The basal layer passes upwards into a 70 cm thick bed of mottled, brown mudstone, with a 15–20 cm thick interlayer of mottled siltstone to fine-grained sandstone in its lower part. The deposits show dispersed coalified plant fragments. The top of the mudstone layer is marked by a level rich in coalified plant fragments, locally forming a shiny coal layer as much as 2 cm thick.

The overlying part of the succession begins with a 37 cm thick bed of grey-brown, mottled to subtly parallel laminated mudstone (with plant roots?) that grades upwards into siltstone and subsequently to an argillaceous sandstone as much as 30 cm thick. The latter grades upwards into a 22 cm thick layer of dark-brown mudstone capped by a 5–10 cm thick coal seam. The sandstone is rich in large coalified plant debris and is cut by plant roots (Fig. 24C). This basal part of the Czerna Formation is tectonically duplexed in the eastern part of the quarry (with only remnants presently visible), whereas small thrusts occur in its western part, now covered by the quarry waste (see Leszczyński 2010, fig. 3).

The coal seam overlying the duplexed part shows burrows reminiscent of the ichnogenus *Thalassinoides*. The coal seam is overlain by a brown mudstone, 33–45 cm thick, showing a mottled structure and locally penetrated by plant roots (Fig. 24C). This mudstone is overlain by a bed of impure coal, up to 20 cm thick (see log height 12.7 m in Fig. 24). Over the duplex structure, this coal seam occurs amalgamated into one bed with the lower-lying seam. The upper coal seam is brittle with sand insertions, similar to the lower-lying seam. The coal shows sand insertions with tortuous shapes and some dish shaped lamellation in cross-section. They resemble structures described by Kamola (1984) as various ichnospecies of *Thalassinoides*. The tortuous ones with lamellae resemble structures shown by Seilacher (1955) as cf. *Phycodes palmatum* Hall (1852), and to some extent *Teichichnus zigzag* Frey and Bromley 1985. Their tortuosity may be in part a result of compaction. The bundles of lens-shaped sand insertions may possibly represent the ichnogenus *Phycodes*. Some lenses showing a striated surface and an obliquely laminated interior in cross section may represent the ichnogenus *Teichichnus*. The branched, rope-sized burrows represent

two *Thalassinoides* isp. Another feature of the coal seam is the occurrence, at its top, of tree trunk fragments containing casts of the wood borings *Teredolites clavatus* Leymerie, 1842 (Leszczyński 2010, fig. 10E, F). Compositionally, this coal bed corresponds to the "log-ground" of Savrda et al. (1993): that is, a ground consisting of a high concentration of allochthonous wood strewn across a depositional surface.

The overlying unit is a highly to completely bioturbated argillaceous sandstone passing upwards into a sandstone-mudstone heterolithic packet (Fig. 24 log, B), showing variable bioturbation intensity (Fig. 26K–M). This whole unit is 165 cm thick. The argillaceous sandstone shows a mottled structure with remnants of flaser and wavy bedding. Trace fossils of the ichnogenera *Asterosoma*, *Palaeophycus*, *Ophiomorpha*, *Thalassinoides*, *Planolites*, and *Taenidium* are the dominant recognizable ichnotaxa (Leszczyński 2010), particularly in the lower part of the muddy-sandstone unit. In places, the sediment fabric seems to show *Asterosoma* and inferred *Cylindrichnus* overprinted by *Thalassinoides* isp., a thickly mud-lined burrow tentatively called *Palaeophycus* isp., *P.* cf. *tubularis* Hall, 1847, and *Planolites* isp. indet. (Fig. 26L). Elsewhere in the lower part of the unit, the ichnofabric is dominated by roughly horizontally winding burrows of the ichnogenus *Ophiomorpha* and *Palaeophycus* (Leszczyński, 2010, fig. 12B). Most burrows in the lower part of the argillaceous sandstone resemble *Ophiomorpha irregulaire* Frey, Howard and Pryor, 1978 (Leszczyński, 2010, fig. 12A, C, D). They are accompanied by rare burrows showing annulations of pelleted mud lining as in *O. annulata* (Książkiewicz 1977; see Leszczyński 2010, fig. 12A, B). Bedding-parallel to oblique burrows, resembling the ichnogenus *Taenidium*, occur locally in the argillaceous sandstone. Specimens of *Taenidium baretti* (Bradshaw,1981) (Leszczyński 2010, fig. 12C, D) and *Taenidium serpentinum* Heer, 1877 (see Leszczyński 2010, fig. 12B) were recorded in the *Ophiomorpha*-dominated division. In total, the trace fossil assemblage appears to represent the *Cruziana* Ichnofacies in the proximal expression of a stressed environment.

The upper part of the heterolithic packet comprises interbedded drab to pale-coloured argillaceous sandstone, arenitic sandstone, and grey to dark-brown sandy mudstone and mudstone. These deposits show variable intensities and styles of bioturbation. The proportion of sandstone relative to mudstone decrease upwards, as the mudstone also becomes more clayey. The less bioturbated divisions show wavy to lenticular bedding. Current ripple lamination with variable and often bidirectional inclination, combined-flow ripples, and wave ripples are recognizable in the poorly bioturbated sand lenses and layers. The icnofabric primarily consists of irregular tan to drab sediment mottles. Distinct trace fossils are represented by several ichnotaxa dominated by 1 mm thick, bedding-parallel to vertical, mud-lined and sand-filled burrows and similarly thick, unlined, mud-filled burrows. Some thin, mud-lined burrows are U-shaped and Y-shaped and resemble *Arenicolites* (Fig. 26M) and *Psilonichnus*. They are analogous with burrows of the polychaete *Capitella* cf. *capitula* described from the upper offshore of Georgia, U.S.A. (Hertweck et al. 2007). The mud-lined burrows showing different orientations to bedding seem to correspond to the trace fossil *Bornichnus tortuosus* Bromley and Uchman (2003) described from the Lower–Middle Jurassic tidal flat deposits of Bornholm (Denmark). Ichnotaxa also include *Schaubcylindrichnus* isp. indet., ?*Phycosiphon* isp. indet., *Planolites* isp. indet. and other taxonomically undetermined forms. Some *Schaubcylindrichnus* specimens resemble the ichnospecies S. *coronus* Frey and Howard, 1981. They tend to occur in bundles of congruent, sand-lined tubes. Some rock parts contain aggregations of taxonomically undetermined sand-filled burrows resembling diminutive *Planolites* in cross-section and small burrows showing concentric structure in cross-section. The trace fossil assemblage would seem to represent a single ecological suite. The forms of structures, the inferred ichnotaxa and the sedimentological and ichnological context of these deposits indicate the *Cruziana* Ichnofacies of a highly stressed environment.

The heterolithic packet passes gradually upwards into a 1 m thick bed composed of grey to greenish-grey and green clayey mudstone sandwiched by several thin clay ironstone (siderite) interbeds and topped by a coaly mudstone layer several centimetres thick (log height 16.0 m in Fig. 24). The latter is

the highest unit in the local sedimentary succession of the Nowogrodziec Member. No distinct bioturbation structures have been found in the mudstone deposit. Examination of three samples from its lower, middle, and upper parts revealed an absence of foraminifers or other microfossils.

The overlying coaly mudstone is highly burrowed in its upper part, where bioturbation obscures its upper boundary and adds to its gradual passage into the overlying sandstone. Bioturbation is dominated by densely packed sand-filled burrows *Asterosoma ludwigae* Schlirf, 2000, accompanied by *Thalassinoides* isp. indet., *Chondrites* isp. indet. (Leszczyński 2010, fig. 14D–F; Fig. 26N) and some other taxonomically undetermined ichnotaxa. *Asterosoma* dominates in the whole bioturbated division, whereas *Thalassinoides* is most densely distributed from 10 to 20 cm above the lower boundary of the mudstone bed and *Chondrites* is recorded only from 5 to 9 cm above this boundary. *Asterosoma* is intersected by *Thalassinoides* isp. Both ichnotaxa cross-cut *Chondrites* isp. Burrowing becomes less distinct upwards, in the drab coloured argillaceous sandstone; however, the mottled appearance of its splitting surfaces suggests profound bioturbation. The ichnofossils are typical of taxonomically impoverished archetypal *Cruziana* Ichnofacies (see MacEachern et al. 2007).

The overlying part of the sedimentary succession (above log height 15.8 m in Fig. 24) consists of two coarsening- to fining-upwards divisions comprising seven lower-order coarsening-upward divisions. The top part of this unit is strongly reworked by Quaternary surficial processes. The whole unit is rather poorly preserved, being strongly jointed, irregularly impregnated with iron oxides, and commonly penetrated by recent plant roots (Fig. 26O). Massive or cross-stratified sandstone deposits are present, and a sand-dominated heterolithic deposit occurs at its top. The heterolithic deposit shows wavy to lenticular bedding and a chaotic structure. The lamination of current ripples, combined-flow ripples, and wave ripples is visible locally. The sandstone deposit is pale to orange and yellowish in colour and shows a generally massive structure. Some of its parts display ripple lamination and medium-scale cross-stratification. It shows sparse to abundant bioturbation. Thorough examination revealed the occurrence of *Asterosoma* isp. indet. (see Leszczyński 2010, fig. 15C, D), *Paleophycus* cf. *tubularis*, *Ophiomorpha* cf. *irregulaire* (see Leszczyński 2010, fig. 15D, E), *O.* cf. *nodosa*, and *Planolites* isp. Argillaceous sandstone shows rich casts and molds of various bivalves (e.g., *Cyrena cretacea*), partly concentrated on bedding surfaces. The sandstone of the lower part of the thickest coarsening-upwards unit shows bivalve shells in life position and fragments of vertical to nearly vertical, cylindrical, smooth-walled burrows resembling *Skolithos linearis* Haldeman, 1840 (see Leszczyński 2010, fig. 16C, D) and *Arenicolites*-like trace fossils. The trace fossils in heterolithic deposits represent the *Cruziana* Ichnofacies in a distal to proximal expression of a stressed environment, whereas the assemblage recorded in massive, poorly bioturbated sandstones seems to represent the *Skolithos* Ichnofacies.

Small thrusts and tectonic duplexing occur in the lower part of the Czerna Formation (Leszczyński 2010, fig. 3), although these former features in the western quarry segment are now covered by the quarry waste, whereas the duplexed body, ca. 13 m in length, has been removed by mining operations.

Palaeobotany of the stop and its surroundings: The Nowogrodziec Member of the Czerna Formation has been the focus of recent palaeobotanical investigations by a joint Polish–Czech–German team (see Halamski et al. 2020 and references therein). The earliest plant fossils have been found directly at the boundary between the Żerkowice Member and the Czerna Formation (see Assemblage 4 in Halamski et al. 2020). This assemblage is dominated by the angiosperm *Dewalquea haldemiana* (Fig. 16I) and the matoniaceous fern *Konijnenburgia* cf. *galleyi* (Fig. 16K). Both have thick coriaceous leaves and may be interpreted as dwellers of xerophytic habitats (dryland and/or fern savannas). The next assemblage (Assemblage 5 in Halamski et al. 2020) comes from about 6–8 m of overlying dark siltstone containing irregular coal intercalations (including, therefore, parts B–C of the lithological column given in Fig. 24) This assemblage is dominated by the conifer *Geinitzia reichenbachii* (Fig. 16J) and clearly corresponds to backswamp forests.

The mesoflora and microflora have been recently studied on the basis of collections from

the upper part of the Nowogrodziec Member (corresponding to the megafloral Assemblage 5, stratigraphy as above). The mesoflora is relatively poor, and recent investigations failed to locate the rich mesofloral level from which the material described by the Czech palaeobotanist Ervín Knobloch was reportedly derived (Knobloch and Mai 1986).

The microflora consists of 126 taxa, including 105 terrestrial palynomorphs (54 bryophyte, lycophyte, and pteridophyte spores, 16 gymnosperms, 35 angiosperms; Halamski et al. 2020). Marine palynomorphs, in particular dinocysts, are extremely infrequent. Therefore, in contrast to initial expectations, the position of the Coniacian–Santonian boundary could not be verified on the basis of microflora.

The microflora from this area had previously been investigated by the pioneering palynologists F. Thiergart and W. Krutzsch. Thiergart (1942) described a characteristic schizeaceous fern spore *Appendicisporites appendicifer*. Krutzsch (1966) distinguished the "Löwenberger Bild" as an informal palynostratigraphic unit within the Cretaceous. Locality data for Krutzsch's samples are not available, but he presumably collected them at Rakowice Małe, the largest quarry in the region. However, his palynofloral list is notably different from the findings of recent authors even at the genus level (see Halamski et al., 2020, p. 858 for details). An interesting direction for future research would be to explore the details and reasons for these differences.

Genesis: The sandstones in the lower part of the sedimentary succession (Żerkowice Member) show features (lithofacies and trace fossils) indicative of a shoaling tidal bar complex overlain by the encroaching basin margin shoreface and foreshore (Fig. 24). In contrast, the lower part of the Czerna Formation (Nowogrodziec Member), indicates sedimentation on a vegetated coastal limnic plain increasingly invaded by seawater. The change of depositional environment recorded by the Czerna Formation is attributed to a separation of the coastal plain from the open sea by a sand barrier formed within the transgressive systems tract (Figs 28D, 29). Siltstones with plant roots and driftwood fragments showing the trace fossil *Teredolites clavatus*, together with coal seams containing *Thalassinoides* isp., are thought to represent a coastal plain with paludal sedimentation and incursions of marine water. The fining-upwards top part of the Nowogrodziec Member – showing an almost archetypal *Cruziana* Ichnofacies suggesting highly stressed brackish conditions – indicates extensive marine drowning and lagoonal sedimentation. The termination of the drowning, marked as a maximum flooding surface (Fig. 29), is indicated by the coaly mudstone at the top of the Nowogrodziec Member. A punctuated normal regression with prograding brackish bay shoreface and deltas is inferred from lithofacies, ichnofossils and body fossils for the deposits overlying the Nowogrodziec Member and topping the examined succession (Fig. 29). The trace fossils indicate *Cruziana* Ichnofacies and *Skolithos* Ichnofacies in an expression of slightly stressed environments.

Stop 9

Active open pit (Kopalnie Surowców Mineralnych Surmin-Kaolin S.A. in Nowogrodziec; Quarzwerke GmbH group) near the town of Nowogrodziec (German *Naumburg am Queis*; Fig. 41); 51° 12' 45'' N, 15° 22' 31'' E; pit ca. 500×550 m in area, ca. 25 m deep, active, with 10 extraction horizons.

Structure and stratigraphy: Bolesławiec Syncline; Czerna Formation (German *Überquader*), Santonian(?)

Subject: Sedimentological features; origin and economic significance.

Fig. 41. Location of stop 9. For explanation of symbols see Fig. 30.

Remarks: Sedimentary succession composed of lenses and beds of brittle, trough and rarely planar cross-stratified or structureless, very coarse- to fine-grained, greyish-white to white, subordinately orange-brown, quartzose sandstones, minor granule to pebble quartzose conglomerates, and light-grey to white poorly cemented siltstones, mudstones (muds), and claystones (clays). The lenses and beds of the fine-grained sediments are 0.2–3.0 m thick, mostly 0.5–1.5 m, and constitute ca. 25% of the whole succession (Galos 2020). The succession dips homoclinally £12° to the northeast (Fig. 27).

These are typical kaolins. Here, white-firing clay is extracted from both the coarse-grained and fine-grained sediments by washing the crushed output from parts of the succession where the proportion of good quality clay minerals is >20%.

Genesis: The mainly lenticular beds of both coarse- and fine-grained sediments, common cross-stratification of sandy, and erosional gravelly horizons indicate an alluvial origin of the sedimentary succession. The white colour of sediments results from bleaching by highly acidic pore waters (e.g., Rushton et al., 2020 and references therein)

Stop 10

Osiecznica (German *Wehrau*), **the birthplace of** Abraham Gottlob Werner (1749–1817), the founder of Neptunism theory (Fig. 42); 51° 19' 36.3'' N, 15° 25' 23.3'' E. Rock tors on the left bank of the Kwisa river gorge.

Structure and stratigraphy: Bolesławiec Syncline; upper Cenomanian Wilków Sandstone Member (German *Unterquader*) of the Rakowice Wielkie Formation

Subject: Sedimentological features and origin of late Cenomanian deposits at the norththeastern margin of the North Sudetic Synclinorium; natural resources of the local Cretaceous and their use.

Remarks: The rock tors show diffusely interbedded, structureless to crudely cross-stratified, medium- to coarse-grained quartzose, noncalcareous sandstones and granule to

Fig. 42. Location of stop 10. For explanation of symbols see Fig. 30.

fine pebble conglomerates with poor kaolinitic and ferrous cement and amuddy matrix. The rock colour is whitish grey to drab, zonally orange-brown. Deposits in nearby outcrops are covered by grey, thin-bedded sandy marlstones. The Cenomanian age of these sediments is based on the occurrence of *Pecten asper* Lamarck, found in an old quarry ("Napoleon") south of the Bolesławiec–Kliczków road and in excavations to the north of it (see Przybylski and Ihnatowicz 2012). The sandstones are vertically and horizontally fractured. They used to be mined in quarries a few kilometres to the southeast.

The village of Osiecznica is presently the second-largest glass sand pit processing plant in Poland. The Coniacian Żerkowice Sandstone exploited here is an almost loose sand, containing >99% SiO_2. The sedimentological features of these sandy and overlying muddy deposits are described in the main text of the guidebook.

Genesis: The sediments in the tors show features indicative of deposition in a high wave-energy shoreface, dominated by longshore currents and sea storms.

REFERENCES

Alexandrowicz, S.W. 1976. Foraminifera from the brackish Santonian deposits in the North Sudetic Basin (Western Poland). Rocznik PTG, Annales de la Société Géologique de Pologne, 46, 183–195.

Allen, J.R.L. 1982. Sedimentary Structures: Their Character and Physical Basis, Vol. 2. Developments in Sedimentology, 30B, 643 p. Elsevier; Amsterdam.

Allmon, W.D. and Cohen, P.A. 2008. Palaeoecological significance of turritelline gastropod-dominated assemblages from the mid-Cretaceous (Albian–Cenomanian) of Texas and Oklahoma, USA. Cretaceous Research, 29, 65–77.

Andert, H. 1934. Die Fazies in der sudetischen Kreide unter besonderer Berücksichtigung des Elbsandsteingebirges. Zeitschrift der Deutschen Geologischen Gesellschaft, 86, 616–636.

Aramowicz, A., Anczkiewicz, A.A. and Mazur, S. 2006. Fission-track dating of apatite from the Góry Sowie Massif, Polish Sudetes, NE Bohemian Massif: Implications of post-Variscan denudation and uplift, Neues Jahrbuch für Mineralogie – Abandlungen, 182, 221–229.

Badura, J. 2005. Szczegółowa mapa geologiczna Polski, 1:50 000, arkusz Bolesławiec (621). Wydawnictwa Geologiczne; Warszawa.

Badura, J., Przybylski, B. and Zuchiewicz, W. 2004. Cainozoic evolution of Lower Silesia, SW Poland: A new interpretation in the light of sub-Cainozoic and sub-Quaternary topography, Acta Geodynnamica Geomaterialia, 1 (135), 6–29.

Badura, J., Pécskay, Z., Koszowska, E., Wolska, A., Zuchiewicz, W. and Przybylski, B. 2005. New age and petrological constraints on Lower Silesian basaltoids, SW Poland, Acta Geodynamica et Geomaterialia, 2 (139), 6–15.

Barbacka, M. Pacyna, G. and Halamski, A.T. in press. Achievements of Polish palaeobotany during the last 100 years. Palaeozoic and Mesozoic floras. 3. Mesozoic macrofossils. Annales Societatis Botanicorum Poloniae.

Beddingfield, S.D. and McClintock, J.B. 1993. Feeding behavior of the sea star *Astropecten articulatus* (Echinodermata: Asteroidea): an evaluation of energy-efficient foraging in a soft-bottom predator. Marine Biology, 115, 669–676.

Berg, G. 1913. Beiträge zur Geologie von Niederschlesien mit besonderer Berücksichtigung der Erzlagerstätten. Abhandlungen der Königlich Preußischen Geologischen Landesanstalt. Neue Folge, 64, 1–63.

Berg, G. 1938. Erläuterungen zu Blatt Landeshut, Lieferung 193. Preußische Geologische Landesanstalt, Berlin.

Beyrich, E. 1849. Das Quadersandsteingebirge in Schlesien. Zeitschrift der Deutschen Geologischen Gesellschaft, 1, 390–393.

Beyrich, E. 1855. Ueber die Lagerung der Kreideformation im schlesischen Gebirge. Abhandlungen der Königlichen Akademie der Wissenschaften zu Berlin, 26, 56–80.

Biernacka, J. 2012. Provenance of Upper Cretaceous quartz-rich sandstones from the North Sudetic Synclinorium, SW Poland: Constraints from detrital tourmaline. Geological Quarterly, 56, 315–332.

Biernacka, J. and Józefiak, M. 2009. The Eastern Sudetic Island in the early-to-middle Turonian: Evidence from heavy minerals in the Jerzmanice sandstones, SW Poland. Acta Geologica Polonica, 59, 45–565.

Birkenmajer, K., Jeleńska, M., Kądziałko-Hofmokl, M. and Kruczyk, J. 1966. Age of deep-seated fractures zones in Lower Silesia (Poland), based on K-Ar and paleomagnetic dating of Tertiary basalts. Annales de la Société géologique de Pologne, 46, 545–552.

Birkenmajer, K., Pécskay, Z., Grabowski, J., Lorenc, M.W. and Zagożdżon, P.P. 2004. Radiometric dating of the Tertiary volcanics in Lower Silesia, Poland. IV. Further K-Ar and paleomagnetic data from late Oligocene to early Miocene basaltic rocks of the Fore-Sudetic block. Annales Societatis Geologorum Poloniae, 64, 1–19.

Blake, D.B. and Guensburg, T.E. 2016. An asteroid (Echinodermata) faunule from the Oxfordian Swift Formation (Upper Jurassic) of Montana. Journal of Paleontology, 90, 1160–1168.

Bobiński, W., Gawlikowska, E. and Kłonowski, M. 1999. Important geosites of the Polish Sudetes. Polish Geological Institute Special Papers, 2, 19–26.

Born, A. 1921. Über Jungpaläozoische kontinentale Geosynklinalen Mitteleuropas. Abhandlungen der Senckenberg Gesellschaft für Naturforschung, 360, 506–583.

Bossowski, A. 1991. Wykroty N-14. Profile Głębokich Otworów Wiertniczych Państwowego Instytutu Geologicznego, 62, 1–45.

Botor, D., Anczkiewicz, A.A., Mazur, S. and Siwecki, T. 2019. Post-Variscan thermal history of the Intra-Sudetic Basin (Sudetes, Bohemian Massif) based on apatite fission track analysis. International Journal of Earth Sciences, 108, 2561–2566.

Bradshaw, M.A. 1981. Palaeoenvironmental interpretations and systematics of Devonian trace fossils from the Taylor Group (Lower Beacon Supergroup), Antarctica. New Zealand Journal of Geology and Geophysics, 24, 615–652.

Bromley, R.G. and Uchman, A. 2003. Trace fossils from the Lower and Middle Jurassic marginal marine deposits of the Sorthat Formation, Bornholm, Denmark. Bulletin of the Geological Society of Denmark, 50, 185–208.

Burkowicz, A., Galos, K. and Guzik, K. 2020. The resource base of silica glass sand versus glass industry development: The case of Poland. Resources, 9, 1–20.

Caregnato, F.F., Wiggers, F., Tarasconi, J.C. and Veitenheimer-Mendes, I.L. 2009. Taxonomic composition of mollusks collected from the stomach content of *Astropecten brasiliensis* (Echinodermata: Asteroidea) in Santa Catarina, Brazil. Revista Brasileira de Biociências, 7, 252–259.

Čech, S. 2011. Palaeogeography and Stratigraphy of the Bohemian Cretaceous Basin (Czech Republic) – an overview. Geologické výzkumy na Moravě a ve Slezsku, 1, 18–21.

Charpentier, J.F.W. 1768. Mineralogische Geographie der Chursächsischen Lande, 432 p. S.L. Crusius; Lepizig.

Chrząstek, A. and Jewticz, S. 2019. Trace fossils and associated mollusc fossils from the Coniacian sandstones (Żeliszów Quarry, Żerkowice Quarry) from the North Sudetic Synclinorium – new palaeoecological and palaeoenvironmental implications. In: Muszer, J., Chrząstek, A. and Niedźwiedzki, R. (Eds), XXIV Konferencja Naukowa Sekcji Paleontologicznej Polskiego Towarzystwa Geologicznego, "Od prekambru do holocenu – zmiany bioróżnorodności zapisane w skałach". Materiały konferencyjne. PTG, UWr, Zakład Geologii Stratygraficznej Instytutu Nauk Geologicznych, Zakład Paleozoologii Instytutu Biologii Środowiskowej, Wrocław 2019, 17–18. [in Polish]

Chrząstek, A., Muszer, J., Solecki, A. and Sroka, A.M. 2018. *Rosarichnoides sudeticus* igen. et isp. nov. and associated fossils from the Coniacian of the North Sudetic Synclinorium (SW Poland). Geological Quarterly, 62, 181–196.

Chrząstek, A. and Wojewoda, J. 2011. Mesozoic of South-Western Poland (The North Sudetic Synclinorium). In: Żelaźniewicz, A., Wojewoda, J. and Ciężkowski, W. (Eds), Mezozoik i Kenozoik Dolnego Śląska [Mesozoic and Cenozoic of the Lower Silesia]. pp. 1–10. WIND; Wrocław. [In Polish with English summary]

Chrząstek, A. and Wypych, M. 2018. Coniacian sandstones from the North Sudetic Synclinorium revisited: palaeoenvironmental and palaeogeographical reconstructions based on trace fossil analysis and associated body fossils. Geologos, 24, 29–53.

Clifton, H.E. and Dingler, J.R. 1984. Wave-formed structures and paleoenvironmental reconstruction. Marine Geology, 60, 165–198.

Cloos, H. 1922. Der Gebirgsbau Schlesiens und die Stellung seiner Bodenschätze, 106 p. Gebrüder Borntraeger; Berlin.

Cohen, K.M., Finney, S.C., Gibbard, P.L. and Fan, J.-X. 2013. The ICS International Chronostratigraphic Chart. Episodes, 36, 199–204.

Csiki-Sava, Z., Buffetaut, E., Ősi, A., Pereda-Suberbiola, X. and Brusatte, S.L. 2015. Island life in the Cretaceous – faunal composition, biogeography, evolution, and extinction of land-living vertebrates on the Late Cretaceous European archipelago. ZooKeys, 469, 1–161.

Cymerman, Z., Ihnatowicz, A., Kozdrój, W. and Przybylski, B. 2005a. Szczegółowa mapa geologiczna Polski, 1:50 000, arkusz Lwówek Śląski (658). Wydawnictwa Geologiczne; Warszawa.

Cymerman, Z., Ihnatowicz, A., Kozdrój, W. and Przybylski, B. 2005b. Szczegółowa mapa geologiczna Polski, 1:50 000, arkusz Lubań (656). Wydawnictwa Geologiczne; Warszawa.

Danišík, M., Migoń, P., Kuhlemann, J., Evans N.J., Dunkl, I. and Frisch, W. 2010. Thermochronological constraints on the long-term erosional history of the Karkonosze Mts., Central Europe. Geomorphology, 116, 68–89.

Dercourt, J., Gaetani, M., Vrielynck, B., Barrier, E., Biju-Duval, B., Brunet, M. F., Cadet, J.P., Crasquin, S. and Snadulescu, M. 2000. Atlas Peri-Tethys, Palaeogeographical Maps. CCGM/CGMW, Paris: 24 maps and explanatory notes, I–XX, 269 pp.

Drescher, R. 1863. Ueber die Kreide-Bildungen der Gegend von Löwenberg. Zeitschrift der Deutschen Geologischen Gesselschaft, 14, 291–366.

Drozdowski, S., Engel, W. and Falecki, W. 1978. Dokumentacja geologiczna złoża rud miedzi Wartowice w kategorii C. Archives, Przedsiębiorstwo Geologiczne; Wrocław.

Dunne, L.A. and Hempton, M.R. 1984. Deltaic sedimentation in the Lake Hazar pull-apart basin, southeastern Turkey. Sedimentology, 31, 401–412.

Dyjor, S. 1995. Young Quaternary and recent crustal movements in Lower Silesia, SW Poland. Folia Quarternaria, 66, 51–58.

Ehling, A. 2006. Eigenschaften, Abbau und Verwendung schlesischer Bausandsteine – ein aktueller Vergleich mit der Historie. Zeitschrift der Deutschen Gesellschaft für Geowissenschaften, 158, 351–360.

Frey, R.W. and Bromley, R.G. 1985. Ichnology of American chalks: the Selma Group (Upper Cretaceous), western Alabama. Canadian Journal of Earth Sciences, 22, 801–828.

Frey, R.W. and Howard, J.D. 1981. Conichnus and Schaubcylindrichnus: redefined trace fossils from the Upper Cretaceous of the Western Interior. Journal of Paleontology, 55, 800–804.

Frey, R.W., Howard, J.D. and Pryor, W.A. 1978. Ophiomorpha: its morphologic, taxonomic and environmental significance. Palaeogeography, Palaeoclimatology, Palaeoecology, 23, 199–229.

Galos, K. 2010. Ball clays for the production of porcelain tiles in Poland. Gospodarka Surowcami Mineralnymi, 26, 21–43.

Goeppert, H.R. 1841. Über die fossile Flora der Quadersandsteinformation in Schlesien, als erster Beitrag zur Flora der Tertiärgebilde. Nova Acta Academiae Caesareae Leopoldinae Naturae Curiosorum, 19, 99–134.

Goeppert, H.R. 1844. Uebersicht der fossilen Flora Schlesiens. In: Wimmer, F. (Ed.), Flora von Schlesien, preussischen und österreichischen Antheils. Zweiter Band, 156–225. Ferdinand Hirt; Breslau.

Górniak, K. 1991. The influence of sedimentary and early diagenetic conditions on the mineral composition of alluvial sediments (an example of sandy-clayey sediments of the North-Sudetic Trough). Prace Geologiczne PAN Oddział w Krakowie, 136, 1–95. [In Polish with English summary]

Górniak, K. 1996. The role of diagenesis in the formation of kaolinite raw materials in the Santonian sediments of the North-Sudetic Trough (Lower Silesia, Poland). Applied Clay Science, 12, 313–328.

Greguš, J., Kvaček, J. and Halamski, A.T. 2013. Revision of Protopteris and Oncopteris tree fern stem casts from the Late Cretaceous of Central Europe. Acta Musei Nationalis Pragae, Series B – Historia Naturalis, 69, 69–82.

Halamski, A.T. 2020. Upper Cretaceous megafloras of Poland – history of research, collections, and results of taxonomic revisions. In: Skrzyński, G., Badura, M. and Noryśkiewicz, A. (Eds), Sympozjum Sekcji Paleobotanicznej Polskiego Towarzystwa Botanicznego 4.12.2020. pp. 8–13. Polskie Towarzystwo Botaniczne, Warszawa. [In Polish, English summary]

Halamski, A.T., Kvaček, J., Svobodová, M., Durska, E. and Heřmanová, Z. 2020. Late Cretaceous mega-, meso-, and microfloras from Lower Silesia. Acta Palaeontologica Polonica, 65, 811–878.

Halamski, A.T. and Taylor, P.D. 2022. Angiosperm tree leaf as a bryozoan substrate: a case study from the Cretaceous and its taphonomic consequences. Lethaia, 55, 1–7.

Haldeman, S.S. 1840. Supplement to Number One of "A Monograph of the Limniades, or Freshwater Univalve Shells of North America" Containing Descriptions of Apparently New Animals in Different Classes, and the Names and Characters of the Subgenera in Paludina and Anculosa. 3 p. Philadelphia.

Hall, J. 1847. Palaeontology of New York. Volume 1. 338 p., C. Van Benthuysen; Albany.

Hall, J. 1852. Palaeontology of New York. Volume 2, 362 p., C. Van Benthuysen; Albany.

Haq, B.U. 2014. Cretaceous eustasy revisited. Global and Planetary Change, 114, 44–58.

Harries, P.J. and Ozanne, C.R. 1998. General trends in predation and parasitism upon inoceramids. Acta Geologica Polonica, 48, 377–386.

Hein, F.J. 1986. Tidal/littoral offshore shelf deposits – Lower Cambrian Gog Group, Southern Rocky Mountains, Canada. Sedimentary Geology, 52, 155–182.

Heer, O. 1877. Flora fossilis Helvetiae. Die vorweltliche Flora der Schweiz. 182 p. J. Wurster; Zürich.

Heřmanová, Z., Kvaček, J., Halamski, A.T., Zahajská, P. and Šilar, J. 2019. Reinterpretation of fossil reproductive structures *Zlivifructus microtriasseris* (Normapolles complex, Fagales) from the Czech and Polish Late Cretaceous. Review of Palaeobotany and Palynology, 268, 88–94.

Heřmanová, Z., Kvaček, J., Dašková, J. and Halamski, A.T. 2020. Plant reproductive structures and other mesofossils from Coniacian/Santonian of Lower Silesia, Poland. Palaeontologia Electronica, 23, a61.

Hertweck, G., Wehrmann, A. and Liebezeit, G. 2007. Bioturbation structures of polychaetes in modern shallow marine environments and their analogues to Chondrites group traces. Palaeogeography, Palaeoclimatology, Palaeoecology, 245, 382–389.

Jahn, A. 1980. Tertiary relief of the Sudetes. Geographia Polonica, 43, 5–23.

Jarmołowicz-Szulc, K. 1984. Geochronological study of a part of the northern cover of the Karkonosze granite by fission track method. Archiwum Mineralogiczne, 39, 139–183.

Jerzmański, J. 1955. Szczegółowa mapa geologiczna Sudetów w skali 1:25 000, arkusz Złotoryja. Instytut Geologiczny; Warszawa.

Kamola, D.L. 1984. Trace fossils from marginal-marine facies of the Spring Canyon Member, Blackhawk Formation (Upper Cretaceous), East-Central Utah. Journal of Paleontology, 58, 529–541.

Kley, J. and Voigt, T. 2008. Late Cretaceous intraplate thrusting in central Europe: effect of Africa–Iberia–Europe convergence, not Alpine collision. Geology, 36, 839–842.

Knobloch, E. and Mai, D.H. 1986. Monographie der Früchte und Samen in der Kreide von Mitteleuropa. Rozpravy Ústředního ústavu geologického, 47, 1–219.

Komar, P.D. and Miller, M.C. 1965. The initiation of oscillatory ripple marks and the development of planebed at high shear stresses under waves. Journal of Sedimentary Petrology, 45, 696–603.

Kowalski, A. 2021. Late Cretaceous palaeogeography of NE Bohemian Massif: diachronous sedimentary successionsin the Wleń Graben and Krzeszów Brachysyncline (SW Poland). Annales Societetis Geologorum Poloniae, 91, 1–36.

Kozdrój, W., Ihnatowicz, A. and Przybylski, B. 2005. Szczegółowa mapa geologiczna Polski, 1:50 000, arkusz Złotoryja (659). Wydawnictwa Geologiczne; Warszawa.

Krutzsch, W. 1966. Die sporenstratigraphische Gliederung der Oberkreide im nordlichen Mitteleuropa. Abhandlungen des Zentralen Geologischen Institutes, 8, 79–111.

Książkiewicz, M. 1977. Trace fossils in the flysch of the Polish Carpathians. Palaeontologia Polonica, 36, 1–208.

Leeder, M.R., Ord, D.M. and Collier, R. 1988. Development of alluvial fans and fan deltas in neotectonic extensional settings: implications for the interpretation of basin-fills. In: Nemec, W. and Steel, R.J. (Eds), Fan Deltas – Sedimentology and Tectonic Settings, pp. 163–185. Blackie; London.

Leszczyński, S. 2010. Coniacian–?Santonian paralic sedimentation in the Rakowice Małe area of the North Sudetic Basin, SW Poland: sedimentary facies, ichnological record and palaeogeographical reconstruction of an evolving marine embayment. Annales Societatis Geologorum Poloniae, 80, 1–24.

Leszczyński, S. 2018. Integrated sedimentological and ichnological study of the Coniacian sedimenta-

tion in North Sudetic Basin, SW Poland. Geological Quarterly, 62, 666–816.

Leszczyński, S. and Nemec, W. 2020. Sedimentation in a synclinal shallow-marine embayment: Coniacian of the North Sudetic Synclinorium, SW Poland. The Depositional Record, 6, 144–161.

Lewicka E. and Galos K. 2004. Gospodarka iłami ceramicznymi w Polsce. In: Surowce mineralne Polski. Surowce skalne. Surowce ilaste, pp. 341–369. Wydawnictwo Instytutu Gospodarki Surowcami Mineralnymi i EnergetycznymiPolskiej Akademii Nauk; Kraków.

Lorenc, S. and Mroczkowski, J. 1968. The sedimentation and petrography of Zechstein and lowermost Triassic deposits in the vicinity of Kochanow (Intra-Sudetic Trough). Geologia Sudetica, 13, 23–39.

MacEachern, J.A., Bann, K.L., Pemberton, S.G. and Gingras, M.K. 2007. The ichnofacies paradigm: High resolution paleoenvironmental interpretation of the rock record. In: MacEachern, J.A., Bann, K.L., Gingras, M.K. and Pemberton, S.G. (Eds), Applied Ichnology. Society of Economic Paleontologists and Mineralogists, Short Course Notes, 52, 27–64.

McBride, R.A. 2003. Offshore sand banks and linear sand ridges. In Middleton. G.V. (Ed.), Encyclopedia of Sediments and Sedimentary Rocks, pp. 636–639. Kluver Academic Publishers; Dordrecht.

Migoń, P. and Lidmar-Bergström, K. 2001. Weathering mantles and their significance for geomorphological evolution of central and northern Europe since the Mesozoic. Earth Science Reviews, 56, 285–324.

Milewicz, J. 1956. Zaburzenie utworów kredowych w Rakowicach Małych. Przegląd Geologiczny, 4, 361–364.

Milewicz, J. 1958. Podział stratygraficzny osadów kredowych w niecce północno-sudeckiej. Przegląd Geologiczny, 6, 386–388.

Milewicz, J. 1960. The Cretaceous of the Jerzmanice Graben (Sudetes). Biuletyn Instytutu Geologicznego, 239, 36–66. [In Polish with English summary]

Milewicz, J. 1964. Złoża górnokredowych iłów ceramicznych na tle budowy geologicznej depresji północnosudeckiej. Biuletyn Instytutu Geologicznego, 280, 216–259.

Milewicz, J. 1965. Facje górnej kredy wschodniej części niecki północnosudeckiej. Biuletyn Instytutu Geologicznego, 160, 15–80.

Milewicz, J. 1966. Kreda z głębokiego otworu Węgliniec IG 1. Kwartalnik Geologiczny, 10, 1144–1146.

Milewicz, J. 1968. The geological structure of the North-Sudetic Depression. Biuletyn Instytutu Geologicznego, 226, 5–26.

Milewicz, J. 1969. Distribution of Cretaceous Rocks in the North Sudetic Basin. Kwartalnik Geologiczny, 23, 819–825. [In Polish with English summary]

Milewicz, J. 1985. A proposal of formal stratigraphic subdivision of the infill of the North Sudetic Depression. Przegląd Geologiczny, 33, 385–389. [In Polish with English summary]

Milewicz, J. 1988. Makrofauna z osadów kredowych otworu wiertniczego Węgliniec IG 1. Kwartalnik Geologiczny, 32, 389–404.

Milewicz, J. 1996. Upper Cretaceous of the North Sudetic Depression (litho- and biostratigraphy, paleogeography, tectonics and remarks on raw materials). Prace Geologiczno-Mineralogiczne, 61, 1–59.

Milewicz, J. 2006. O osadach santońskich na obszarze basenu północnosudeckiego. Przegląd Geologiczny, 54, 693–694.

Mitura, J., Cieśliński, S. and Milewicz, J. 1969. Inoceramy kredowe z niecki północnosudeckiej. Biuletyn Instytutu Geologicznego, 216, 169–166.

Mohr, B. 2009. A truly European forest: A historic Lower Silesian Palaeobotanical Collection (Late Cretaceous) at the Museum of Natural History (Berlin). Earth Sciences History, 28, 276–292.

Musstow, R. 1968. Beitrag zur Stratigraphie und Paläogeographie der Oberkreide und des Albs in Ostbrandenburg und der östlichen Niederlausitz. Geologie, 16, 1–61.

Nieć, M. and Ratajczak, T. 2004. Złoża kopalin kaolinowych, iłów biało wypalających się i kopalin haloizytowych. In: Ney, R. (Ed.), Surowce Mineralne Polski. Surowce skalne. Surowce ilaste, pp. 31–66. Wydawnictwo Instytutu Gospodarki Surowcami Mineralnym i Eneregetycznymi Polskiej Akademii Nauk; Kraków.

Oberc, J. 1962. Sudety i Obszary Przyległe. In. Pożaryski, W. (Ed.), Budowa Geologiczna Polski, vol. 4, part 2, 306 p. Wydawnictwa Geologiczne; Warszawa.

Partsch, J. 1896. Schlesien. Eine Landeskunde für das deutsche Volk, 1. Teil: Das ganze Land. 420 p. Ferdinand Hirt; Breslau.

Postma, G. 1990. An analysis of the variation in delta architecture. Terra Nova, 2, 124–130.

Pożaryski, W., Brochwicz-Lewiński, W., Brodowicz, Z., Jaskowiak-Szoenejch, M., Milewicz, J., Sawicki, L. and Uberna, T. 1969. Geological Map of Poland and Adjoining Countries (without Cenozoic). Wydawnictwo Geologiczne; Warszawa.

Przybylski, B. and Ihnatowicz, A. 2005. Szczegółowa mapa geologiczna Polski, 1:50 000, arkusz Nowogrodziec (620). Wydawnictwa Geologiczne; Warszawa.

Przybylski, B. and Ihnatowicz, A. 2012. Objaśnienia do szczegółowej mapy geologicznej Polski, 1:50 000, arkuszNowogrodziec (620). 37 p. Wydawnictwa Geologiczne; Warszawa.

Rampino, M.R. and Sanders, J.E. 1981. Evolution of the barrier islands of southern Long Island, New York., Sedimentology, 28, 36–46.

Randhaber, K. 1906. Ein Beitrag zur Kenntniss der Bunzlauer Tone. 65 p. Kaemerer & CO; Halle.

Raumer, K., 1819. Das Gebirge Nieder-Schlesiens, der

Grafschaft Glatz und eines Theils von Böhmen und der Ober-Lausitz, geognostisch dergestellt. 182 p. G. Reimer; Berlin.

Retallack, G.J. 2001. Soils of the Past. 600 p. Blackwell; Oxford.

Reynaud, J.Y., Tessier, B., Proust, J.N., Dalrymple, R., Marsset, T., De Batist, M. and Lericolais, G. 1999. Eustatic and hydrodynamic controls on the architecture of a deep shelf sand bank (Celtic Sea). Sedimentology, 46, 603–621.

Rushton, J.C., Wagner, D., Pearce, J.M., Rochelle, C.A. and Purser, G. 2020. Red-bed bleaching in a CO_2 storage analogue: Insight from Entrada Sandstone fracture-hosted mineralization. Journal of Sedimentary Research, 90, 48–66.

Sanders, J.E. and Kumar, N. 1965. Evidence of shoreface retreat and in-place "drowning" during Holocene submergence of barriers, shelf off Fire Island, New York. Geological Society of America Bulletin, 86, 65–66.

Saul, L.R. and Squires, R.L. 1998. New Cretaceous gastropods from California. Palaeontology, 41, 461–488.

Savrda, C.E., Ozalas, K., Demko, T.H., Hutchinson, T.A. and Scheiwe, T.D. 1993. Log grounds and the ichnofossil *Teredolites* in transgressive deposits of the Clayton Formation (Lower Paleocene), western Alabama. Palaios, 8, 311–324.

Scupin, H. 1910. Über sudetische prätertiäre junge Krustenbewegungen und die Verteilung von Wasser und Land zur Kreidezeit in der Umgebung der Sudeten und des Erzgebirges. Zeitschrift für Naturwissenschaften, 82, 321–344.

Scupin, H. 1913. Die Löwenberger Kreide und ihre Fauna. Palaeontographica-Supplementbände, 6, 1–266.

Scupin, 1935. Die stratigraphischen Beziehungen der mittel- und nordsudetischen Kreide. Zeitschrift der Deutschen Geologischen Gesellschaft, 86, 523–538.

Scupin, H. 1936. Zur palaeographie des Sudetischen Kreidemeeres. Zeitschrift der Deutschen Gesellschaft für Geowissenschaften, 88, 309–325.

Seilacher, A. 1955. Spuren und Fazies im Unterkambrium. In: Schindewolf, O. H. and Seilacher, A. (Eds), Beitrage zur Kenntnis des Kambriums in der Salt Range (Pakistan), pp. 373–399. Akademie der Wissenschaften und Literatur, Mainz.

Skoček, V. and Valečka, J. 1983. Palaeogeography of the Late Cretaceous quadersandstein of central Europe. Palaeogeography Palaeoclimatology Palaeoecology, 44, 61–92.

Snedden, J.W., and Dalrymple, R.W. 1999. Modem shelf sand ridges: from historical perspective to a unified hydrodynamic and evolutionary model. In: Bergman, K.M and Snedden, J.W. (Eds), Isolated Shallow Marine Sand Bodies: Sequence Stratigraphic Analysis and Sedimentological Perspectives. Society for Sedimentary Geology (SEPM) Special Publication, 64, 13–28.

Sobczyk, A., Sobel, E.R. and Georgieva, V. 2019. Meso-Cenozoic cooling and exhumation history of the Orlica-Śnieżnik Dome (Sudetes, NE Bohemian Massif, Central Europe): Insights from apatite fission-track thermochronometry. Terra Nova, 32 (2), 122–133.

Sohl, N.F. 1987. Cretaceous gastropods: contrasts between Tethys and temperate provinces. Journal of Paleontology, 61, 1085–1111.

Sohl, N.F and Kollmann, H.A. 1985. Cretaceous Actaeonellid Gastropods from the Western Hemisphere. US Geological Survey Professional Paper, 1304, 1–97.

Solecki, A. 2011. Structural development of the epi-Variscan cover in the North Sudetic Synclinorium area. In: Żelaźniewicz, A., Wojewoda, J. and Ciężkowski, W. (Eds), Mezozoik i Kenozik Dolnego Śląska, pp. 19–36. WIND; Wrocław [In Polish, with English abstract.]

Sztromwasser, E. 1995. Szczegółowa mapa geologiczna Polski, 1:50 000, arkusz Chojnów (622). Wydawnictwa Geologiczne, Warszawa.

Stoch, L. 1962. Mineralogia glin kaolinitowych okolic Bolesławca. Prace Geologiczne, 6, 1–120.

Śliwiński, W., Raczyński, P. and Wojewoda, J. 2003. Sedimentation of the epi-Variscan cover in the North-Sudetic Basin. In: Ciężkowski, W., Wojewoda, J. and Żelaźniewicz, A. (Eds), Sudety zachodnie od wendu do czwartorzędu, pp. 119–126. Wind, Wrocław. [In Polish with English summary]

Thiergart, F. 1942. Mikropaläobotanische Mitteilungen 1–3. Jahrbuch der Reischsamtes für Bodenforschung, 62, 109–116.

Uličný, D. 2001. Depositional systems and sequence stratigraphy of coarse-grained deltas in a shallow-marine, strike-slip setting: The Bohemian Cretaceous Basin, Czech Republic. Sedimentology, 48, 599–628.

Uličný, D., Čech, S. and Grygar, R. 2003. Tectonics and depositional systems of a shallow marine, intra-continental strike-slip basin: Exposures of the Český Ráj region, Bohemian Cretaceous Basin. Geolines, 16, 133–148.

Uličný, D., L. Špičáková, L., Grygar, R., Svobodová, M., Čech, S. and Laurin, J. 2009. Palaeodrainage systems at the basal unconformity of the Bohemian Cretaceous Basin: Roles of inherited fault systems and basement lithology during the onset of basin filling. Bulletin of Geosciences, 84, 566–610.

Ulrych, J., Dostál, J. Adamovič, J., Jelínek, E., Špaček, P., Hegner, E. and Balogh, K. 2011. Recurrent Cenozoic volcanic activity in the Bohemian Massif (Czech Republic). Lithos, 123, 133–144.

Ventura, B., Lisker, F. and Kopp, J. 2009. Thermal and denudation history of the Lusatian Block (NE Bohemian Massif, Germany) as indicated by apatite fission-track data. The Geological Society, London, Geological Society Special Publications, 324, 181–192.

Villier, L., Kutscher, M. and Mah, C.L. 2004. Systematics and palaeoecology of middle Toarcian Asteroidea (Echinodermata) from the "Seuil du Poitou", Western France. Geobios, 37, 807–825.

Voigt, S., Wagreich, M., Surlyk, F., Walaszczyk, I., Uličný, D., Čech, S., Voigt, T., Wiese, F., Wilmsen, M., Niebuhr, B., Reich, M., Funk, H., Michalík, J., Jagt, J.W.M., Felder, P.J. and Schulp, A.S. 2008. Cretaceous. In: McCann, T. (Ed.), Geology of Central Europe. Volume 2: Mesozoic and Cenozoic, pp. 923–998. Geological Society; London.

Voigt, T., Kley, J. and Voigt, S. 2021. Dawn and Dusk of Late Cretaceous Basin Inversion in Central Europe. Solid Earth, 12, 1443–1461.

Walaszczyk, I. 2008. North Sudetic Basin (Outer Sudetic Cretaceous). In: T. McCann (Ed.), The Geology of Central Europe, 2 (Mesozoic and Cenozoic), pp. 959–960. Geological Society; London.

Walendowski, H. 2001. Piaskowce bolesławieckie w architekturze. Świat Kamienia, 6.

Williger, G. 1882. Die Löwenberger Kreidemulde, mit besonderer Berücksichtigung ihrer Fortsetzung in der preussischen Ober-Lausitz. Jahrbuch der königlichen preussischen geologischen Landesanstalt, 1881, 55–125.

Wilmsen, M., Uličný, D. and Košťák, M. 2014. Cretaceous basins of Central Europe: deciphering effects of global and regional processes – a short introduction. Zeitschrift der Deutschen Gesellschaft für Geowissenschaften, 165, 495–499.

Wilson, K. and Mohrig, D. 2021. Modern coastal tempestite deposition by a non-local storm: Swell-generated transport of sand and boulders on Eleuthera, The Bahamas. Sedimentology, 68, 2043–2068.

Wojewoda, J. 1986. Fault scarp induced shelf sand bodies in Upper Cretaceous of Intrasudetic Basin. In: Teisseyre A.K. (Ed.), 6th IAS Regional Meeting. Excursion Guidebook, Excursion A-1, pp. 31–52. Committee of Geological Sciences, Polish Academy of Sciences, Ossolineum; Wrocław.

Wojewoda, J. 1996. Upper Cretaceous littoral-to-shelf succession in the Intrasudetic Basin and Nysa Trough, Sudety Mts. In: Wojewoda, J. (Ed.), Obszary Źródłowe: Zapis w Osadach, pp. 81–96. WIND; Wrocław.

Wojewoda, J. 2020. Geoatrakcje pogranicza – Góry Stołowe i Broumowskie Ściany. B. Kokot vel Kokociński, Nowa Ruda, 300 p.

Wood, M.L. and Ethridge, F.G. 1988. Sedimentology and architecture of Gilbert- and mouth bar-type fan deltas, Paradox Basin, Colorado. In: Nemec, W. and Steel, R.J. (Eds), Fan Deltas – Sedimentology and Tectonic Settings, pp. 251–263. Blackie; London.

Wright, L.D. 1966. Sediment transport and deposition at river mouths: a synthesis. Geological Society of America Bulletin, 88, 856–868.

Ziegler, P.A. 1986. Late Cretaceous and Cenozoic intraplate compressional deformations in the Alpine foreland. Tectonophysics, 136, 389–420.

Żelaźniewicz, A., Aleksandrowski, P., Buła, Z., Karnkowski P.H., Konon, A., Oszczypko, N., Ślączka, A., Żaba, J. and Żytko, K. 2011. Regionalizacja Tektoniczna Polski. 60 pp. Komitet Nauk Geologicznych Polskiej Akademii Nauk; Wrocław.